

Dissertation zur Erlangung des Doktorgrades
der Fakultät für Chemie und Pharmazie
der Ludwig-Maximilians-Universität München



Precise and multifunctional conjugates for targeted siRNA delivery

vorgelegt von
Christian Dohmen
aus Viersen
2012

Erklärung

Diese Dissertation wurde im Sinne von § 7 der Promotionsordnung vom 28. November 2011 von Herrn Prof. Dr. Ernst Wagner betreut.

Eidesstattliche Versicherung

Diese Dissertation wurde eigenständig und ohne unerlaubte Hilfe erarbeitet.

München, den 27. 04. 2012

.....
(Unterschrift des Autors)

Dissertation eingereicht am:	13. 03. 2012
1. Gutachterin / 1. Gutachter:	Prof. Dr. Ernst Wagner
2. Gutachterin / 2. Gutachter:	Prof. Dr. Wolfgang Friess
Mündliche Prüfung am:	26. 04. 2012

Meinen Eltern

“I’m still confused, but on a higher level”
(Enrico Fermi)

Table of contents

1	Introduction	4
1.1	RNA interference	4
1.1.1	Molecular background of RNA interference	4
1.2	siRNA as pharmaceutical tool	6
1.3	Barriers in macromolecular delivery	6
1.4	Delivery systems for small interfering RNA	9
1.4.1	Basic scaffolds for nucleic acid delivery	9
1.4.2	Design of multifunctional carrier systems	13
1.5	Defined delivery systems	18
1.6	Aim of the thesis	19
2	Materials and Methods	21
2.1	Material	21
2.1.1	Water	21
2.1.2	Solvents	21
2.1.3	Chemicals	21
2.1.4	Chemicals for peptide synthesis	22
2.1.5	siRNAs	23
2.1.6	Polycations	23
2.1.7	Peptides	24
2.1.8	Cell culture	24
2.2	Methods	24
2.2.1	Loading of a 2-chlorotriyl chlorid resin	24
2.2.2	General solid phase supported peptide synthesis procedure	25
2.2.3	Kaiser test	26
2.2.4	Synthesis of Fola-PEG ₂₄ -K-(Stp ₄ -C) ₂ and its analogues	26
2.2.5	Synthesis of A-PEG ₂₄ -K-(Stp ₄ -C) ₂ and its analogues	27
2.2.6	Synthesis of Fola-PEG ₂₄ -C	28
2.2.7	Synthesis of Fola-PEG ₂₄ -Azide	29
2.2.8	Synthesis of the endosomolytic Inf7-siRNA hybrid	29
2.2.9	Synthesis of the nonreducible control Inf7-Mal-siRNA	30
2.2.10	Synthesis of the targeted Fola-PEG ₂₄ -ss-siRNA hybrid	31

2.2.11 Synthesis of siRNA hybrids <i>via</i> copper(I) catalyzed 1,3-dipolar cycloaddition	32
2.2.12 Analytical RP-HPLC	33
2.2.13 MALDI-TOF-MS analysis	34
2.2.14 ¹ H-NMR	34
2.2.15 Analytical agarose gel electrophoresis	35
2.2.16 Particle formation	35
2.2.17 Gel migration assay	35
2.2.18 Size measurement	36
2.2.19 Zeta potential measurement.....	37
2.2.20 Erythrocyte leakage assay	37
2.2.21 Fluorescence microscopy.....	38
2.2.22 Flow cytometric analysis	39
2.2.23 Reporter gene silencing	39
2.2.24 Endogenous target silencing	40
2.2.25 Reporter gene expression.....	41
2.2.26 <i>In vivo</i> assays.....	41
3 Results.....	43
3.1 Enhancing endosomal escape by endosomolytic active siRNA conjugates	43
3.1.1 Design and synthesis of an Inf7-siRNA hybrid	44
3.1.2 Functional evaluation of the Inf7-siRNA hybrid	48
3.1.3 Silencing activity of the Inf7-siRNA hybrid <i>in vitro</i>	52
3.2 Ligand mediated, targeted siRNA delivery.....	54
3.2.1 Design and synthesis of the FolicAcid-PEG ₂₄ -siRNA hybrid	55
3.2.2 <i>In vitro</i> gene silencing using FoliA-PEG ₂₄ -siRNA	60
3.2.3 Modified synthesis of targeted siRNA	61
3.2.4 Functional evaluation of FoliA-PEG ₂₄ -click-siRNA	63
3.2.5 Incorporation of FoliA-PEG ₂₄ -click-siRNA into an efficient and functional carrier system	65
3.3 Targeted polycation for cell specific siRNA delivery <i>in vitro</i> and <i>in vivo</i>	71
3.3.1 Design and synthesis of a structural defined targeted polycation.....	72
3.3.2 Showing targeting by DNA delivery - A proof of concept.....	75

3.3.3	Functional evaluation of FoIA-PEG ₂₄ -K(Stp ₄ -C) ₂ in combination with Inf7-siRNA	77
3.3.4	Specific <i>in vitro</i> gene silencing activity of FoIA-PEG ₂₄ -K(Stp ₄ -C) ₂ in combination with endosomolytic active siRNA	81
3.3.5	Biodistribution of siRNA using FoIA-PEG ₂₄ -K(Stp ₄ -C) ₂ in combination with Inf7-siRNA	84
3.3.6	Proving <i>in vivo</i> tumor targeting <i>via</i> intratumoral treatment.	92
4	Discussion.....	94
4.1	An endosomolytic active peptide-siRNA hybrid as structural defined molecule for enhanced endosomal escape in siRNA carrier systems.....	94
4.2	Targeted siRNA as defined structure for enhanced cell specificity and uptake	97
4.3	The combination of a structurally defined, targeted polymer and an endosomolytic active peptide-siRNA hybrid results in a delivery system for specific gene silencing <i>in vitro</i> as well as <i>in vivo</i>	101
5	Summary	105
6	References	107
7	Appendix	116
7.1	Abbreviations	116
7.2	Supporting Info Chapter 3.3.....	119
7.3	Publications	121
7.3.1	Original papers.....	121
7.3.2	Patents	122
7.3.3	Book chapters	122
8	Acknowledgements	123

1 Introduction

1.1 RNA interference

In 1998 an article entitled “Potent and specific genetic interference by double-stranded RNA in *Caenorhabditis elegans*” was published by Andrew Fire and Craig C. Mello.¹ In their work they discovered that the introduction of double-stranded RNA (dsRNA) encoding for a certain gene into cells, led to the down regulation of its gene product. This down regulation was more efficient for an introduced double strand than for the separate introduction of its single strands. For single strands it was thought, that they hybridize with their target messenger RNA (mRNA) leading to degradation and thus avoid translation (antisense strategy).² As the effect of dsRNA was significantly higher, the scientists hypothesized a catalytic process. This finding, termed RNA interference (RNAi) was awarded with the Nobel Prize in Physiology or Medicine in 2006.

One year after this discovery (1999) Tuschl *et al.* published their results on this field.³ They had found that the dsRNA was cleaved into 21-23 nt long fragments when introduced into the cell. They concluded that these fragments led to gene silencing. In 2001 Tuschl and co-workers could demonstrate that their hypothesis was right. They introduced synthetic, 21 nt long dsRNA, called small interfering RNA (siRNA), into mammalian cells resulting in a specific gene knockdown.⁴ These findings did not only revolutionize the field of cell biology and its understanding due to the opportunity to selectively down regulate single genes on post transcriptional level; it also opened a completely new, very potent platform for drug development.

1.1.1 Molecular background of RNA interference

Since its discovery the knowledge of RNA interference increased rapidly. The process starting with the introduction of dsRNA or synthetic siRNA into cells, resulting in a specific target gene silencing is understood in its details. An overview of the processes and structures included in the RNA mediated silencing of a gene is shown in Fig. 1.1.

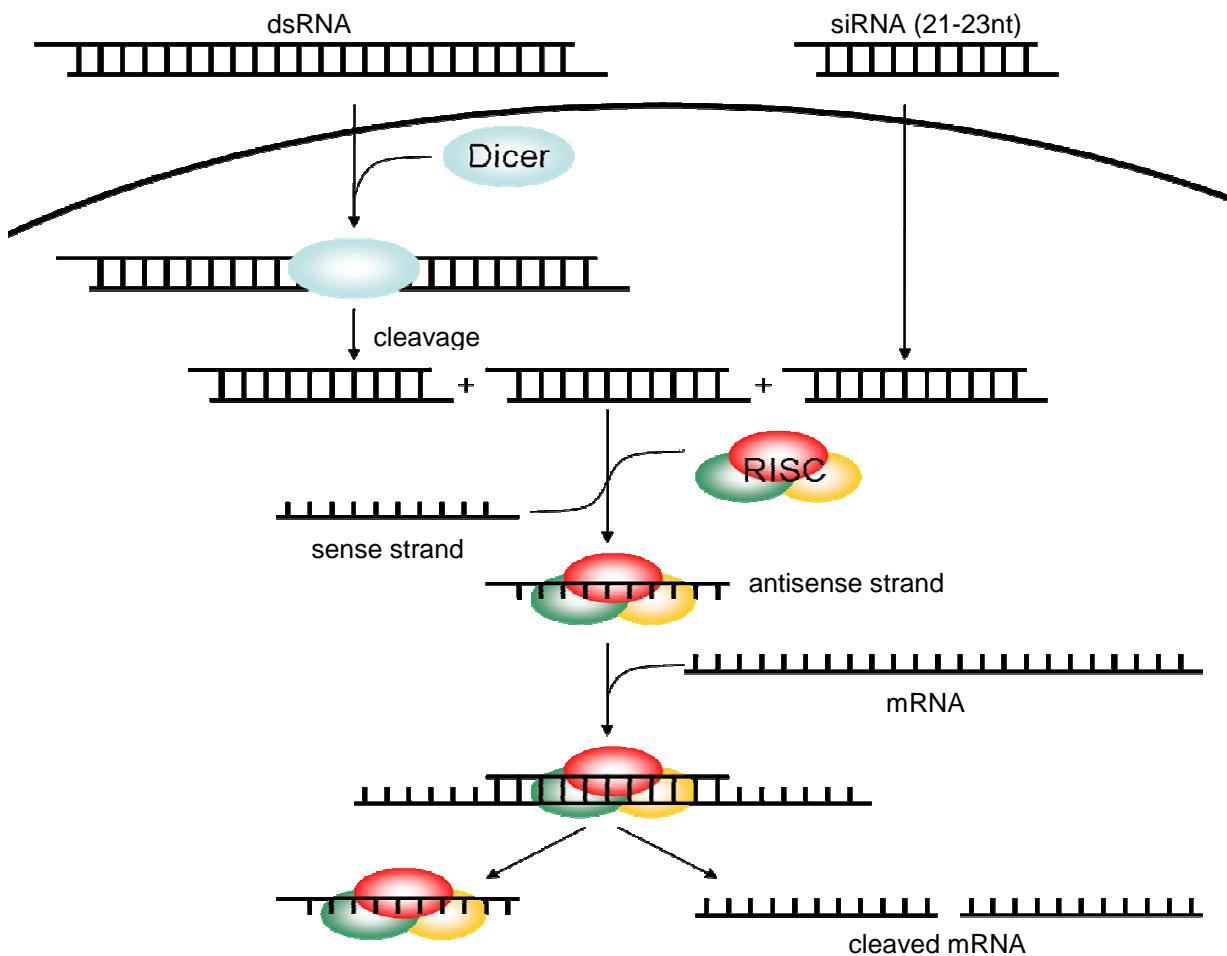


Fig. 1.1 Mechanisms of gene silencing by introduction of dsRNA and siRNA. RISC: RNA induced silencing complex, mRNA: messenger RNA, siRNA: small interfering RNA, dsRNA: double-stranded RNA.

When dsRNA enters the cell, it is recognized by an enzyme called Dicer.⁵ This enzyme cleaves the dsRNA into fragments of 21 – 23 nt also known as siRNA. Instead of the introduction and cleavage of dsRNA, synthetically produced siRNA can be introduced immediately.⁴ Once in the cytosol, these fragments are recognized by a multi-protein complex called RNA-induced silencing complex (RISC). Argonaute 2, as part of the RISC unwinds the siRNA. While the sense strand is released and degraded, the antisense strand remains incorporated in the RISC.⁶ If complementary mRNA is accessible, the complex attaches to it, resulting in cleavage of the mRNA followed by degradation.⁷⁻⁸ The RISC-antisense strand complex remains stable during this process and therefore is able to attach to a new corresponding mRNA propagating and catalyzing gene silencing. This process displays an important epigenetic tool for the regulation of gene expression.

1.2 siRNA as pharmaceutical tool

As RNAi technology results in the down regulation of a specific target gene, it is a potent tool for cell biological science. Moreover, since the first *in vivo* test using siRNA in 2002,⁹ its potential as pharmaceutical drug has been studied extensively.¹⁰⁻¹¹ Many diseases are based on a genetic dysfunction. Besides reduction of the expression of an upregulated gene up to complete silencing, siRNA treatment can also lead to upregulation of a gene e.g. by down regulation of its suppressor proteins.¹² In comparison to chemical drugs, siRNA has the advantage to work very specific on the target gene, almost without cross reactivity to any other process. Compared to other high specific macromolecular drugs (e.g. antibodies or peptides) it can target almost any cellular process based on a gene product, making former undruggable targets accessible. If a formulation is able to deliver the siRNA to a certain target cell, every mechanism can be regulated without modifying the drug characteristics (structure, solubility, charge, etc.). The only adoption that has to be made is the target-directed siRNA nucleotide sequence. Due to these advantages siRNA has been investigated for various diseases including inflammation, viral infections and cancer.¹³⁻¹⁸ Especially in case of cancer, siRNA reveals potent new therapy methods.¹⁹⁻²⁰ As many genes are deregulated in all tumors, RNAi technology can help to reorganize the cancer cell or simply force apoptosis.²¹

The key problem hampering a rapid development of pharmaceutical drugs is the problem, every macromolecule bears: the delivery process.

1.3 Barriers in macromolecular delivery

siRNA has similar limitations as many other macromolecules like proteins, peptides, antibodies or DNA during the delivery process.

Depending on their function, macromolecules have to act at the surface of the target cell, or inside the cell. Antibodies, proteins and peptides acting e.g. as inhibitor of cell surface receptors or inducing a receptor based signalling cascade have just the need to get access to the target cell,²²⁻²³ while siRNA, antisense RNA or intracellular acting proteins, peptides and antibodies have to enter the cell and reach the cytosol or,

especially in case of DNA, enter the nucleus. While getting to the place of need, these molecules are faced with many problems. Local injection followed by diffusion of the delivered molecule to the cell of interest is one method to get huge amounts of a macromolecular drug to its target cell. But just a few cells or tissues can be addressed *via* this method. Direct injection in the eye has in example been used for the treatment of age related macula degeneration.²⁴ Especially strong vascularized organs like liver or kidney, but most important metastatic tumor tissue can be addressed easier by systemic delivery *via* blood supply. According to Paul Ehrlich's philosophy of the "magic bullet", the macromolecular drug should find its target cell itself after systemic injection, avoiding any interaction with blood compounds or non-targeted cells. In reality this process raises many hurdles for the drug. After injection into the blood stream the macromolecule is surrounded by a tremendous amount of different molecules, starting from serum albumin over blood cells, the immune system (phagocytic cells etc.) and enzymes like proteases, peptidases or nucleases. They interact either unspecific *via* ionic or hydrophobic interactions or very specific (e.g. enzymatic degradation). During the circulation, the macromolecule passes all different kinds of tissues and organs, raising new limitations. Especially clearance by liver and kidney is a problem during macromolecular delivery.²⁵⁻²⁶ The kidney has a size cut off of around 8 nm and thus allows renal clearance of small proteins peptides and especially siRNA with a size below this cut off. On the other hand organs with very small capillaries like the lung have to be passed. Thus huge delivery vehicles resulting from a potential aggregation have to be avoided, because they could lead to a hampered blood flow, followed by inefficient blood supply.

If a delivery vehicle for the macromolecule is designed in an appropriate manner, a stable circulation throughout the body should be enabled. After overcoming these bottlenecks the macromolecule has to reach its target cell/tissue. When arrived, it has to leave the blood circulation and attach to the cell surface depending on its function. For proteins, peptides and antibodies acting from the extracellular side of the cellular membrane it is rather easy to address to the target cell. In general these drugs are designed to attach and activate or inhibit a certain antigen or cell surface receptor. Thus the drug is designed to recognize its target cell. In case of macromolecular drugs acting intracellular, the delivery process becomes more complex, because they have to overcome the cellular membrane. As this lipid bilayer is designed to hamper macromolecules from uncontrolled cell entrance, this barrier is not easy to overcome.

For macromolecules there are two options to pass the membrane and get inside the cell (Fig. 1.2 II, III).

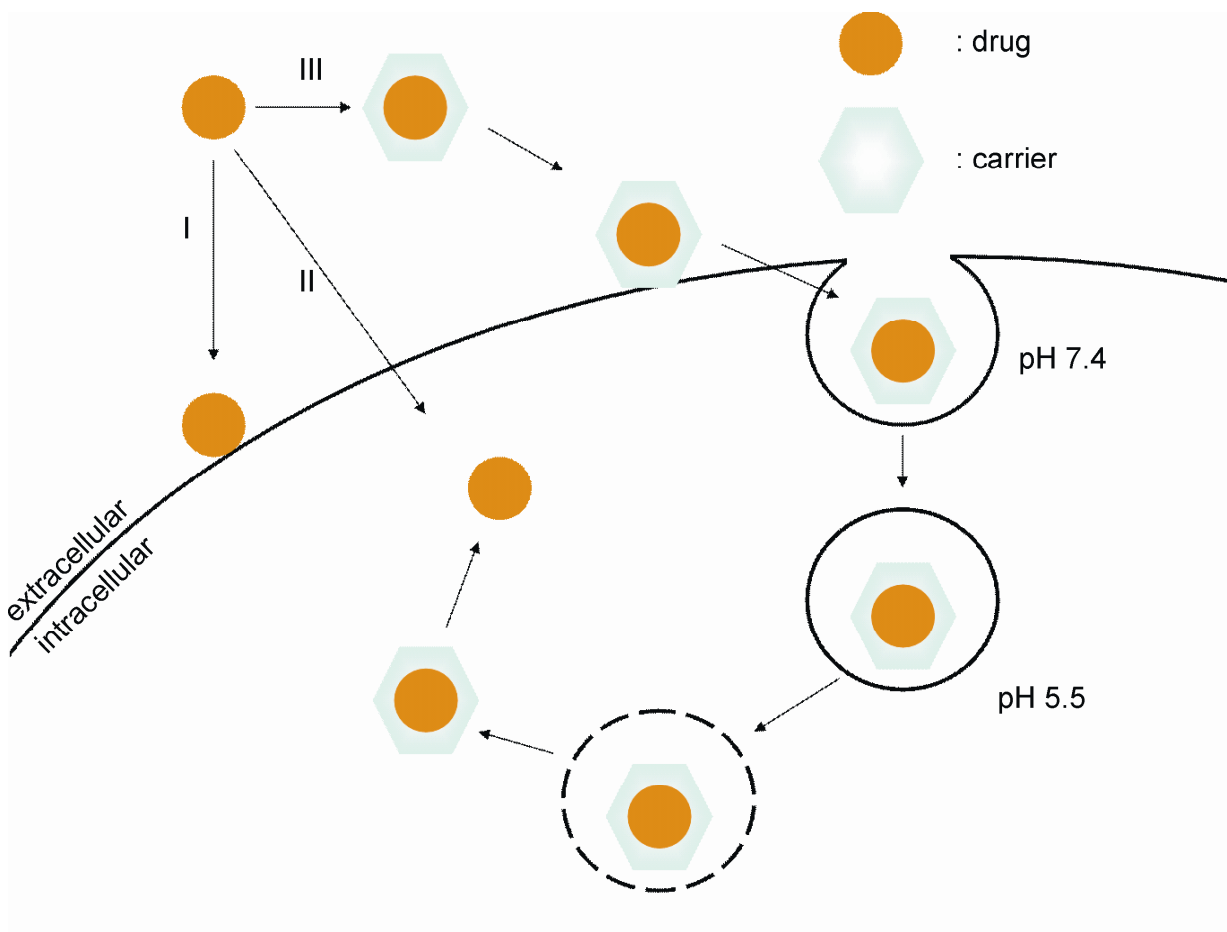


Fig. 1.2 Cell association and entry mechanisms for macromolecular delivery. I: Interaction of an extracellular acting drug with the cell surface, II: Direct transduction through the cell membrane, III: Internalization *via* a carrier system.

One possibility is crossing the layer directly using cell penetrating peptides (CPP)²⁷ or peptide transduction domains (PTD)²⁸⁻²⁹ (Fig. 1.2 II). These peptides are able to interact with the cellular membrane helping a conjugated macromolecule to attach to, and enter the cell. For some drugs, peptides and proteins this method works to certain extend, but the efficiency is strongly influenced by the physical properties (charge, size, hydrophobicity) of the attached macromolecule. Although it has been reported that the delivery of free oligonucleotides or negatively charged molecules through the plasma membrane is possible to certain extend,³⁰⁻³³ especially for negatively charged nucleic acids, the interaction with the negatively charged cell surface is difficult.

The second option of cell entrance is clathrin- or caveolae mediated endocytosis (Fig. 1.2 III). Endocytosis is a natural process that enables a controlled uptake of macromolecules. General processes initiating endocytosis are e.g. the attachment of special ligands to its receptors. The transferrin receptor is for example internalized after attachment of a Fe^{3+} loaded transferrin molecule.³⁴ This process allows the uptake of iron-ions into the cytosol. In case of receptors that start an intracellular signal cascade, the receptor is internalized after ligand attachment to avoid multiple activation of the cascade. Besides these receptor based processes, rather unspecific ionic interactions can lead to the invagination of the cellular membrane resulting in endocytosis.³⁵ Although the biological functions are very different, these processes can be used to get a macromolecule *via* an endosome across the cellular membrane. In case of direct crossing *via* cell penetrating peptides, the payload gets immediately into the cytosol, where many of the molecules (especially siRNA) are addressed to. In case of endocytosis, the drug enters the cell entrapped in a small compartment. As an endosome gets acidified and further processed to a lysosome after cell entrance, the macromolecular structures have to escape out of the endosome to avoid lysosomal degradation. After cell entrance, all modifications that have been done to the payload have to be cleaved off to enable the development of a fully active non modified structure. All these steps have to be fulfilled during delivery. If just one of these steps is inefficient, the efficiency of all other steps is nonrelevant, because the whole process is disabled.

1.4 Delivery systems for small interfering RNA

Nucleic acids as macromolecules to be delivered to certain cell populations have to overcome all single delivery steps described in the last chapter. Carrier systems and ideas to overcome these hurdles are pointed out in detail in the following section.

1.4.1 Basic scaffolds for nucleic acid delivery

Due to extensive disadvantages of systemic delivery of naked siRNA, starting from enzymatic degradation³⁶ over renal clearance, interaction with blood compounds,

activation of the immune system³⁷ and the inefficient uptake by target cells,³⁸ many approaches of systemic delivery use vehicles. As also known from the field of gene delivery, these vehicles can be classified into three major groups, illustrated in Fig. 1.3: viruses, liposomes and polycations.³⁹⁻⁴¹

As natural gene delivery vehicles, viruses are able to deliver their genes to target cells. Due to a long term evolution process they are ideally adapted to overcome the general problems of delivery. Although viruses are very complex, efficient vehicles, they also have limitations for the use as siRNA delivery system.

In general viruses are targeted to one cell type, thus it is difficult to target a special cell population that is no common target of a natural virus. Although work has been described, developing methods for genetic and chemical de-/retargeting,⁴²⁻⁴³ reaching certain cell populations without cross reactivity remains a challenge.

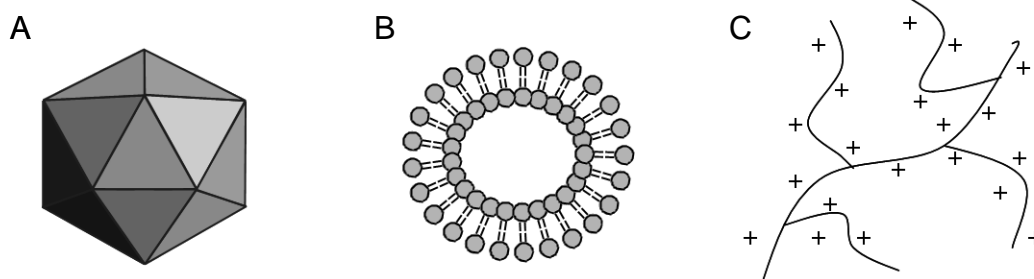


Fig. 1.3 Overview of basic types of carrier-systems for nucleic acid delivery. A: Virus, B: Liposome, C: Polycation.

As viruses have been modified and adapted in an evolutive manner for millions of years, same did the immune defence of the organisms. Thus viral delivery in general is restrained by recognition by the immune system, during the blood circulation as well as during cell entrance.⁴⁴ Therefore the virus has to be genetically or chemically modified to avoid an immune response.⁴⁵ The most prominent disadvantage of viral systems for siRNA delivery is the lack of compatibility. For gene delivery the gene of interest is introduced into a plasmid. A special packaging cell line is transfected with this plasmid, leading to the amplification of the DNA and incorporation into intracellular produced viruses. The virus can be isolated out of the medium and used for delivery.⁴⁶ siRNA is a completely chemically synthesized structure. Thus it is impossible to get it into a virus by the described *in vitro* virus production method. To obviate this problem, DNA has been packed into viral particles such as AAV vectors, bearing a sequence encoding for the sense and antisense strand separated by a short nontargeting region

called loop.⁴⁷⁻⁴⁸ When the transgene is transcribed in the target cell after transfection, it produces mRNA that can self assemble to a double stranded RNA with high similarity to siRNA (small hairpin RNA, shRNA). This method bears common disadvantages of DNA delivery, because it often is associated with the integration of the nucleic acid into the cell genome and thus can hardly be controlled when introduced once.⁴⁹⁻⁵⁰

To circumvent the numerous disadvantages of viral delivery, synthetic structures have been designed.⁵¹ These so called artificial viruses overcome the hurdles of delivery by mimicking viral processes, but avoid their negative aspects. Two major classes of vehicles have been developed: liposomes and polyplexes. Besides of them, a various amount of different systems combining parts of both vehicle types like lipoplexes,⁵² cationic lipids,⁵³ lipidoids,⁵⁴ etc. have been designed.

Liposomes are small particles composed of one or several lipid bilayers that entrap a hydrophilic core. Multilamellar liposomes originate spontaneously by mixing a hydrophobic with a hydrophilic phase. Further treatment e.g. extrusion or sonication result in unilamellar vehicles. Drugs can be integrated into this carrier system either in the hydrophilic inner compartment or the hydrophobic layer. Liposomes build very stable particles and remain stable during the delivery process. In case of siRNA deliver, the payload is in the inner, hydrophilic compartment. The delivery process after reaching the target cell can be performed in two different manners. The first, less frequent option is the fusion of the liposome with the target cell, releasing the siRNA into the cytosol. The second, more frequent option includes endocytosis of the liposome into an endosome. The endosomal escape then takes place by either membrane fusion or endosome disruption. Most trials using lipid formulations for nucleic acid delivery address liver cells or liver tumors for therapy. As the liver shows high affinity to lipidic particles, they are very efficient in this tissue. This advantage in liver targeting displays a disadvantage in the treatment of other tissues. As liposomes and other hydrophobic particles are easily directed to the liver, they need a strong shielding to get efficiently into other tissues.⁵⁵

In contrast, polyplexes are particles that are formed spontaneously by mixing anionic and cationic structures under aqueous conditions.⁵⁶ Due to ionic interactions they aggregate in a controlled way (depending on the mixing ratio), resulting in compact structures. In case of pDNA or siRNA, building the anionic fraction, different types of polycationic polymers have been used to form polyplexes for the delivery process.

Linear structures like poly-lysine (PLL),⁵⁷ linear polyethylenimine (LPEI),⁵⁸ chitosan⁵⁹ or branched structures like polyamidoamine (PAMAM),⁶⁰ branched polyethylenimine (brPEI)⁶¹ or polypropylenimine (PPI)⁶² have been used in several described experiments (Fig 1.4).

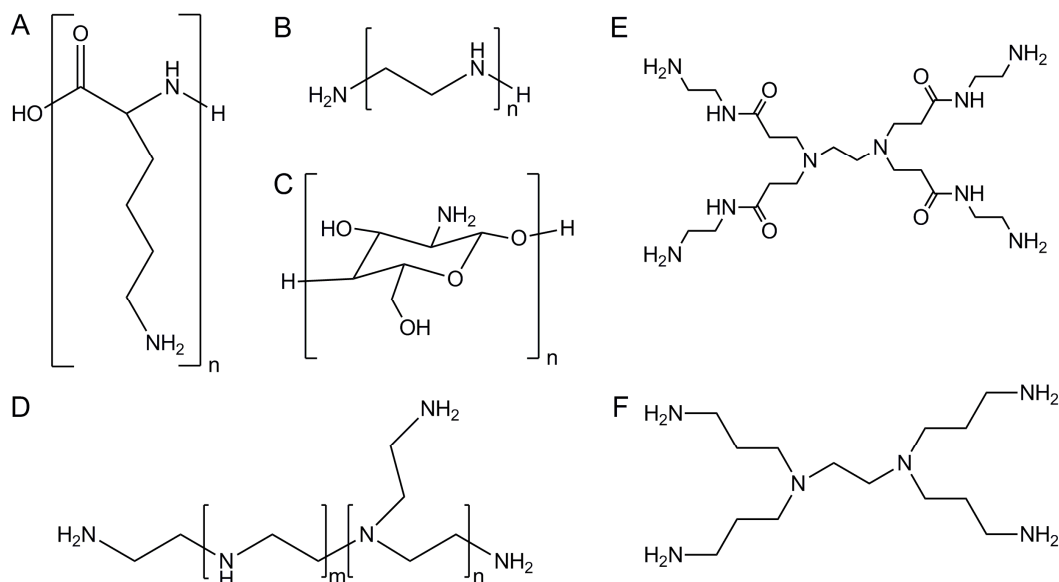


Fig. 1.4 Polycationic polymers for nucleic acid delivery. A: Poly-lysine (PLL), B: linear polyethylenimine (LPEI), C: chitosan, D: branched polyethylenimine (brPEI), E: polyamidoamine (PAMAM), F: polypropylenimine (PPI).

As pointed out in Fig. 1.4 most used structures are based on a polyamine backbone, giving the needed positive charge at physiological pH. As gold standard for the delivery of nucleic acids LPEI has been used in several experimental settings.⁶³⁻⁶⁵ This molecule bears many advantages during the delivery process. Once mixed with the nucleic acid, it builds stable polyplexes under physiological conditions. These polyplexes in general have a positive zeta potential due to the excess of positive charged polymer. This enables the attachment to the target cell surface *via* ionic interactions, followed by endocytosis. In the endosome, PEI leads to an escape *via* the so called 'proton sponge effect'.⁶⁶⁻⁶⁷ Due to its strong buffering capacity, the polycation hampers the acidification of the endosome. Thus more and more protons get into the endosomal compartment, followed by chloride as counter ion. This leads to a strong osmotic pressure, resulting in an influx of water. If the osmotic pressure is to strong, the endosome bursts and releases the polyplex into the cytosol.⁶⁷ However PEI like particles have been described that do not have a good transfection

efficiency.⁶⁸ It also seems to be important that the polycationic charge is presented on the surface for interaction and destabilization of the endosomal membrane in addition to the proton sponge effect.⁶⁹ Many hurdles during the delivery process can be overcome by simple polyplex formation. Standard PEI is a very inefficient carrier for siRNA *in vitro*.⁷⁰ Aigner *et al.* however demonstrated efficient delivery in a mouse model *in vivo*.⁷¹ Beside this obscurity, many problems occur during *in vitro* as well as *in vivo* delivery. The introduction of polymeric, charged structures into the cell led in many cases to strong toxic side effects. The cell can not degrade the high molecular weight polymers, which results in accumulation and interactions with DNA, proteins and membranes.⁷² *In vivo* the strong positive charged polyplexes interact with compounds of the blood circulation, resulting in strong aggregation and thus toxicity. Without modification they might interact with every cell they pass by unspecific cell attachment, leading to undesired side effects. On the other hand, for example succinylation of PEI to block some of the positive polymer charges has resulted in an efficient siRNA carrier with strongly reduced cytotoxicity⁶¹

It could be shown that with proper modifications nonviral carrier systems may have tremendous advantages over viral systems.⁵¹ Although they have many side effects and are less efficient, they bear the potential to deliver nucleic acids to cells and have the advantage of a huge design space. To reduce side effects and raise efficiency new concepts, based on these scaffolds have been developed.

1.4.2 Design of multifunctional carrier systems

The different basic types of artificial carrier systems, with their limitations as described in the last section can presumably just act as scaffold for an efficient multifunctional siRNA carrier system. Compared with a viral delivery vehicle, they just build the 'inner core'. Reducing side effects and raising specificity of synthetic carrier systems was obtained in further studies, using more complex functionalized structures attached to these scaffolds.⁷³ Modifications and structures, addressing every delivery step are pointed out in the following section.

1.4.2.1 Stabilization

Stabilization of the carrier system is a key issue especially in case of polyplex mediated siRNA delivery. Use of high-molecular weight polycationic polymers used for delivery may increase stability of polyplexes, but also triggers high toxicity due to cellular accumulation processes, leading to aggregation of intracellular compounds. In contrast short fragments (e.g. oligoethylenimine (OEI)) show a dramatically decreased toxicity, but also do not build stable polyplexes. A combination of both structures giving high stability of the polyplex by reduction of toxicity would result in a favourable polymer. Thus linker structures have been introduced into the polycationic backbone either pre- or post-polyplex formation. These linkers crosslink short polymers, resulting in high molecular weight structures with increased polyplex stability. To reduce the toxicity of these huge structures, bioreversible linkers have been used. These linkers degrade, reacting on the intracellular environment.^{62, 74-75} Thus high molecular weight structures are cleaved into several small molecules after the payload has been delivered. Hence toxicity is strongly reduced. Used linkers include (i) disulfides, reacting on the reductive cytosolic environment,⁷⁶ (ii) acetal linkers cleaved under acidic endosomal conditions⁷⁴ or (iii) peptide structures cleaved by peptidases.⁷⁷ Besides the mentioned covalent binding, structures resulting in noncovalent interactions were internalized to further enhance stability, like hydrophobic domains (e.g. fatty acids or tyrosines).⁷⁸⁻⁸⁰ These modifications result in self organizing molecules generating highly stable polyplexes. In a different approach siRNA was covalently attached to a polymeric delivery vehicle *via* a disulfide bond to increase the stability and avoid the dissociation of carrier system and cargo.^{57, 81} The resulting hybrid led to efficient knockdown while the stability under physiological conditions was drastically increased.

1.4.2.2 Shielding

Protection of the carrier surface from interactions with blood compounds and nontargeted cells is one of the key issues using several delivery systems. All carriers, viruses as well as liposome- and polycation based vector systems have the problem of

undesired interactions with compounds during blood circulation, resulting in aggregation, destabilization or unwanted transfection of nontargeted cells. Thus the hydrophobic or charged surface has to be shielded. The most prominent molecule used for shielding is poly (ethylene glycol) (PEG).⁸²⁻⁸⁴ It is a highly soluble, uncharged polymer that prevents molecules from interactions when coupled to it. The covalent attachment can be performed either during synthesis, attaching the poly (ethylene glycol) *via* a linker to a free amino or thiol group^{57, 85} or after loading the carrier (post-pegylation).⁸⁶ Apart from PEG, hydroxyethylene starch (HES) or poly(N-(2-hydroxypropyl)methacrylamide) (pHPMA)⁸⁷⁻⁸⁸ are feasible molecules for shielding. Besides hampering the interaction with other molecules or cells, shielding also raises the circulation time in the blood flow due to a decreased clearance⁸⁹ and avoids recognition by the liver or the immune system.

1.4.2.3 Targeting

An ideally stabilized, shielded particle is able to circulate for an extended time in the blood flow without interacting with any cell. Hence a maximal shielded particle is not able to interact with the target cell. Thus additional to a shielding domain, a kind of 'homing structure' to the target tissue has to be incorporated into the carrier system. In case of tumor targeting, different strategies allow the accumulation in the target tissue. Non targeted structures have already shown to work very efficient in case of DNA delivery into tumors. This phenomenon can be explained by the enhanced permeability and retention (EPR) effect.⁹⁰ When growing tumors reach a certain size, where they are limited in nutrient supply, they recruit their own blood vessels. These vessels are functional but not perfect in structure and orientation. They show large fenestrations between the endothelial cells, resulting in leakiness.⁹¹ Molecules that pass these vessels leave the blood circulation by diffusion and migrate into the tumor tissue as do the carrier systems. Small molecules diffuse back into the blood flow, when the drug concentration decreases. Big molecules, which are hampered in migration once they entered the tissue, accumulate there. This passive targeting has been a common method in case of tumoral delivery for many systems.⁹²

A more specific, active targeting is addressing receptors on the cell surface.⁹³ Almost all tissues differ in the expression level of certain receptors, making them

distinguishable. Thus the incorporation of ligand structures, analogues of them or antibodies addressing these receptors enable a specific interaction with the desired tissue, while other tissues remain untransfected.

For the intracellular delivery of siRNA, endocytosis after cell attachment is required. Therefore receptors, leading to this process after ligand binding are the once most prominently used for delivery issues. In case of tumor targeting the transferrin receptor (Tf-R), the epidermal growth factor receptor (EGF-R), the folic acid receptor (FolA-R) or integrins (e.g. $\alpha_v\beta_3$) are the most described structures used for specific targeting.⁹⁴⁻⁹⁸ They are highly upregulated in tumor tissue, and lead to endocytosis after ligand attachment.⁹⁹⁻¹⁰² In first experiments the native ligands (transferrin, the epidermal growth factor, folic acid, etc.) have been used. Although they are ligands with high binding affinity, they lead to very heterogenic structures when coupled to a carrier system. Their huge size and limitation in specific coupling, led to the development of smaller structures. By phage display several peptidic molecules have been investigated for their binding affinity to receptors like the Tf- or the EGF-receptor. The resulting peptides B6 (for Tf-R targeting)¹⁰³ and GE11 (for EGF-R targeting)¹⁰⁴ show a good binding affinity, while allowing a more defined attachment to the carrier system.¹⁰⁵ However, often their specificity and affinity to the receptor always remains lower than that of the native ligands. Targeting integrin $\alpha_v\beta_3$ is possible *via* different types of peptide structures containing the amino acid sequence arginine-glycine-aspartic acid (RGD).¹⁰⁶⁻¹⁰⁷

Additionally, cells can be targeted using antibodies. They are defined structures with a specific, high binding affinity. Especially the EGF-receptor has been topic of several studies using antibodies to inhibit tumor growth.¹⁰⁸⁻¹⁰⁹ As these antibodies fulfil the requirements for a good targeting structure, they were used on carriers as well.

With a K_d of 10^{-10} M, folic acid is one of the ligands with the highest binding affinity.¹¹⁰ Its receptor is upregulated in different tumors,¹¹¹⁻¹¹² while it is almost absent in other tissues¹¹³⁻¹¹⁴ despite of the apical membrane of epithelial cells in the kidney proximal tubules¹¹⁵ and activated monocytes and macrophages.¹¹⁶ As small molecule it can be attached rather defined to a carrier system. Using the carboxyl function for coupling, it can only be attached *via* its α - or γ -carboxyl group.¹¹⁷⁻¹¹⁸ A huge disadvantage using random coupling conditions is the strong reduction of binding affinity after coupling *via* the α -carboxyl group.¹¹⁹

1.4.2.4 Endosomal escape

After cell entrance *via* endocytosis, the endosomal escape is the last hurdle during the delivery process. Although some liposomes with special, systemically not very stable lipid composition can fuse with the membrane, endosomal escape remains a bottleneck. Polymers like PEI can use the proton sponge effect to avoid lysosomal degradation. As a certain amount of polymer is needed within one endosome to mediate enough buffering capacity for the proton sponge effect, and not all endosomes are acidified with the same efficiency,¹⁰¹ this method of endosomal escape is also not optimal. Hence it can be maximized using further strategies. Moreover new structures lacking a buffering capacity¹²⁰ can be tested as feasible carrier systems, if combined with endosomolytic agents. To enhance the escape of the endosomal compartment, different structures have been developed. One reasonable approach is the use of peptides that bear an endosomolytic activity.¹²¹ In 1992 Wagner and colleagues reported a peptide based on the sequence of the amino-terminus of the influenza virus hemagglutinin for use in gene transfer.¹²² Permutation of the sequence revealed a peptide (Inf7) that is highly lytic at endosomal pH (pH 5.5), while it is not lytic at physiological pH (pH 7.4).¹²³ Thus this peptide displays a useful tool for endosomal escape. It is non-functional in the extracellular environment and does not lead to erythrocyte lysis or toxicity after cell entrance, while it develops a highly lytic activity in the endosomal environment. A further peptide used to overcome this bottleneck is melittin.¹²⁴⁻¹²⁵ As main substance of bee venom it is highly lytic¹²⁶ but in contrast to Inf7 does not show advantageous pH dependency, causing highest lytic potential at neutral pH, thus significant toxicity in the delivery process.¹²⁷ Meyer *et al.* could show that the modification of the peptide with dimethylmaleic anhydride (DMMAAn) leads to a strong reduction of its lytic activity at neutral pH. Due to the acid lability of the modification it is cleaved in the endosome, recovering its lytic potential, resulting in increased pDNA and siRNA delivery *in vitro*.^{57, 120, 128} Furthermore synthetic peptides mimicking natural lytic peptides have been designed. GALA and KALA, consisting of the repeating structure glutamic acid (or lysine for KALA)-alanine-leucine-alanine build a random structure at neutral pH, while forming an amphipathic alpha-helix in an acidic environment. These structures are able to interact with lipid bilayers, resulting in enhanced endosomal escape.¹²⁹ The molecules have been shown to mediate gene and siRNA delivery either free¹³⁰ or in combination with a

carrier system.¹³¹⁻¹³⁴ These systems show that charge (of the polymer) as well as a certain hydrophobicity of the peptides is required to enhance the endosomal escape. Thus the combination of polycationic backbones and fatty acids, having comparable properties, has been a further reasonable approach overcoming this crucial step of delivery.^{80, 89}

1.5 Defined delivery systems

As described in the last sections, an ideal carrier system for siRNA delivery is composed of a backbone, a shielding domain, a targeting ligand, an endosomal escape domain and further stabilizing molecules. In comparison to first approaches using nonmodified polymers, complexity increased exponential in the last years. As the main chemistry did not change, the products became very heterogenic and undefined, due to different reasons. The polymers used in most strategies (PEI, PLL, PEG, etc.) are synthesized using common random polymerization techniques. Thus the backbone itself often (e.g. for PEIs) already lacks definition. The attachment of the substructures (fatty acids, peptides, proteins, PEG etc.) is performed using linker molecules. These are randomly attached to the backbone of the polymer (e.g. to amino groups).¹³⁵⁻¹³⁶ After coupling different substructures the polydispersity of the molecules in one batch is very high. Hence the exact reproduction of a batch is almost impossible, because many factors have influence on the synthesis. Moreover the exact determination of the composition is very difficult, because efficient methods like RP-HPLC or mass analysis are no feasible methods for this kind of structures. The most relevant disadvantage of these structures is the inability to get an exact structure-activity relationship. As the polymers are very heterogenic, experiments can just give an average result of knockdown efficiency, toxicity, etc. In contrast, defined polymers with an exact structure regarding amount and position of attached molecules could give very precise data and enable the design of more efficient delivery systems. A strategy to overcome these problems is the solid phase supported peptide synthesis (SPPS). The method first described by Merrifield *et al.*¹³⁷ allows the synthesis of defined structures. On solid support, a molecule is synthesized using a high excess of educts and washing them away after reaction is completed by a simple filtration step. This method was adapted by Hartmann *et al.*¹³⁸⁻¹³⁹ to synthesize defined polycationic

structures. After adaption and modification, this strategy was used in our group to synthesize more than 300 molecules combining polycationic, crosslinking and hydrophobic properties. The results published by Schaffert *et al.* reveal that these defined structures enable the determination of a highly precise structure - activity relationship.⁸⁰ However the design space of this strategy was limited to lipid modified polycationic structures up to now.

1.6 Aim of the thesis

RNAi is one of the leading techniques, having the possibility to result in efficient drugs for an increasing amount of diseases and arises treatment options on targets that were undruggable up to now. The crucial limitation in the development of efficient pharmaceuticals remains the delivery process. Although many different types of feasible chemical carrier systems with a high efficiency have been evaluated *in vitro*, the *in vivo* delivery process makes new demands on the delivery vehicles. New properties and functional domains have to be included during their design. This has shown to result in very efficient but very complex and heterogenic structures e.g. carrier PLL-PEG-DMMAAnMel-ss-siRNA published by Meyer *et al.* from our group.⁵⁷ The use of very polydisperse, polymeric scaffolds for the synthesis in combination with the high degree of functionalization makes the resulting delivery system a very heterogenic product. This fact displays an own limitation in the development of efficient delivery systems:

Resulting polymers make an analysis of structure as well as purity of the carrier system with state-of-the-art analytics impossible. Achieved physicochemical and biological data give just an average of effects of the heterogenic mixture, eliminating the determination of a clear structure activity relationship. The polydispersity of the carrier mixture results in a strong batch dependency and thus a low reproducibility of the synthesis. All these aspects are clear disadvantages regarding the development of efficient systems as well as their aspired clinical testing, requiring GMP production methods.

General aim of this thesis was the development of new efficient, polyplex based carrier systems containing functional substructures that address all limitations during the delivery process including:

- Polyplex formation and stability
- Shielding
- Receptor mediated cell-targeting
- Endosomal escape
- Biodegradability and low toxicity

Specific aims were:

- Generation of monodisperse constructs by solid-phase supported synthesis, enabling state-of-the-art analytics and a controllable modification.
- Introduction of functionalities by modifying either the polymeric backbone or the siRNA itself, building covalent conjugates.
- Biophysical and biological characterization of the novel functionalized siRNA polyplexes.

2 Materials and Methods

2.1 Material

2.1.1 Water

Water is defined in this thesis as deionized water with a conductance below 0.06 μS .

2.1.2 Solvents

Acetonitrile, HPLC grade	Sigma-Aldrich, Steinheim, Germany
Dichlorormethane, for analysis	AppliChem, Darmstadt, Germany
N,N-Dimethylformamide, peptide grade	Iris Biotech, Marktredwitz, Germany
Deuterium oxide	Sigma-Aldrich, Steinheim, Germany
Ethanol, for analysis	Sigma-Aldrich, Steinheim, Germany
Methanol, for analysis	Sigma-Aldrich, Steinheim, Germany
Methyl tertiary butyl ether	AppliChem, Darmstadt, Germany
n-Hexane	Sigma-Aldrich, Steinheim, Germany
TFA	Iris Biotech, Marktredwitz, Germany

2.1.3 Chemicals

Boric acid	Sigma-Aldrich, Steinheim, Germany
3-Hydroxypicolinic acid	Sigma-Aldrich, Steinheim, Germany
5,5'-Dithiobis-(2-nitrobenzoic acid)	Merck, Darmstadt, Germany
Ethylenediaminetetraacetic acid	Sigma-Aldrich, Steinheim, Germany
Hepes	Biomol, Hamburg, Germany
3-Hydroxypicolinic acid	Sigma-Aldrich, Steinheim, Germany
Potassium cyanide (KCN)	Merck, Darmstadt, Germany
Sodium chloride (NaCl)	VWR, Darmstadt, Germany
<i>tris</i> (2-Carboxyethyl) phosphine	Sigma-Aldrich, Steinheim, Germany
Trisma® Base	Sigma-Aldrich, Steinheim, Germany

2.1.4 Chemicals for peptide synthesis

Reactor:

Syringe reactor (PP reactor with PE frit) MultiSynthech, Witten, Germany

Resins:

2-Chlorotrityl chloride resin
(200-400 mesh, 1.56 mmol Cl⁻/g resin) Iris Biotech, Marktredwitz, Germany
Ala-Wang resin (0.35 mmol/g) Novabiochem, Hohenbrunn, Germany

Natural amino acids (all L-type):

Boc-Cys(Trt)-OH Novabiochem, Hohenbrunn, Germany
Dde-Lys(Fmoc)-OH Iris Biotech, Marktredwitz, Germany
Fmoc-Cys(Trt)-OH Iris Biotech, Marktredwitz, Germany
Fmoc-Ser(tBu)-OH Iris Biotech, Marktredwitz, Germany
Fmoc-Lys(Fmoc)-OH Iris Biotech, Marktredwitz, Germany
Fmoc-Glu(OH)-tBu Iris Biotech, Marktredwitz, Germany

Artificial amino acids:

(S)-5-Azido-2-(Fmoc-amino)pentanoic acid Sigma-Aldrich, Steinheim, Germany
*N*¹⁰-(Trifluoroacetyl)pteroic acid Clausen & Kaas, Fraum, Denmark
Fmoc-N-amido-dPEG®24-acid Quanta Biodesign, Powell, Ohio
Succinoyl-tetraethylenpentamine (Stp) In-house synthesis¹⁴⁰

Reagents:

1 M ammonium hydroxide solution Roth, Karlsruhe, Germany
Diisopropylethylamin (DIPEA) Iris Biotech, Marktredwitz, Germany
Hydrazine monohydrate Iris Biotech, Marktredwitz, Germany
1-Hydroxybenzotriazol Hydrat (HoBt) Sigma-Aldrich, Steinheim, Germany
Ninhydrine Sigma-Aldrich, Steinheim, Germany
Phenol Sigma-Aldrich, Steinheim, Germany
Piperidine Sigma-Aldrich, Steinheim, Germany
PyBop® MultiSynthech, Witten, Germany
Pyridine Sigma-Aldrich, Steinheim, Germany

2.1.5 siRNAs

Table 2.1 Used siRNA molecules. Small letters: 2'-methoxy-RNA, s: phosphorothioate. These nucleic acids were synthesized by the Roche Kulmbach GmbH (now Axolabs GmbH, Kulmbach, Germany).

siRNA	target	label	sequence
siGFP	eGFP-Luc	---	AuAucAuGGccGAcAAGcAdTsdT UGCUUGUCGGCcAUGAuAUdTsdT
siCtrl	---	---	AuGuAuuGGccuGuAuuAGdTsdT CuAAuAcAGGCcAAuAcAUdTsdT
siAHA1-Cy7	AHA1*	Cy7	GGAuGAAGuGGAGAuuuAGudTsdT (Cy7)(NHC ₆)ACuAAUCUCcACUUCAUCCdTsdT
C ₆ -ss-C ₆ -siGFP	eGFP-Luc	---	(C ₆ SSC ₆)AuAucAuGGccGAcAAGcAdTsdT UGCUUGUCGGCcAUGAuAUdTsdT
C ₆ -ss-C ₆ -siCtrl	---	---	(C ₆ SSC ₆)AuGuAuuGGccuGuAuuAGdTsdT CuAAuAcAGGCcAAuAcAUdTsdT
C ₆ -ss-C ₆ -siEG5	EG5 / KSP	---	(C ₆ SSC ₆)ucGAGAAucuAAAcuAAcudTsdT AGUuAGUuAGAUUCUGAdTsdT
C ₆ -ss-C ₆ -siAHA1-Cy5	AHA1*	Cy5	(C ₆ SSC ₆)GGAuGAAGuGGAGAuuuAGudTsdT (Cy5)(NHC ₆)ACuAAUCUCcACUUCAUCCdTsdT
Hexynyl-ss-C ₆ -siGFP	eGFP-Luc	---	(Hexynyl)(C ₆ SSC ₆)AuAucAuGGccGAcAAGcAdTsdT UGCUUGUCGGCcAUGAuAUdTsdT
Hexynyl-ss-C ₆ -siCtrl	---	---	(Hexynyl)(C ₆ SSC ₆)AuGuAuuGGccuGuAuuAGdTsdT CuAAuAcAGGCcAAuAcAUdTsdT
Hexynyl-ss-C ₆ -siAHA1-Cy5	AHA1*	Cy5	(Hexynyl)(C ₆ SSC ₆)GGAuGAAGuGGAGAuuuAGudTsdT (Cy5)(NHC ₆)ACuAAUCUCcACUUCAUCCdTsdT

2.1.6 Polycations

Table 2.2 Used defined polycations.¹⁴⁰

polymer ID	structure	type	protonable amines	molecular weight [Da]
46	C-Stp ₃ -C-K-OleA ₂	i-shape	9	1695
49	C-Stp ₂ -K(K-OleA ₂)-Stp ₂ -C	t-shape	13	2095
76	C-Stp-K(K-OleA ₂)-Stp-C	t-shape	7	1552
229	C-Stp ₃ -C-K-LinA ₂	i-shape	9	1691
230	C-Gtp-Gtt-Stp-C-K-LinA ₂	i-shape	8	1676
386	C-Stp ₃ -K(Stp ₃ -C) ₂	three arm	27	2860

2.1.7 Peptides

Inf 7: H₂N-GLFEAIEGFIENGWEGMIDGWYGC-amide, Biosyntan (Berlin, Germany)

2.1.8 Cell culture

All cell culture consumables (dishes, well plates, t-flasks) were purchased from NUNC, Langensfeld, Germany) or TPP (Trasadingen, Switzerland). Growth media and additives (FCS, Glutamine, Penicillin/Streptomycin) were purchased from Invitrogen (Karlsruhe, Germany). Cells were ordered at the American Type Culture Collection (ATCC, Wesel, Germany). Used cell lines are listed in table 2.3.

Table 2.3 Used cell lines.

name	description	ATCC-Nr.	medium
Neuro2A	Wildtype murine neuroblastoma cells	CCL-131	DMEM
Neuro2A-Luc	Murine neuroblastoma cells expressing the eGFP-Luciferase fusion gene	---	DMEM
KB	Wildtype human nasopharyngeal epidermoid carcinoma cells	CCL-17	RPMI, w/o folic acid
KB-Luc	Human nasopharyngeal epidermoid carcinoma cells expressing the eGFP-Luciferase fusion gene	---	RPMI, w/o folic acid

2.2 Methods

2.2.1 Loading of a 2-chlorotrityl chloride resin

All chemical syntheses were performed using either a preloaded Wang-resin or 2-chlorotrityl chloride-resin (CTC-resin, 200-400 mesh, Iris Biotech, Marktredwitz). For stability reasons, the CTC-resin was loaded immediately prior to use.

The resin (1.56 mmol chloride/g) was swollen in anhydrous DCM for 10 min. 0.45 eq./g (150% of the desired loading) of the Fmoc protected amino acid per gram resin and DIPEA (0.9 eq./g) were dissolved in anhydrous DCM, added to the resin and mixed for 1 h. After coupling, a mixture of DCM/MeOH/DIPEA (80/15/5; v/v/v) was added for 30 min to cap residual reactive chloride groups.

To determine the resin loading, a small amount of resin (~5 mg) was washed twice with DCM and two times with n-hexane and dried under vacuo. 1 mg dry resin (triplicates) was mixed with 1 ml 20% (v/v) piperidine in DMF and incubated for 1 h. The cleaved Fmoc-protection group was quantified, measuring the adsorption at 301 nm. The loading was calculated using following equation:

$$\text{loading}[\text{mmol} / \text{g}] = \frac{1000 \times A_{301}}{m[\text{mg}] \times 7800 \times D}$$

where D is the dilution factor. After determination of the resin loading, the complete resin was incubated four times for 10 min with 20% (v/v) piperidine in DMF, washed three times with DMF, three times with DCM, three times with n-hexane and dried under vacuo.

2.2.2 General solid phase supported peptide synthesis procedure

Solid phase based peptide synthesis was used in this thesis to generate peptide ligands, defined carriers and targeted structures for siRNA delivery. Common Fmoc based synthesis first published by Merrifield *et al.*¹³⁷ was performed. As solid support either Wang- or 2-chlorotrityl chloride resin was used. The desired amount of resin was filled into a syringe reactor of appropriate size (2 mL, 5 mL, 10 mL, PP reactor with PE frit, Multisynthech, Witten, Germany) and fixed on a vacuum station. The general synthesis procedure was performed as described in table 2.4. After reaction and washing steps, solvents and non reacted reagents were removed by vacuum filtration.

Table 2.4 General synthesis protocol.

Step Nr.	Description	V [mL/g resin]	Time [min]
1	20% piperidine/DMF	10	4 x 10 min
2	DMF wash	10	5 x 1 min
3	AA/PyBop/HoBt/DIPEA 4/4/4/8 eq. In DMF/DCM (1/1)	10	1 x 60 min
4	DMF wash	10	5 x 1 min
5	DCM wash	10	5 x 1 min
6	Kaisertest	10	

2.2.3 Kaiser test

The Kaiser test was used as in process control to detect free amino groups on the resin and thus to determine if the attachment of a building block has been completed. For that purpose a few resin beads were taken out of the reactor, filled in an Eppendorf tube and washed three times with 1 mL methanol. After the solvent has been removed, 2 drops of each of the following solutions were filled into the reaction tube, 5% ninhydrine in EtOH (w/v), 80% phenol in EtOH (w/v) and KCN in pyridine (2 mL 0.001 M KCN in 98 mL pyridine). The mixture was incubated in a heating block at 100°C for 4 min. An intense blue color indicated free amine residues.

2.2.4 Synthesis of FoIA-PEG₂₄-K-(Stp₄-C)₂ and its analogues

After swelling Cys(Trt)-NH₂ loaded 2-chlorotriyl chloride resin (0.1 mmol, 0.35 mmol/g) in DCM for 30 min, the backbone was synthesized with succinoyl-tetraethylenpentamine (Stp) as building block. First 4 Stp units were attached, using the coupling conditions described under 2.5.2. After the Fmoc-protection group of the fourth Stp unit was cleaved, Dde-Lys(Fmoc)-OH was coupled as branching domain. The coupling of 4 further Stp units was performed on the lysine side chain, using

standard reaction conditions. After removal of the last Fmoc-protection group Boc-Cys(Trt)-OH was attached as last amino acid to finish the backbone HO-C(Trt)-Stp₄-K(Stp₄-C(Trt)-Boc)-Dde. The Dde protective group was removed with 2% hydrazine monohydrate in DMF (v/v) (10-30 times for 5 min) until no significant absorption at 300 nm was measurable in the supernatant of the deprotection mixture. In between the deprotection steps the resin was washed twice with DMF. Fmoc-PEG₂₄-OH dissolved in 1 mL DCM/DMF (1/1, v/v) was added under standard coupling conditions. The vessel was agitated until Kaiser test indicated complete conversion. After Fmoc cleavage, Fmoc-Glu(OH)-tBu and *N*¹⁰-(Trifluoroacetyl)pteroic acid were attached in additional steps. The resin was washed 5 times with DMF and 5 times with DCM, before the TFA group was removed, incubating the resin with 1 M ammonium hydroxide/DMF (1/1, v/v) four times for 30 min. In between the cleavage steps, the resin was washed with DCM. After completion of the reaction the resin was washed three times with DCM, three times with n-hexane and dried for 12 h over KOH in vacuo. The peptidic structure was cleaved of the resin by suspending it in a solution of TFA/H₂O/TIS (95.0/2.5/2.5, v/v/v) and incubated for 2 h. The cleavage solution was collected by filtration. To increase the yield, the resin was washed twice with TFA and once with DCM. After concentrating the flow-through by evaporation, the solution (approx. 1 mL) was dropped slowly in a 1/1 mixture (v/v, 40 ml) of cooled (0°C) MTBE and n-hexane. The resulting precipitate was centrifuged at 4°C for 10 min and 2000-3000 rpm. The solvents were decanted and the pellet was washed twice with ice-cold MTBE. The resulting pellet was dissolved in 50% (v/v) acetonitrile in water and lyophilized.

A structural analogue bearing serines instead of cysteines was synthesized in an analogues procedure using Ser(tBu)-NH₂ loaded CTC-resin. The backbone was terminated with Boc-Ser(tBu)-OH instead of Boc-Cys(Trt)-OH.

2.2.5 Synthesis of A-PEG₂₄-K-(Stp₄-C)₂ and its analogues

After swelling Ala-Fmoc loaded wang resin (0.1 mmol, 0.35 mmol/g) in DMF over night, the resin was washed 3 times with DCM. After removing the Fmoc protection group under standard conditions Fmoc-PEG₂₄-OH and Fmoc-Lys(Fmoc)-OH were attached consecutively using the under 2.2.2 described coupling procedure. After

subsequent removal of the protection group four Stp units were attached to each amine of the branching lysine. For this purpose the coupling protocol was modified. The used ratio of AA/PyBop/HOBt/DIPEA was set to 8/8/8/16 based on resin bound polymer, resulting in the common 4/4/4/8 ratio per free amine. After the Stp coupling step was repeated 4 times Boc-Cys(Trt)-OH was attached using the modified protocol to finish the synthesis. The resin was washed three times with DCM, three times with n-hexane and dried for 12 h in vacuo. To cleave the peptidic structure, the resin was suspended in a solution of TFA/H₂O/TIS (95.0/2.5/2.5, v/v/v) for 2 h. The cleavage solution was collected by filtration and the resin washed twice with TFA and once with DCM. After concentrating the product by evaporation, the solution (approx. 1 mL) was dropped slowly in a mixture of cooled (0°C) MTBE and n-hexane (1/1, v/v, 40 ml). The resulting precipitate was centrifuged at 4°C for 10 min (2000-3000 rpm). The solvents were decanted and the pellet was washed twice with ice-cold MTBE. The resulting precipitate was dissolved in 50% (v/v) acetonitrile in water and lyophilized. Structural analogues lacking the PEG chain were synthesized the same way.

2.2.6 Synthesis of FoIA-PEG₂₄-C

After swelling Cys(Trt)-NH₂ loaded 2-chlorotriyl chloride resin (0.1 mmol, 0.35 mmol/g) in DCM for 30 min, Fmoc-PEG₂₄-OH, Fmoc-Glu(OH)-tBu and N¹⁰-(Trifluoroacetyl)pteroic acid were attached consecutively, using the standard synthesis protocol. After washing the resin five times with DMF and five times with DCM, the TFA group was removed, incubating the resin with 1 M ammonium hydroxide solution/DMF (1/1, v/v) four times 30 min. In between the cleavage steps the resin was washed with DCM. After completion of the reaction the resin was washed three times with DCM, three times with n-hexane and dried for 12 h in vacuo. The peptidic structure was cleaved from the resin, suspending it in a solution of TFA/H₂O/TIS (92.5/2.5/2.5, v/v/v) for 2 h. The cleavage solution was collected by filtration and the resin washed twice with TFA and once with DCM. After concentrating the product by evaporation, the solution (approx. 1 mL) was dropped slowly in a 1/1 mixture (v/v, 40 ml) of cooled (0°C) MTBE and n-hexane. The resulting precipitate was centrifuged at 4°C for 10 min (2000-3000 rpm). The solvents were decanted and the

pellet was washed twice with ice-cold MTBE. The resulting pellet was dissolved in 50% (v/v) acetonitrile in water and lyophilized.

2.2.7 Synthesis of FoIA-PEG₂₄-Azide

After swelling (S)-5-Azido-2-(amino)pentanoic acid loaded 2-chlorotrityl chloride resin (0.1 mmol, 0.35 mmol/g) in DCM for 30 min, Fmoc-PEG₂₄-OH, Fmoc-Glu(OH)-tBu and *N*¹⁰-(Trifluoroacetyl)pteroic acid were attached consecutively, using the standard synthesis protocol described under 2.2.2. After washing the resin five times with DMF and five times with DCM, the TFA group was removed, incubating the resin with 1 M ammonium hydroxide solution/DMF (1/1, v/v) four times 30 min. In between the cleavage steps the resin was washed with DCM. After completion of the reaction the resin was washed three times with DCM, three times with n-hexane and dried for 12 h over KOH in vacuo. The peptidic structure was cleaved of the resin by suspending it in a solution of TFA/H₂O/TIS (95.0/2.5/2.5, v/v/v) for 2 h. The cleavage solution was collected by filtration and the resin washed twice with TFA and once with DCM. After concentrating the product by evaporation, the solution was dropped slowly in a 1/1 mixture (v/v, 40 ml) of cooled (0°C) MTBE and n-hexane. The resulting precipitate was centrifuged at 4°C for 10 min (2000-3000 rpm). The solvents were decanted and the pellet was washed twice with ice-cold MTBE. The resulting pellet was dissolved in 50% (v/v) acetonitrile in water and lyophilized.

The structural analogue PEG₂₄-Azide was synthesized the same way, cleaving the peptide off the resin after addition of Fmoc-PEG₂₄-OH and removing its protection group.

2.2.8 Synthesis of the endosomolytic Inf7-siRNA hybrid

For the synthesis of Inf7-siRNA, siRNA with a C₆-s-s-C₆ modification at the 5'-end of its sense strand was used. In a typical experiment 500 nmol siRNA was diluted in 400 µl water and incubated for 30 min with 10 eq. tris(2-carboxyethyl)phosphine (TCEP) to cleave the disulfide bridge and remove the protection group. To remove

TCEP and the cleaved C₆-SH fragment, the HS-C₆-siRNA was purified by ion exchange chromatography using a 1 mL ResourceQ column connected to an Äkta basic system, detecting at 260 nm. The column was equilibrated with buffer A containing 20 mM Hepes, 10 mM NaCl, pH 6.5, 30% (v/v) acetonitrile. Same buffer was used to load the sample onto this column. After the monitored detection wavelength had reached baseline, HS-C₆-siRNA was eluted, applying a sodium chloride gradient of 10 mM/min and a flow rate of 1 mL/min.

To enable the attachment of the Influenza peptide (Inf7, Sequence: H₂N-GLFEAIEGFIENGWEGMIDGWYGC-amide¹²³) *via* its free thiol group, the siRNA was activated using 20 eq. of 2,2'-dinitro-5,5'-dithio-dibenzoic acid (DTNB) diluted in 200 µL buffer containing 20 mM Hepes pH 8.0. The siRNA solution was added dropwise to avoid dimerization. After 30 min incubation the mixture was diluted 2:1 with buffer containing 20 mM Hepes, pH 6.5, 30% (v/v) acetonitrile. The resulting product (TNB-s-s-C₆-siRNA) was purified under the same conditions as described for HS-C₆-siRNA. Attachment of Inf7 was performed, mixing 1.5 eq. of the peptide, diluted in 500 µL 20 mM Hepes pH 8.5, 30% (v/v) acetonitrile with 1 eq. of the activated siRNA. After 2 h incubation at RT, the sample was diluted 2:1 with buffer A. Purification of the resulting Inf7-siRNA was performed on a 1 mL ResourceQ column connected to an Äkta basic system, detecting at 260 nm. The column was equilibrated with buffer A. Same buffer was used to load the sample onto this column. After the monitored detection wavelength had reached baseline, the column was washed using buffer A containing 200 mM NaCl. Inf7-siRNA was eluted setting a gradient of 10 mM NaCl/min and a flow rate of 1 mL/min. Resulting fractions (0.5 mL) were analyzed using analytical agarose gel electrophoresis. Samples containing gel-retarded siRNA compared to unmodified control were pooled. Concentration and buffer exchange for *in vivo* studies was performed, using a Centrifugal filter unit (Amicon Ultra, MWCO: 10000 Da, Millipore, Carrigtwohill, Ireland).

2.2.9 Synthesis of the nonreducible control Inf7-Mal-siRNA

For the synthesis of Inf7-Mal-siRNA, siRNA with a C₆-s-s-C₆ modification at the 5'-end of its sense strand was used. In a typical experiment 500 nmol siRNA was diluted in 400 µl water and incubated for 30 min with 10 eq. tris(2-carboxyethyl)phosphine

(TCEP) to cleave the disulfide bridge and remove the protection group. To remove TCEP and the cleaved C₆-SH fragment, the HS-C₆-siRNA was purified by ion exchange chromatography using a 1 mL ResourceQ column connected to an Äkta basic system, detecting at 260 nm. The column was equilibrated with buffer A containing 20 mM Hepes, 10 mM NaCl, pH 7.4, 30% (v/v) acetonitrile. Same buffer was used to load the sample onto this column. After the monitored detection wavelength had reached baseline, HS-C₆-siRNA was eluted, applying a sodium chloride gradient of 10 mM/min and a flow rate of 1 mL/min.

To connect the thiol modified siRNA with the thiol modified Inf7 peptide by a noncleavable linkage, the linker bis-maleimide-PEG₂ (BM-PEG₂, Thermo Scientific, Rockford, IL) was used. 3.1 mg linker (20 fold excess per HS-C₆-siRNA) was dissolved in 500 µl DMSO and mixed with the purified, deprotected siRNA. After 30 min incubation at RT, the resulting product (Mal-s-C₆-siRNA) was purified under same conditions as described for HS-C₆-siRNA. Attachment of Inf7 was performed, mixing 1.5 eq. of the peptide, diluted in 500 µL 20 mM Hepes pH 8.5, 30% (v/v) acetonitrile with 1 eq. of the activated siRNA. After 2 h incubation at RT, the sample was diluted 2:1 with buffer A. Purification of the resulting Inf7-Mal-siRNA was performed on a 1 mL ResourceQ column connected to an Äkta basic system, detecting at 260 nm. The column was equilibrated with buffer A. Same buffer was used to load the sample onto this column. After the monitored detection wavelength had reached baseline, the column was washed using buffer A containing 200 mM NaCl. Inf7-Mal-siRNA was eluted, setting a gradient of 10 mM NaCl/min and a flow rate of 1 mL/min. Resulting fractions (0.5 mL) were analyzed using analytical agarose gel electrophoresis. Samples containing gel-retarded siRNA compared to unmodified control were pooled.

2.2.10 Synthesis of the targeted FoliA-PEG₂₄-ss-siRNA hybrid

For the synthesis of FoliA-PEG₂₄-ss-siRNA, siRNA with a C₆-s-s-C₆ modification at the 5'-end of its sense strand was used. In a typical experiment 500 nmol siRNA was diluted in 400 µl water and incubated for 30 min with 10 eq. tris(2-carboxyethyl)phosphine (TCEP) to cleave the disulfide bridge and remove the protection group. To remove TCEP and the cleaved C₆-SH fragment, the

HS-C₆-siRNA was purified by ion exchange chromatography using a 1 mL ResourceQ column connected to an Äkta basic system, detecting at 260 nm. The column was equilibrated with buffer A containing 20 mM Hepes, 10 mM NaCl, pH 6.5, 30% (v/v) acetonitrile. Same buffer was used to load the sample onto this column. After the monitored detection wavelength had reached baseline, impurities were eluted using buffer A containing 200 mM NaCl. The elution of the product HS-C₆-siRNA was performed applying a sodium chloride gradient of 10 mM/min and a flow rate of 1 mL/min.

To enable the attachment of the targeting structure *via* its free thiol group, the siRNA was activated using 20 eq. of 2,2'-Dinitro-5,5'-dithio-dibenzoic acid (DTNB) diluted in 200 µL buffer containing 20 mM Hepes pH 8.0. The siRNA solution was added dropwise to avoid dimerization. After 30 min incubation the mixture was diluted 2:1 with buffer containing 20 mM Hepes, 30% (v/v) acetonitrile. The resulting product (TNB-s-s-C₆-siRNA) was purified under the same conditions as described for HS-C₆-siRNA. Attachment of FoIA-PEG₂₄-C was performed, mixing 1.5 eq. of the peptide, diluted in 500 µL 20 mM Hepes pH 8.5, 30% (v/v) acetonitrile with 1 eq. of the activated siRNA. After 2 h incubation at RT, the sample was diluted 2:1 with buffer A. Purification of the resulting FoIA-PEG₂₄-s-s-siRNA was performed on a 1 mL ResourceQ column connected to an Äkta basic system, detecting at 260 nm. The column was equilibrated with buffer A. Same buffer was used to load the sample onto this column. After the monitored detection wavelength had reached baseline, the column was washed using buffer A containing 200 mM NaCl. siRNA was eluted setting a gradient of 10 mM NaCl/min and a flow rate of 1 mL/min. Resulting fractions (0.5 mL) were analyzed using analytical agarose gel electrophoresis. Samples containing gel-retarded siRNA compared to unmodified control were pooled.

2.2.11 Synthesis of siRNA hybrids *via* copper(I) catalyzed 1,3-dipolar cycloaddition

To enable the attachment of a targeting structure *via* copper(I) catalyzed 1,3-dipolar cycloaddition, siRNA modified with a hexynyl-ss-C₆-linker at the 5'-end of its sense strand was used. In a typical experiment 74 nmol siRNA dissolved in 100 µL H₂O was mixed with 296 nmol FoIA-PEG₂₄-Azide in 300 µL DMSO/tertiary butanol (3/1; v/v) and

60 μ L TBTA/CuBr solution (0.1 M TBTA/0.1 M CuBr 2/1 (v/v) each in DMSO/tertiary butanol (3/1 (v/v)) and incubated for 3 h at 37°C under constant shaking. To remove precipitates, the solution was diluted with 1.5 mL buffer A (20 mM Hepes, pH 6.5, 30% acetonitrile) and centrifuged for 5 min at 13000 rpm. The reaction product was purified using a 1 mL ResourceQ column connected to an Äkta basic system, detecting at 260 nm. The column was equilibrated with buffer A containing 20 mM Hepes, 10 mM NaCl, pH 6.5, 30% (v/v) acetonitrile. Same buffer was used to load the sample onto this column. After the monitored detection wavelength had reached baseline, the column was washed using buffer A containing 200 mM NaCl. FoIA-PEG₂₄-click-siRNA was eluted setting a gradient of 10 mM NaCl/min and a flow rate of 1 mL/min. Resulting fractions (0.5 mL) were analyzed using analytical agarose gel electrophoresis. Samples containing gel-retarded siRNA compared to unmodified control were pooled.

2.2.12 Analytical RP-HPLC

The quantitative analysis of the peptide synthesis products was performed using reverse phase high pressure liquid chromatography (RP-HPLC). The used system was a Waters 600 controller connected to a Waters 717plus Autosampler and a Waters 996 Photodiode Array Detector under control of the Millennium software. As analytical column a SunfireTM C18 (5 μ m, 4.6 x 150 mm, Waters, Milford, MA) was used.

In a standard procedure the product was diluted using either water containing 0.1% (v/v) TFA or a mixture of water and acetonitrile (1/1, v/v) containing 0.1% (v/v) TFA to a concentration of 1 mg/mL. 30 μ L of this solution was loaded onto the column using a water/acetonitrile (0.1% (v/v) TFA) mixture of 95/5 (v/v) and a flow of 1 mL/min for 5 min. The product was eluted using a water/acetonitrile gradient from 95/5 (v/v) to 0/100 (v/v) in 20 min. The spectra of detected wavelength ranged between 200 and 800 nm.

2.2.13 MALDI-TOF-MS analysis

2.2.13.1 For peptidic structures

1 mg peptidic structure was dissolved in 1 mL H₂O 0.1% (v/v) TFA. 4 µL of this solution as spotted on a 4 µL matrix droplet consisting of a saturated solution of 2,5-dihydroxybenzoic acid (DHB) in 50% (v/v) acetonitrile containing 0.1% (v/v) TFA. Samples were analyzed using an Autoflex II mass spectrometer (Bruker Daltonics, Bremen, Germany). 50 – 100 spectra of respective probes were averaged for one sample spectrum.

2.2.13.2 For siRNA hybrids

After purification by ion exchange chromatography (see synthesis) the samples were diluted in buffer containing 20 mM Hepes, 500 mM NaCl and 30% (v/v) acetonitrile. As ions decrease the quality of a MALDI spectrum the samples were desalted by dialysis. For that purpose a 5 µl sample droplet was placed on an ultrafiltration membrane (0.2 µm, Millipore, Schwalbach, Germany) swimming in a petri dish filled with water. After 2 h incubation 4 µL of the dialyzed solution was spotted on a 4 µL matrix droplet consisting of a saturated solution of 3-hydroxy picolinic acid (HPA) in 50% (v/v) acetonitrile. Samples were analyzed using an Autoflex II mass spectrometer (Bruker Daltonics, Bremen, Germany). 50 – 100 spectra of respective probes were averaged for one sample spectrum.

2.2.14 ¹H-NMR

The ¹H-NMR spectra were recorded using a JNMR-GX (400 MHz, Joel) with a coupling constant of 0.3 Hz. For the measurement 10-15 mg sample was diluted in deuterated water. Spectra were analyzed using the NMR software MestreNova (MestreLab research).

2.2.15 Analytical agarose gel electrophoresis

The analytical agarose gel electrophoresis was used to analyze fractions of the ion exchange based siRNA-conjugate purification. As the chromatogram always showed different peaks with absorption at 260 nm, product containing fractions were determined by gel electrophoresis.

The analysis was performed using a 2.5% (w/v) agarose gel in TBE buffer (800 mM Tris, 3.8 M boric acid, 2 mM EDTA). For staining GelRed (Biotium Inc., Hayward, CA) was added to the liquid gel. Standard volumes of 3 μ L per fraction of the ion exchange purification were mixed with 7 μ L water, 5 μ L loading dye (30% glycerol, 0.25% bromphenol blue in water) and loaded onto the gel. The electrophoresis was performed using an electric tension of 100 V for 100 min.

2.2.16 Particle formation

Polyplexes for *in vitro* experiments were formed as follows: 270 ng siRNA (free or conjugated) was diluted in 10 μ L HBG (20 mM Hepes, 5% (v/v) glucose pH 7.4). The desired amount of polymer, calculated as protonable polymer nitrogen / siRNA phosphate (N/P 3, 6, 12, 16, 20, 40) was diluted in 10 μ L HBG in a separate Eppendorf tube. The polycation solution was mixed with the siRNA solution rapidly by pipetting up and down 5-10 times. For polyplex formation the mixture was incubated for 40 min at RT.

For *in vivo* experiments, 50 μ g siRNA (free or conjugated) as well as the desired amount of polymer were diluted separately in 125 μ L HBG for intravenous injection or 25 μ L for intratumoral injection. After mixing the solutions rapidly, it was incubated at RT for 40 min to form polyplexes.

2.2.17 Gel migration assay

The gel migration assay was performed to determine the particle formation ability of polymers and siRNA. Due to ionic interactions between siRNA and polymer, the

nucleic acid is encapsulated in polyplexes. The loss of free negative charge and the increased size of the particle in comparison to free siRNA hampers its migration into the agarose gel. Thus hampered migration is a signal for interactions between nucleic acid and polymer.

The assay was performed in a 2.0% (w/v) agarose gel in TBE buffer (800 mM Tris, 3.8 M boric acid, 2 mM EDTA). For staining GelRed (Biotium Inc., Hayward, CA) was added to the liquid gel. Polyplexes were formed under *in vitro* conditions as described under 2.2.16. After incubation for 40 min and gentle addition of 5 μ L loading buffer (30% (w/v) glycerol, 0.25% (w/v) bromophenol blue in water) the samples were filled into the pockets of the agarose gel. Gel electrophoresis was performed using an electric tension of 80 V for 60 min.

2.2.18 Size measurement

2.2.18.1 Laser light scattering

The particle size of polyplexes with a diameter above 10 nm were measured by laser-light scattering using a Zetasizer Nano ZS (Malvern Instruments, Worcestershire, U.K.). Polyplexes were formed under *in vitro* or *in vivo* conditions as described under 2.2.16 with following modification: To achieve results the amount of siRNA polymer and buffer was increased by the same factor to result in 10 μ g siRNA. After polyplex formation the solution was gently filled up to 1 mL with 20 mM HEPES, pH 7.4 before measurement. Average values were calculated with the data of 10 runs with standard deviations. Three experimental replicates were measured.

2.2.18.2 Fluorescence correlation spectroscopy (FCS)

The particle size of polyplexes with a diameter below 10 nm were measured by fluorescence correlation spectroscopy (FCS) using an Axiovert 200 microscope with a ConfoCor2 unit (Carl Zeiss, Jena, Germany). A HeNe laser (633 nm, average power

of 50 μ W at the sample) was used for excitation. The objective was a 40x (NA = 1.2) water immersion approachmate (Carl Zeiss, Jena, Germany).

Particles were formed under *in vitro* or *in vivo* conditions as described under 2.2.16 in a volume of 10 μ L HBG with a final concentration of 14.8 μ M siRNA, including 50 nM Cy5 labelled Inf7-siRNA at indicated N/P ratios. After polyplex formation the particles were gently filled up with 200 μ L HBG, transferred to a eight well LabTek chamber slide (NUNC, Wiesbaden, Germany) for measurement. Three experimental replicates were measured. These measurements were performed together with Christina Troiber.

2.2.19 Zeta potential measurement

The measurement of the zeta potential is a method to determine the surface charge of a particle or polyplex. Polyplexes were formed under *in vitro* or *in vivo* conditions as described under 2.2.16 with following modification: To achieve results the amount of siRNA, polymer and buffer was increased by the same factor to result in 10 μ g siRNA. After polyplex formation for 40 min, the solution was gently filled up to 1 mL with 20 mM HEPES, 1 mM NaCl, pH 7.4. The zeta potential was measured using a Zetasizer Nano ZS (Malvern instruments, Worcestershire, U.K.). Average values were calculated with the data of 10 runs with standard deviations. Three experimental replicates were measured.

2.2.20 Erythrocyte leakage assay

In the erythrocyte leakage assay the membrane disruptive activity of compounds was explored. For this purpose erythrocytes were chosen as model structure. Disruption of the membrane leads to a release of hemoglobin, which can be measured at absorption of 405 nm. In relation to an untreated control and complete lysed cells, the relative lytic activity of a compound can be quantified.

For this purpose fresh citrate treated murine blood was washed with phosphate buffer saline (PBS) and centrifuged at 800 g and 4°C for 10 min. This procedure was

repeated until the supernatant showed no red appearance. After decanting the buffer, the erythrocytes were counted and diluted in three different samples with PBS pH 7.4, pH 6.5 or pH 5.0 to a concentration of 5×10^7 erythrocytes/mL. The tested structure (peptide or siRNA-conjugate) was diluted to a concentration of 10 μ M using PBS buffer pH 7.4, pH 6.5 or pH 5.0. 75 μ L erythrocyte solution was mixed with 75 μ L structure containing solution in a well of a 96-well V-bottom plate (NUNC, Roskilde, Denmark) and incubated at 37°C for 60 min. All mixtures were prepared in triplicate for all three pH ratios. As negative control 75 μ L cells were mixed with 75 μ L PBS buffer, as positive control 75 μ L 1% (w/v) Triton X-100 at indicated pH ratios was used. After incubation, intact and lysed blood cells were removed by centrifugation at 800 g and 4°C for 10 min, 80 μ L of the supernatant was transferred into a new 96-well plate (TPP 96F, Trasadingen, Switzerland). The amount of released haemoglobin was determined, measuring the absorption at 405 nm in a microplate reader (Spectrafluor Plus, Tecan Austria GmbH, Grödig, Austria). Three experimental replicates were measured. The lysis of erythrocytes was calculated in relation to 100% lysis (Triton X-100 treated erythrocytes) and 0% lysis (buffer treated erythrocytes).

2.2.21 Fluorescence microscopy

For the qualitative analysis of siRNA uptake, KB cells or Neuro2A cells were seeded into 8 well LabTek chamber slides (NUNC, Wiesbaden, Germany), at a density of 2×10^4 cells/well. After 24 h, culture medium was replaced with 240 μ L fresh growth medium.

For the uptake of targeted siRNA 1.5 μ g Cy5-labeled nucleic acid was dissolved in 60 μ L HBG, added to each well of the chamber slides and incubated for thirty minutes at 37°C. For the uptake of targeted polyplexes, polyplexes were formed under *in vitro* conditions as explained under 2.2.16 using 200 ng Cy5-labeled siRNA. After polyplex formation for 40 min the complexes were added to each well of the chamber slides and incubated for 30 min at 37°C.

After treatment, cells were washed twice with 500 μ L PBS. To stain nuclei, Hoechst 33342 dye (Thermo scientific, Rockford, IL) was added. Cellular uptake was assayed by excitation of Cy5 at 635 nm and detection of emission at 665 nm. A Zeiss Axiovert

200 fluorescence microscope was used to collect the images. Data were analyzed and processed by AxioVision LE™ software.

2.2.22 Flow cytometric analysis

Fluorescence microscopy was used during this thesis for qualitative determination of cell association and cellular uptake of targeted structures and polymers.

Cells were seeded into 24-well plates at a density of 5×10^4 cells/well. After 24 h, culture medium was replaced by 400 μ L fresh growth medium. Targeted polyplexes or targeted siRNA conjugates (using Cy5 labelled siRNA) were added to each well at a siRNA concentration of 200 nM. After incubated at 37°C for 30 min, cells were washed twice with PBS, detached with trypsin/EDTA and taken up in PBS containing 10% (v/v) FCS. Flow cytometry was performed using a Cyan™ ADP flow cytometer (Dako, Hamburg, Germany). Cellular uptake was assayed by excitation of Cy5 at 635 nm and detection of emission at 665 nm. To discriminate between viable and dead cells, cells were appropriately gated by forward/sideward scatter and pulse width and counterstained with DAPI. 1×10^4 gated events per sample were collected. Data were recorded by Summit software (Summit, Jamesville, NY, USA) and evaluated by FlowJo® software.

2.2.23 Reporter gene silencing

To demonstrate RNAi mediated gene silencing, cell lines stably expressing the fusiogenic protein eGFP-Luciferase (composed of eGFP and Luciferase) were used. In this thesis siRNA directed against eGFP has been transfected. As this siRNA leads to the down regulation of the fusiogenic protein, luciferase activity could be used for read out. For detection of unspecific silencing effects due to cross reactivity of siRNA or toxicity of the carrier system a non-targeting control sequence siCtrl has been tested in comparison under same conditions.

In a typical experiment 5×10^3 cells in 100 μ L medium were seeded in a well of a 96 well plate (TPP, Trasadingen, Switzerland). After incubation for 24 h at 37°C and 5%

CO₂ the medium was replaced by 80 µL fresh culture medium. Polyplexes were formed as explained under 2.2.16 and added to the well. Each polymer nitrogen to siRNA phosphate (N/P) ratio has been tested in triplicate. For targeted delivery, the medium containing polyplexes was replaced by fresh culture medium after 30 min at 37°C and 5% CO₂. For reporter gene silencing cells were incubated for additional 48 h at 37°C and 5% CO₂. To quantify the knockdown of the eGFP-Luciferase fusion protein, the medium was removed, replaced by lysis buffer (Promega, Mannheim, Germany) and incubated for 30 min at RT. The luciferase activity in the cell lysate was measured using a luminometer (Lumat LB9507 instrument, Berthold, Bad Wildbad, Germany). Luciferase light units were detected from 35 µL cell lysate and 10 s integration after injection of luciferin. Silencing efficiency was evaluated as percent of reduced luciferase activity compared to HBG treated cells. Three experimental replicates were measured.

2.2.24 Endogenous target silencing

To study the effectiveness of the tested carrier systems, besides the highly upregulated artificial transgene eGFP-Luciferase, an endogenous target was used to perform silencing experiments. As candidate the kinesin spindle protein (KSP, EG5) was chosen. As reported by Judge *et al.*¹⁴¹ the silencing of this gene leads to a characteristic mitotic figure formation, called 'aster'.

In a typical experiment 1×10^4 cells in 200 µL medium were seeded in a well of an eight well LabTek chamber slide (NUNC, Wiesbaden, Germany). After incubation for 24 h at 37°C and 5% CO₂ the medium was replaced by 180 µL fresh culture medium. Polyplexes containing 1 µg siRNA were mixed as described under 2.2.16 at N/P 16 and added to the well. After 30 min incubation medium containing polyplexes was replaced by fresh culture medium. After 24 h medium was removed, cells washed five times with 200 µL PBS and fixed with a 4% paraformaldehyde solution. After staining nuclei with DAPI, aster formation was determined, using a Zeiss Axiovert 200 (fluorescence microscope, Carl Zeiss AG, Germany).

2.2.25 Reporter gene expression

For testing certain characteristics (e.g. targeting ability) of the siRNA carrier systems, DNA was chosen as model cargo in certain settings, due to similar characteristics, a comparable delivery route and a more sensitive read out. As cargo gene, luciferase encoded in a plasmid (pCMVLuc, Plasmid Factory, Bielefeld, Germany) was chosen. In a typical experimental setting 1×10^4 cells in 100 μL culture medium were seeded per well of a 96-well plate (TPP, Trasadingen, Switzerland). After incubation for 24 h at 37°C and 5% CO_2 , medium was exchanged against 80 μL fresh culture medium. Polyplexes were prepared as followed. 200 ng pDNA in 10 μL HBG and polymer at different nitrogen to phosphate (N/P) ratios in 10 μL HBG were mixed by pipetting. After incubation for 30 min the 20 μL polyplex solution was added to the cells. Polyplexes were removed by medium exchange after 30 min and replaced by 90 μL fresh medium and 10 μL PBS containing 10 μM chloroquine when indicated. 24 h after transfection, medium was replaced by 100 μL lysis buffer (Promega, Mannheim, Germany). After 30 min incubation at RT the luciferase activity was determined analyzing 35 μL of the lysate in a luminometer (Lumat LB9507 instrument, Berthold, Bad Wildbad, Germany). Luciferase light units were recorded from a 10 s integration time after luciferin injection. The transfection efficiency was evaluated as relative light units (RLU) per 10000 seeded cells.

2.2.26 *In vivo* assays

In vivo assays in mice were performed by Laura Schreiner and Daniel Edinger, therefore will be described in detail in their PhD theses (in preparation). As key results proofing special characteristic of the carriers are presented here as well, used methods are listed in the following section.

2.2.26.1 Near infrared imaging of siRNA distribution

5×10^6 KB cells were injected subcutaneously in the neck of female Rj:NMRI-nu (nu/nu) mice (Janvier, Le Genest-St-Isle, France). After tumors reached a size of 100 mm^3 , polyplexes containing $50 \mu\text{g}$ Cy7 labelled siRNA at N/P ratio of 16 in $50 \mu\text{L}$ (intratumoral injection) or $250 \mu\text{L}$ (intravenous injection) HBG were injected. Detection was performed using an IVIS Lumina system with Living Image software 3.2 (Caliper Life Sciences, Hopkinton, USA).

2.2.26.2 Determination of silencing efficiency by aster formation

5×10^6 KB cells were injected subcutaneously in the neck of female Rj:NMRI-nu (nu/nu) mice (Janvier, Le Genest-St-Isle, France). After tumors reached a size of 100 mm^3 , polyplexes containing $50 \mu\text{g}$ Inf7-siRNA at N/P ratio of 16 in $50 \mu\text{L}$ (intra tumoral injection) or $250 \mu\text{L}$ (intra venous injection) HBG were injected 48 h and 24 h prior to euthanasia. Tumors were harvested and either embedded in tissueTek, cut into $5 \mu\text{m}$ slices and stained with DAPI or fixed in formalin, embedded in paraffin, cut into $4.5 \mu\text{m}$ slices and stained by hematoxylin and eosin (HE) staining.

2.2.26.3 Urine analysis

4 h after systemic administration of siRNA polyplexes or free siRNA into female Rj:NMRI-nu (nu/nu) mice (see 2.26.1 and 2.26.2) urine was collected by punctation. Urine samples were analyzed by agarose gel electrophoresis without further dilution as described under 2.17. If indicated, $2 \mu\text{L}$ of a 0.5 M TCEP solution and $2 \mu\text{L}$ of a heparin solution were added.

3 Results

Aim of this thesis was the design of highly defined carrier systems for siRNA mediated gene silencing *in vitro* as well as *in vivo*. These carrier systems should contain functional substructures, addressing limitations during the delivery process. This includes stabilization in the extracellular environment, specific cell attachment followed by endocytosis, endosomal escape and release of the siRNA in the intracellular environment. In contrast to already existing, functional macromolecules these carrier systems should be synthetically defined, pure structures enabling a precise chemical analysis and the study of a clear structure activity relationship.

3.1 Enhancing endosomal escape by endosomolytic active siRNA conjugates

The endosomal escape is one of the major bottlenecks during the delivery process of siRNA *in vitro* as well as *in vivo*. Polyplexes that enter the cell *via* endocytosis have to escape out of the endosome to avoid lysosomal degradation. As described in chapter 1.4.2.4 many different strategies are known to enhance the endosomal escape. Incorporation of substructures with a high buffering capacity leads in example to a process called proton sponge effect. In contrast the introduction of certain peptides enhances the endosomal escape by active disruption of the endosomal membrane. The incorporation of endosomolytic activity to polyplexes and lipoplexes was mainly limited to covalent attachment of functional domains randomly to the delivery vehicle. This has two disadvantages: (i) The random attachment leads to an undefined product with a low reproducibility but more important (ii) the endosomal escape of siRNA, not the carrier polymer is critical for the delivery. The polymer might separate from siRNA before endosomal entry / escape. Thus this strategy leads to a new limitation for endosomal escape, the polyplex stability.

To overcome the hurdle of endosomal escape without generating new bottlenecks, it was hypothesized that the direct covalent attachment of a lytic peptide to the siRNA would enhance its activity due to a highly efficient endosomal escape. In the following chapter the synthesis of this peptide siRNA hybrid, its purification, analysis and biological evaluation is described.

3.1.1 Design and synthesis of an Inf7-siRNA hybrid

The modification of siRNA is difficult, because it can vary its recognition by the RISC complex and thus the silencing ability. The influence on the silencing efficiency is limited by different factors, including position, type and stability of attachment as well as the properties of the attached macromolecule. Thus it was decided to modify the siRNA at the 5'-end of its sense strand. This position was thought to be one of the least influencing positions regarding reduction of silencing activity. To further avoid an unexpected influence of the connected peptide on the siRNA, it was decided to conjugate it *via* a disulfide linkage. Disulfides are known to be cleaved under the reductive cytosolic environment, releasing an almost unmodified siRNA. Furthermore this linkage enables a simple synthesis and purification strategy. As lytic molecule Inf7, a peptide based on the amino-terminus of the influenza virus hemagglutinin was chosen. Its strong lytic activity, which is limited to the endosomal environment, is described in chapter 1.4.2.4.

As shown in Fig. 3.1, the synthesis of Inf7-siRNA was divided into three steps, each intermitted by a purification step. For conjugation, siRNA with a thiol modification at the 5'-end of its sense strand was chosen.

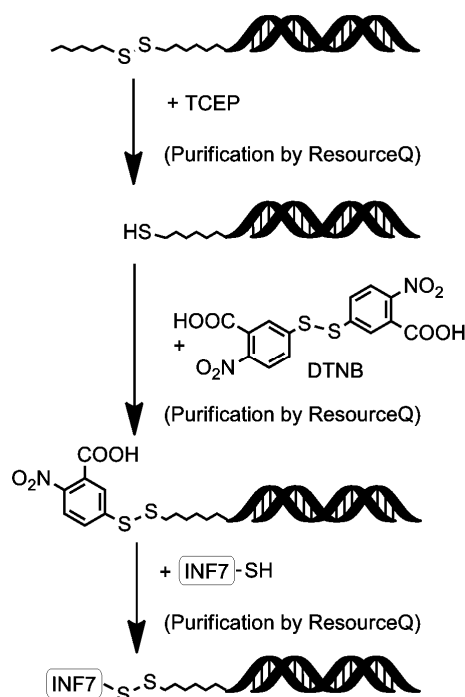


Fig. 3.1 Synthesis of the Inf7-siRNA hybrid. After deprotection of the thiol group and purification by ion exchange chromatography, the thiol bearing siRNA was activated with DTNB. Additional purification of the product allowed the defined attachment of the cysteine terminated influenza peptide *via* a disulfide bridge. DTNB: 5,5'-dithiobis-(2-nitrobenzoic acid); TCEP: (2-carboxyethyl)phosphine.

To avoid dimerization under storage conditions, the thiol group was protected as disulfide. Thus the first step was to deprotect the thiol group in a reductive environment using tris(2-carboxyethyl)phosphine (TCEP). To form new disulfide bridges, TCEP and the cleaved protective group were removed by ion exchange chromatography. The next step was the activation of the free thiol group to enhance the reactivity for disulfide formation with the peptidic cysteine. Thus the thiol bearing siRNA was incubated with 5,5'-dithiobis-(2-nitrobenzoic acid) (DTNB). After purification of the product by ion exchange chromatography, the last step was the conjugation of the influenza peptide (Inf7) *via* its thiol group at the C-terminal cysteine. After attachment, the product was purified by a last ion exchange chromatographic step. As shown in Fig. 3.2 a sodium chloride gradient was applied to separate the Inf7-siRNA hybrid from free unmodified siRNA. To evaluate synthesis and purification, 0.5 mL fractions were collected. Identification of fractions containing modified siRNA was performed by analysis *via* an agarose gel electrophoresis (Fig. 3.3).

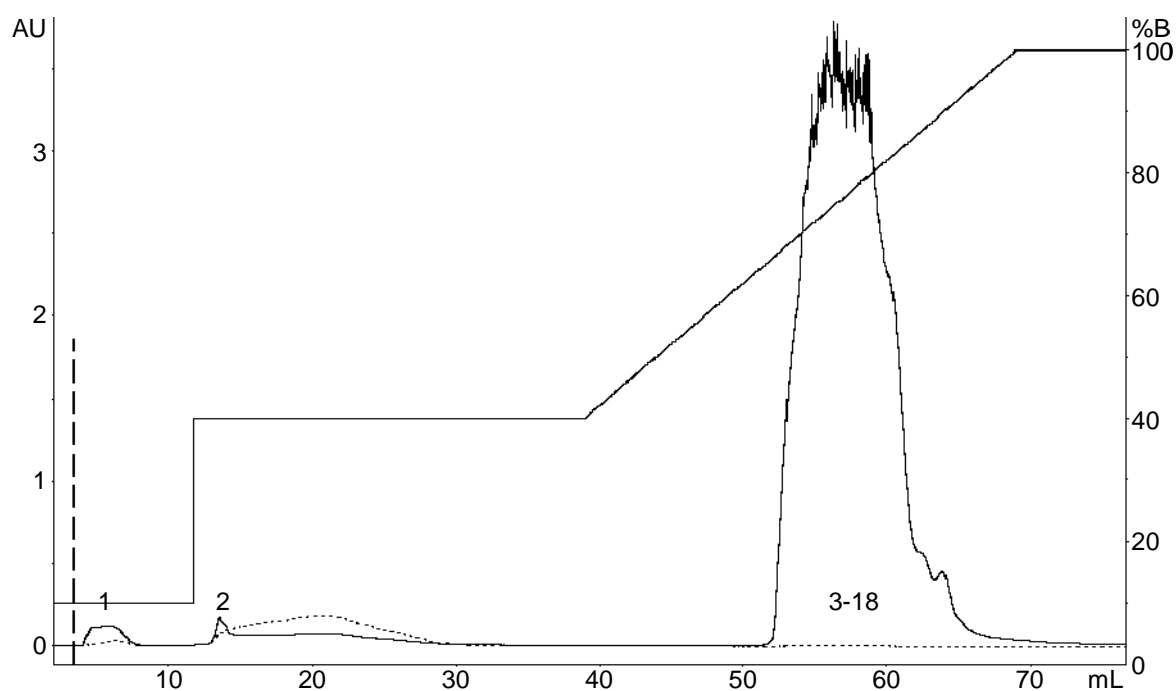


Fig. 3.2 Chromatogram of the ion exchange chromatographic purification of the Inf7-siRNA hybrid. After loading the sample onto a ResourceQ column using 20 mM Hepes, pH 6.5, 50 mM NaCl, 30% acetonitrile the column was washed with the same buffer containing 200 mM sodium chloride. Elution of the product was performed applying a gradient of 10 mM NaCl/min and a flow of 1 mL/min over 30 min. 1-18: collected fractions. Detection wavelength: 260 nm (black line), 412 nm (dashed line).



Fig. 3.3 Agarose gel analysis of the ion exchange chromatographic purification. Fractions, collected during ion exchange chromatographic purification of Inf7-siRNA were analyzed in a 2.5% agarose gel. 100 V were applied for 100 min. C: control (unmodified siRNA), 1-18: Fractions collected during purification.

The chromatogram (Fig. 3.2) shows, that different fractions with absorption at 260 nm elute during the purification process. One fraction during the column loading (fraction 1), one during the washing step with 20% buffer B (fraction 2) and one during the gradient (fractions 3-18). The analysis of the fractions in an agarose gel (Fig. 3.3) proved that the first two peaks do not contain detectable amounts of siRNA, while the fractions collected during the elution of the third peak (3-18) all contain siRNA. As can be seen in the agarose gel, this peak consists of two nucleic acid populations with different behaviour in gel migration. Fractions showing retardation compared to a control of unmodified siRNA were pooled (Fraction 5-9). To identify them as the expected product the sample was analyzed by MALDI-TOF-MS. A representative mass spectrum is shown in Fig. 3.4.

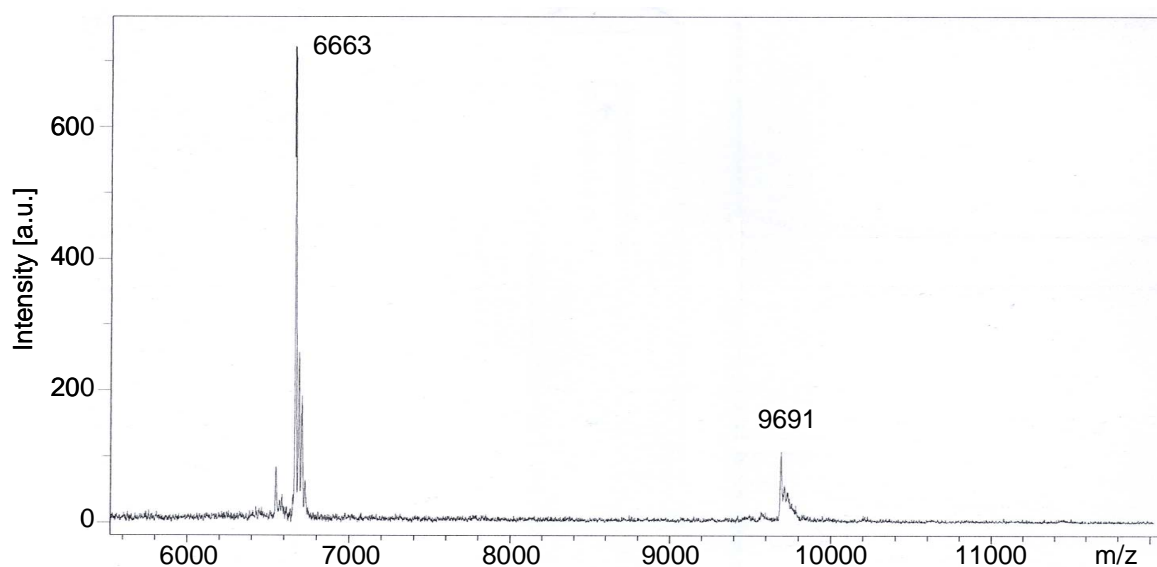


Fig. 3.4 MALDI-TOF-MS spectrum of Inf7-siGFP. After purification *via* ion exchange chromatography and analysis by agarose gel electrophoresis, the Inf7-siRNA conjugate was identified by mass spectrometry. m/z 6663: antisense strand (Calculated mass: 6668 Da); m/z 9691: Inf7-sense strand (Calculated mass: 9691). Used matrix: 3-hydroxypicolinic acid (HPA)

The mass spectrum reveals that the sample consists only of peptide modified siRNA. The two detected peak populations contain the mass peaks of the unmodified antisense strand (m/z 6663) and the peptide conjugated sense strand (m/z 9691). Additional signals arise from salts of the pure highly charged strands.

This synthesis has been performed with different siRNA sequences, depending on the use of the hybrid and the requested read out of the biological system. A complete listing of all synthesized structures is given in table 3.1.

Table 3.1 Overview of synthesized versions of Inf7-siRNA hybrids. Small letter: 2'-methoxy modified ribonucleic acids. Cy5: Cyanine 5.

description	target gene	label	sense strand (5'-3')/ antisense strand (5'-3')
Inf7-siGFP	eGFP-Luc	---	Inf7-SS-C ₆ -AuAucAuGGccGAcAAGcAdTsdT UGCUGUCGGCcAUGAuAUdTsdT
Inf7-siCtrl	---	---	Inf7-SS-C ₆ -AuGuAuuGGccuGuAuuAGdTsdT CuAAuAcAGGCcAAuAcAUdTsdT
Inf7-siEG5	EG5 / KSP	---	Inf7-SS-C ₆ -ucGAGAAucuAAAcuAAcudTsdT AGUuAGUUuAGAUUCUCGAdTsdT
Inf7-siAHA1-Cy5	AHA1	Cy5	Inf7-SS-C ₆ -GGAuGAAGuGGAGAuAGudTsdT (Cy5)ACuAAUCUCcACUUC AUCCdTsdT

The presented data show that the synthesis of a pure and defined Inf7-siRNA hybrid was performed. The synthesis was independent of the siRNA sequence and was reproducible as shown in table 3.1. Thus its functionality and behaviour in a biological environment had to be explored in further steps.

3.1.2 Functional evaluation of the Inf7-siRNA hybrid

Chapter 3.1.1 has proven that the synthesis of the Inf7-siRNA hybrid is possible. What remains unclear is the influence of the covalent attachment to the biological activity of its substructures. This is topic of the following chapter.

3.1.2.1 Influence of covalent siRNA attachment on the lytic activity of the influenza peptide

The biological function of the influenza peptide results from its strong, disruptive interaction with biological membranes. It had to be proven, that the attachment of a negatively charged siRNA with a more than five times higher molecular weight does not influence the interaction between membrane and peptide. Thus the lytic activity of the peptide-siRNA hybrid was compared to that of free peptide in an erythrocyte leakage assay. Erythrocytes were incubated at 37°C with either free Inf7 peptide or the peptide-siRNA hybrid under different pH conditions representing the intracellular- and cytosolic environment (pH 7.4), the endosomal environment (pH 5.5) and an intermediate pH (pH 6.5). Haemoglobin release as indicator for membrane disruption was measured. Results are shown in Fig. 3.5.

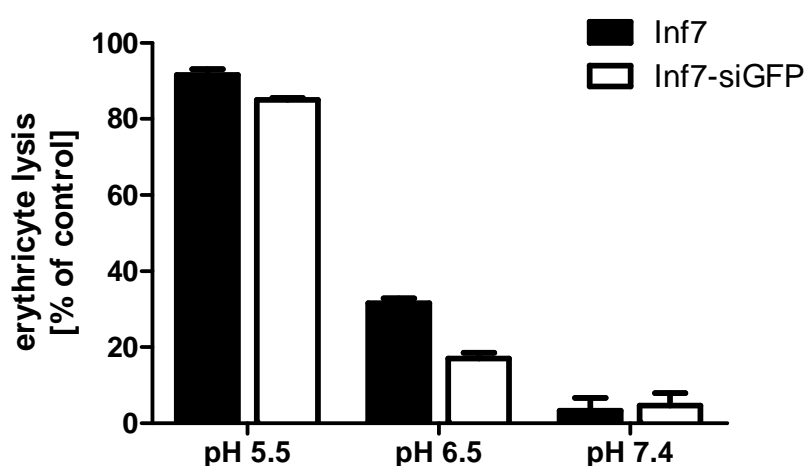


Fig. 3.5 Lytic activity of the Inf7-siRNA hybrid compared to free Inf7 peptide. Erythrocytes were incubated with 5 μ M free Inf7 peptide (black bars) or 5 μ M Inf7-siRNA conjugate (white bars) at indicated pH values. After incubation at 37°C for 60 min the haemoglobin release was determined. The data is presented as relative values compare to complete lysis by treatment with Triton X-100.

The activity of free Inf7 peptide at different pH values in the erythrocyte leakage assay shows, that its lytic force is pH dependent as described previously.¹²³ At pH 7.4 (extracellular and cytosolic pH) there is almost no free haemoglobin measurable (3%), indicating, that the peptide is inactive at this pH. At pH 6.5 32% free haemoglobin can be detected, while at the endosomal pH 5.5 more than 90% of the erythrocytes got lysed by the peptide. The lytic behaviour of Inf7-siRNA is comparable. While there is no lytic activity at pH 7.4 and an intermediate cell lysis at pH 6.5 (17%) the peptide-siRNA hybrid lyses 85% of the erythrocytes at pH 5.5.

This data demonstrates that the covalent attachment of siRNA to the influenza peptide does neither influence its lytic activity nor its pH specificity.

3.1.2.2 Influence of the covalent attachment of the influenza peptide on the activity of siRNA

The influence of the attachment of macromolecules to one or several ends of the siRNA strands on its knockdown efficiency has been investigated intensively.¹⁴² However results are contradictory. In summary one can say, that it strongly depends on the position and type of attachment as well as on the properties of the attached macromolecule, if and how much the siRNAs silencing activity is reduced. Designing the described system, it was decided to attach the peptide at the 5'-end of its sense strand *via* a disulfide linkage to avoid any influence of the attached peptide on the silencing ability. To explore the specific knockdown efficiency and toxicity of the peptide-siRNA conjugate, transfection experiments with defined cationic polymers, known to work very good for siRNA delivery were performed (**46**, **49** for structure see Materials and Methods section), comparing peptide conjugated siRNA with unconjugated siRNA (Fig. 3.6).

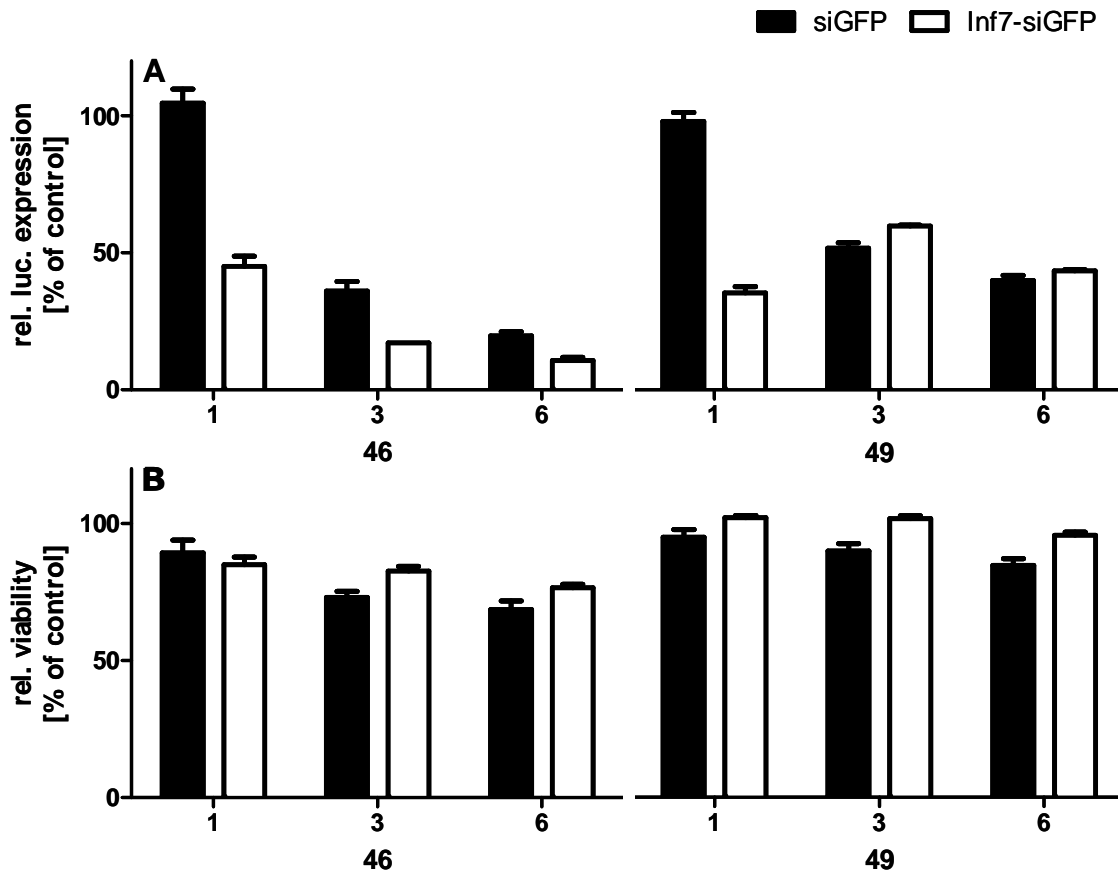


Fig. 3.6 Target gene silencing and toxicity of the Inf7-siRNA hybrid compared to free siRNA. Neuro2A cells stably expressing eGFP-Luciferase were transfected either with 400 nM unmodified siRNA (black bars) or 400 nM Inf7-siRNA hybrid (white bars). For transfection, polycation **46** and **49** were used at indicated N/P ratios (1-6). A: Determination of luciferase-activity; B: Determination of cell viability *via* MTT assay. Results are presented as relative values compared to HBG treated cells.

Transfecting Neuro2A cells with unmodified siRNA (siGFP) using polycation **46** and **49** led to a significant reporter gene knockdown at N/P ratios 3 and 6, while at N/P 1 the expression of the eGFP-Luciferase fusion protein remains unmodified. Regarding cell viability, no significant decrease could be observed. The use of peptide modified siRNA (Inf7-siGFP) led to comparable knockdown results for both polymers at N/P 3 and 6. At N/P 1 the silencing efficiency is even raised compared to unmodified siRNA. In both cases a knockdown to 40-50% of expression could be observed. In cell viability no significant differences were detectable (Fig. 3.6 B).

3.1.2.3 Influence of peptide conjugation on particle formation

Particle formation and stability are two important criteria in the design of carrier systems. During *in vitro* siRNA delivery but more important during *in vivo* delivery, the formed particles have to be stable to protect the siRNA and deliver the cargo to its target cell. The ability to form particles as well as its stability is mainly influenced by electrostatic interactions of polyanion and polycation. Thus modifications of one of these structures could have impact on the particles. To study the influence of the peptide modification of siRNA, its interactions with polycation **49** has been evaluated in a gel shift assay (Fig. 3.7).

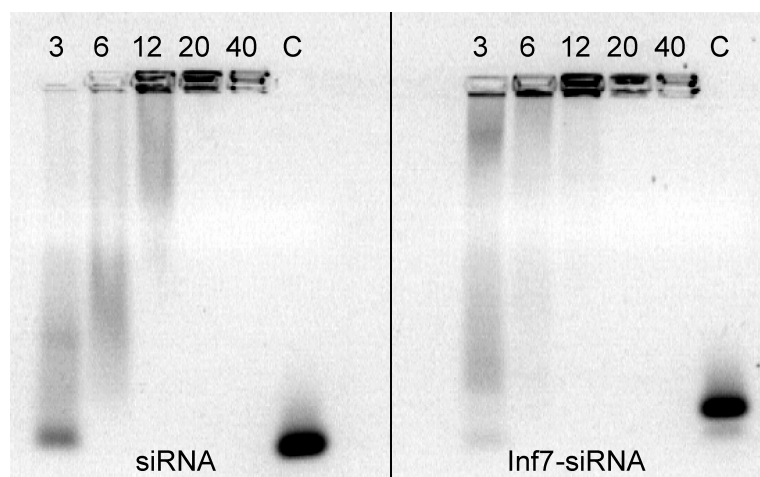


Fig. 3.7 Gel shift assay comparison of polyplex formation ability using siRNA and Inf7-siRNA containing particles. Polycation: **49**, 3-40: nitrogen to phosphate ratio for polyplex formation, C: control (siRNA without polymer).

For unconjugated siRNA the gel shift assay reveals that interactions with the polymer already take place at the lowest N/P ratio. Although just little amounts of completely free siRNA can be observed, most of the material is just slightly hampered to migrate into the gel. At N/P 20 and higher the migration is completely stopped. Inf7-siRNA shows a slightly altered behaviour in this assay. At N/P 3 the migration of the siRNA construct is also just partly influenced. In comparison to unconjugated siRNA, the interaction with the polycation seems to be stronger, because the complete inhibition of movement is already reached at an N/P ratio of 12.

The gel retardation assay just gives limited information of the interactions between both ionic components. It can just verify the impact of the polymer on the siRNA

migration. As a hampered migration can also result from strong aggregation, the particle size of polyplexes formed with modified and unmodified siRNA was compared by dynamic light scattering (DLS) to further explore the influence of the peptide (table 3.2).

The size measurements clearly show that the conjugated as well as the unconjugated siRNA form small defined particles with a diameter of ~17 nm at an N/P of 12 or higher. Both structures led to strong aggregation at N/P 3, making a size measurement impossible. The only difference could be observed at N/P 6. Unmodified siRNA forms particles with a diameter of 321 nm, while Inf7-siRNA based polyplexes have a diameter of 140 nm.

Table 3.2 Particle diameter of siRNA or Inf7-siRNA containing polyplexes measured by dynamic light scattering. N/P: nitrogen to phosphate ratio for polyplex formation, used polycation: **49**.

N/P	Particle diameter [nm]	
	siRNA	Inf7-siRNA
3	---	---
6	321 (\pm 112)	140 (\pm 26)
12	16 (\pm 3)	16 (\pm 2)
20	14 (\pm 2)	15 (\pm 2)
40	8 (\pm 1)	12 (\pm 2)

Summarizing these experiments, the particle formation of siRNA and polycation **49** is not negatively influenced by the attached peptide. Neither ionic interactions nor particle size is dramatically influenced by this structure.

3.1.3 Silencing activity of the Inf7-siRNA hybrid *in vitro*

The purpose of this system was to create siRNA that is independent of the endosomolytic activity of its carrier system. Thus the role of the delivery vehicle should be reduced to protection, particle formation and cell attachment followed by endocytosis. As it has been shown that the biological function of the siRNA as well as

of the peptide remains fully active, the modified siRNA was transfected with a defined polymer lacking efficient endosomal escape ability (**76**, Fig. 3.8).

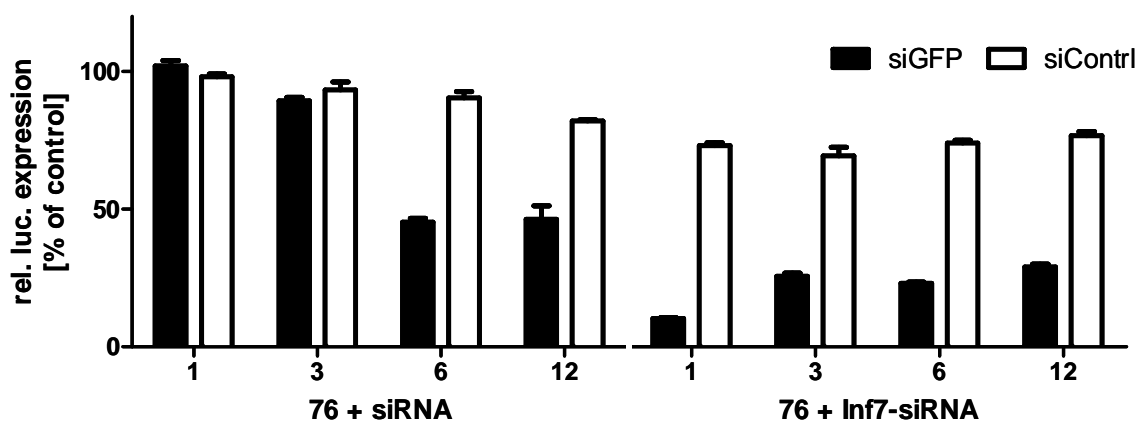


Fig. 3.8 Comparison of luciferase expression after transfection with siRNA and Inf7-siRNA using a polymer with low endosomal escape ability. Neuro2A cells stably expressing eGFP-Luciferase were transfected either with 400 nM Inf7-siRNA (right bars) or 400 nM unmodified siRNA (left bars) using polycation **76**. Luciferase expression was detected. The data is presented as relative values compared to HBG treated cells. The experiment was performed by Thomas Fröhlich as part of his PhD thesis (in preparation).

Transfection of Neuro2A cells stably expressing eGFP-Luciferase with unmodified siRNA using polymer **76** led to a specific knockdown of 50% luciferase expression only at N/P ratios 6 and 12 compared to control siRNA. At N/P 1 and 3 no significant knockdown could be detected. Transfecting the cells with conjugated siRNA resulted in a target gene silencing to ~20% in all N/P ratios. In contrast, conjugated control siRNA showed no knockdown, indicating that the gene silencing is specific.

Summarizing this chapter a defined pure hybrid of influenza peptide and siRNA was synthesized. The covalent attachment does neither influence the peptides lytic activity nor the siRNAs silencing ability. The combination of these two structures leads to a macromolecule that is able to overcome the limitation of endosomal escape independent of the endosome disruptive force of the polycationic carrier system.

3.2 Ligand mediated, targeted siRNA delivery

Overcoming bottlenecks in delivery is the main challenge developing efficient siRNA carrier systems. Beside the endosomal escape (chapter 3.1), specific cell targeting is one of the major limitations in this field. *In vitro* in general just one cell population is existent in one experimental setting. Thus transfecting just a certain subpopulation is no topic in *in vitro* cell culture. The situation changes *in vivo*. Polyplexes should be able to reach the targeted cell population after systemic injection, avoiding interactions with or transfection of other cell populations. Thus they need to be shielded for all cells, having a certain “homing structure” that identifies the addressed tissue or cell population.

In case of tumor homing, this can be done in two different ways: (i) accumulation of polyplexes by enhanced permeability and retention (EPR) effect or (ii) cell specific ligand based targeting. Both described in detail in chapter 1.4.2.3. Since the EPR effect is a more passive tissue targeting, the ligand based cell targeting is very specific. Special receptors are upregulated on certain cell populations while they are absent on other cells. These receptors can be addressed *via* the incorporation of a receptor ligand in the carrier system. If the receptor is internalized by endocytosis after ligand attachment, the whole polyplex enters the cell. In case of tumor targeting, significantly up regulated endocytosed receptors are the transferrin-, the epidermal growth factor- and the folic acid receptor (see chapter 1.4.2.3).

Incorporation of one of these targeting ligands into the carrier system was in common concepts realized by covalent attachment of the ligand to the polycationic backbone (in case of polyplexes) or to lipid structures (in case of lipoplexes and liposomes). This kind of attachment to overcome the hurdle of cell attachment and endocytosis leads to a new crucial limitation, the polyplex stability. As the siRNA is incorporated stable into the polyplex, it has excess to the ligands homing activity. If the polyplex is not stable enough, the siRNA is lost, due to loss of targeting. Especially the process of cell attachment could lead to the release of siRNA out of the polyplex, due to the highly negative charged cell surface.

Thus a more reasonable design of a carrier system would be the covalent attachment of a targeting ligand to the siRNA and its complexation with unmodified polycations. This strategy makes the tumor homing of the therapeutic siRNA independent of the stability of the polyplex although its protecting, stabilizing and endosomolytic effect

retains. In the following chapter, the design, synthesis, purification and biological evaluation of such a siRNA construct is described.

3.2.1 Design and synthesis of the FolicAcid-PEG₂₄-siRNA hybrid

The basic idea of this concept is the synthesis of defined structures. Thus it was decided to synthesis the targeting structure by common solid phase supported peptide synthesis (SPPS). This strategy, first published by Merrifield *et al.*,¹³⁷ enables the generation of highly defined macromolecules, using high excesses of educts during the reaction and easy removal of by-products by simple filtration processes.

As the solid phase peptide synthesis is based on building amide-bonds to grow the structure, the choice of ligands was limited to structures containing such bonds. Thus beside of peptide ligands (e.g. B6 or GE11) derived from phage display, folic acid, composed of glutamic acid and pteronic acid connected *via* an amide bond, was a feasible ligand for this strategy. As folic acid is a ligand with a high binding affinity to its receptor (10^{-10} M),¹¹⁰ it was chosen for a first proof of concept. Being responsible for cell targeting, the ligand should be represented by the polyplex to enable receptor ligand interactions. Therefore a spacer to overcome the distance between incorporated siRNA and exposed ligand was needed. The use of commercially available α -amino-, ω -carboxy-PEG (Fmoc-N-amido-dPEG₂₄-acid, QuantaBiodesign, Powell, Ohio, USA) enabled the introduction of a defined polyethylene glycol spacer on solid phase (see Fig. 3.9).

The covalent attachment of a targeting moiety should not influence the siRNAs silencing efficiency. Hence the ligand construct was attached by a disulfide bond at the 5'-end of its sense strand. As the disulfide bond is cleaved in the cytosol, the siRNA modification is minimal. Taking into account all these features, the synthesis was performed as shown in Fig. 3.9.

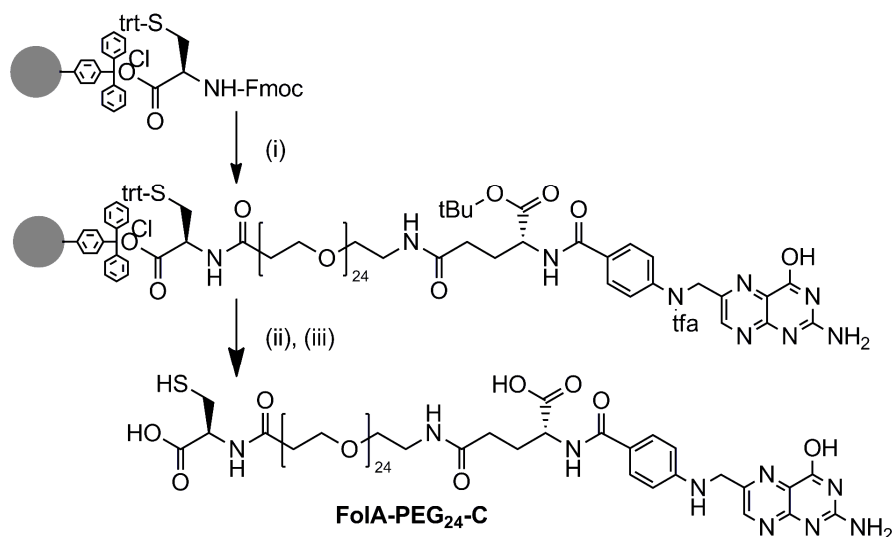


Fig. 3.9 Solid phase synthesis of FoIA-PEG₂₄-C. For synthesis, a 2-Chlorotrytyl chloride resin was chosen. After loading the resin with Cys(Trt)-NH₂, further components were attached, using standard Fmoc based synthesis strategy. (i) Deprotection: 20% (v/v) piperidine in DMF, four times 10 min; (ii) Coupling: AA/PyBop/HOBt/DIPEA (4/4/4/8) in DMF/DCM, 60 min; (iii) tfa-removal: 1 M ammonium hydroxide/DMF (1/1, v/v), four times 30 min; (iv) Cleavage: TFA/TIS/H₂O (95/2.5/2.5), 2 h.

The ligand-spacer complex was generated by SPPS, starting with an Fmoc protected cysteine on solid support, containing a thiol group for the attachment to siRNA. After removing the protective group dPEG₂₄, glutamic acid and N¹⁰-(trifluoroacetyl)pteroic acid were consecutively attached to the growing molecule, resulting in the in Fig. 3.9 shown structure. After removing the trifluoroacetyl protection group with ammonium hydroxide, the peptidic structure was cleaved of the resin and purified by precipitation. The resulting peptide was analyzed by RP-HPLC (Fig. 3.10) and MALDI-TOF-MS (Fig. 3.11).

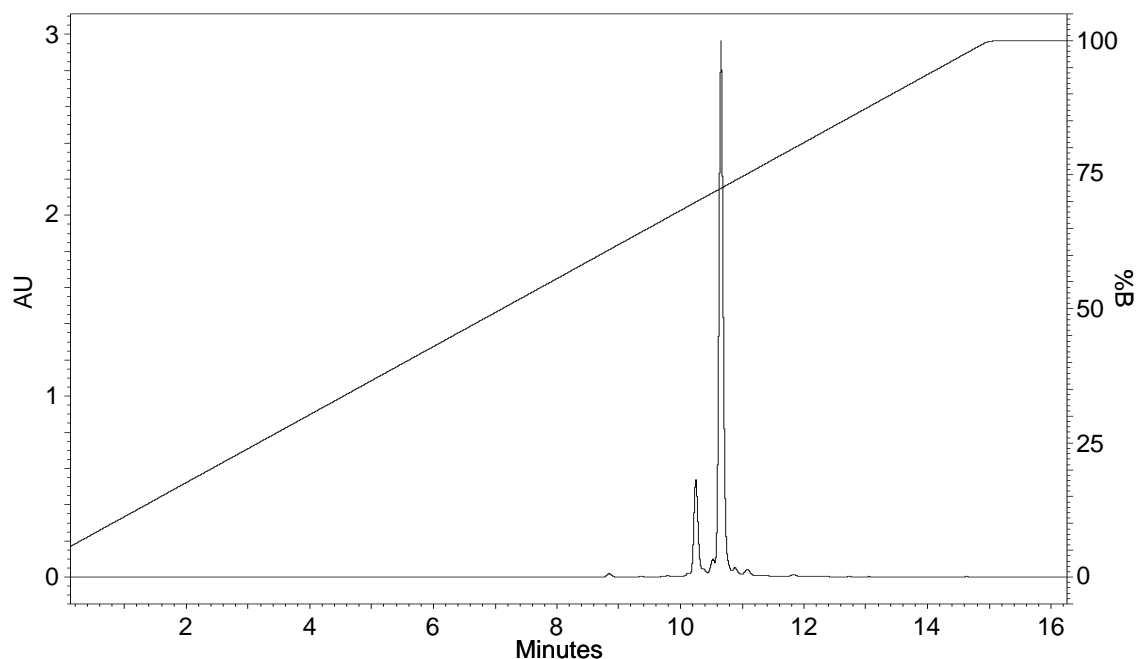


Fig. 3.10 Chromatogram of the analytical RP-HPLC of FoIA-PEG₂₄-C. After cleavage of the peptidic structure and purification by precipitation, the purity was checked by RP-HPLC using a sunfire C18 column (Waters, Milford, MA). A gradient from 5-100% (v/v) acetonitrile in water (0.1% (v/v) TFA) was applied for 20 min.

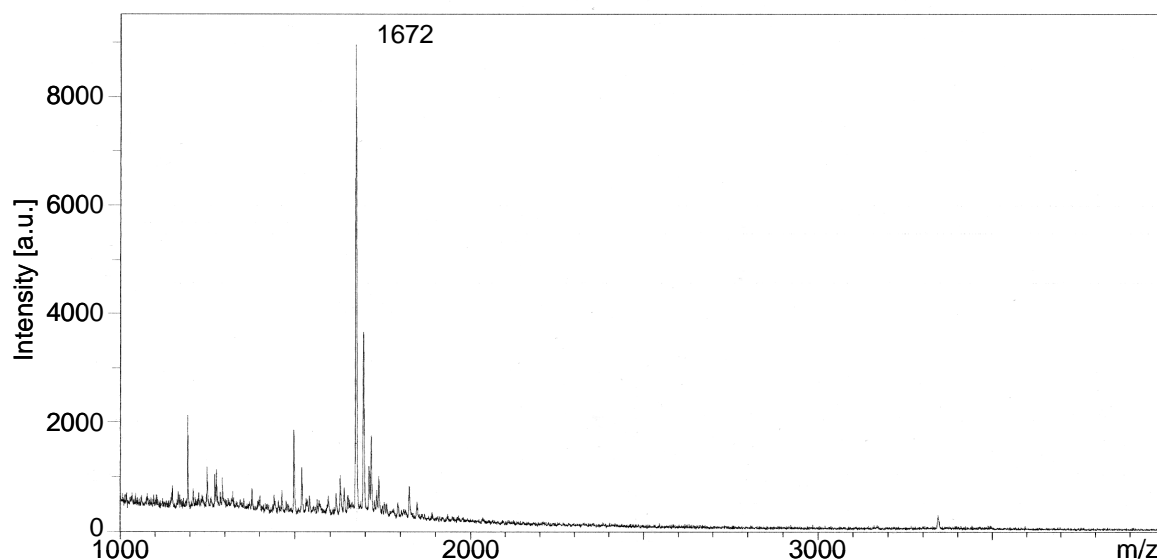


Fig. 3.11 MALDI-TOF-MS spectrum of FoIA-PEG₂₄-C. After cleavage of the peptidic structure and purification by precipitation, the identity was checked by mass spectrometry. Calculated mass: 1673 Da
Used matrix: 2,5-dihydroxybenzoic acid (DHB).

The analysis proved purity as well as identity of the synthesized structure. This defined peptidic ligand was coupled in a second step to the backbone of the siRNA, as

summarized in Fig. 3.12. Same as for the attachment of the influenza peptide, a thiol modified siRNA, protected as disulfide was chosen for the synthesis. Thus it had to be deprotected by the treatment with TCEP, purified by ion exchange chromatography and activated using a high excess of DTNB. After renewed purification by ion exchange chromatography, the peptidic ligand structure was coupled *via* its free thiol group, building a disulfide bond with the siRNA.

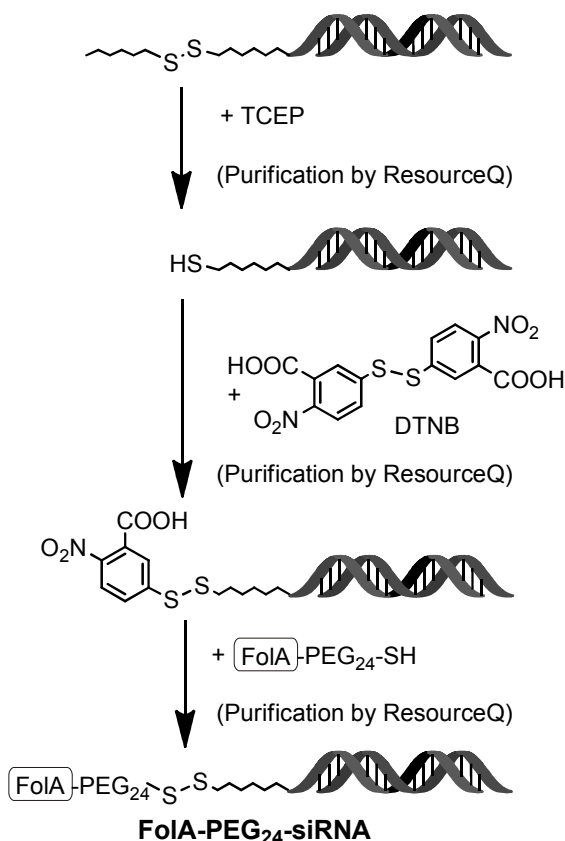


Fig. 3.12 Synthesis of the FoIA-PEG₂₄-siRNA conjugate. After deprotection of the thiol group and purification by ion exchange chromatography, the thiol bearing siRNA was activated with DTNB. Additional purification of the product allowed the defined attachment of the cysteine containing pegylated ligand *via* a disulfide bridge. TCEP: (2-carboxyethyl)phosphine, DTNB: 5,5'-dithiobis-(2-nitrobenzoic acid).

The resulting targeted siRNA was purified by ion exchange chromatography (Fig. 3.13). To identify the product, fractions showing absorption at 260 nm were collected and analyzed by agarose gel electrophoresis (Fig. 3.14).

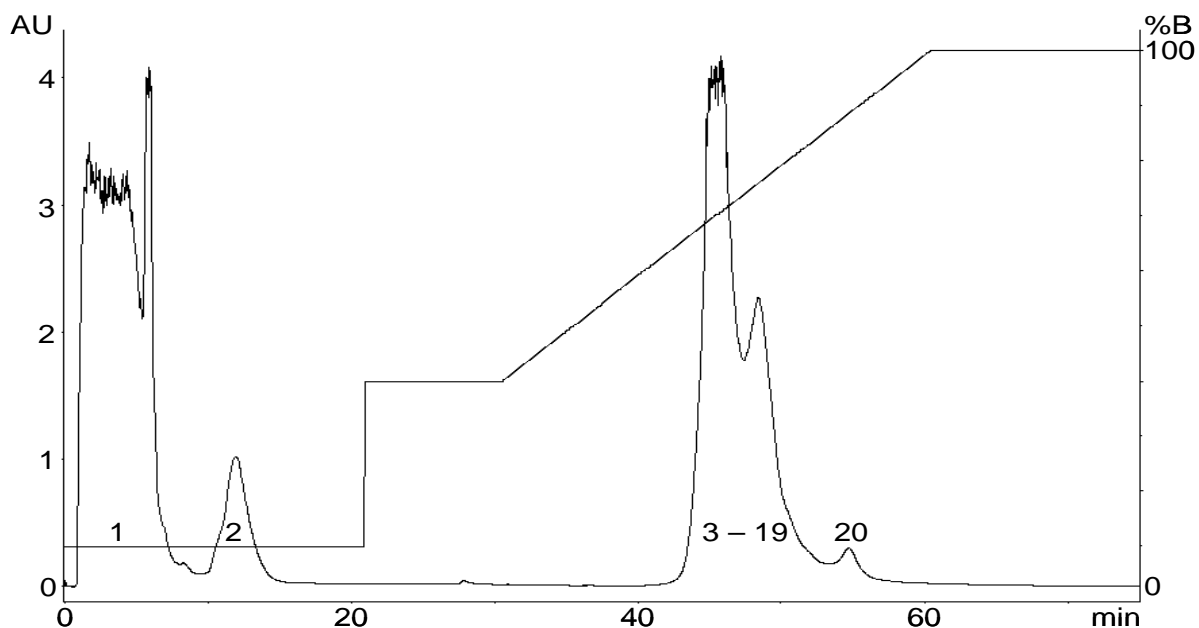


Fig. 3.13 Chromatogram of the ion exchange chromatographic purification of the FoIA-PEG₂₄-siRNA hybrid. After loading the sample onto a ResourceQ column using 20 mM Hepes, pH 6.5, 50 mM NaCl, 30% acetonitrile and a washing step using same buffer with 200 mM NaCl, the elution of the product was performed applying a gradient of 10 mM NaCl/min and a flow of 1 mL/min over 30 min. 1-20: collected fractions. Detection wavelength: 260 nm.

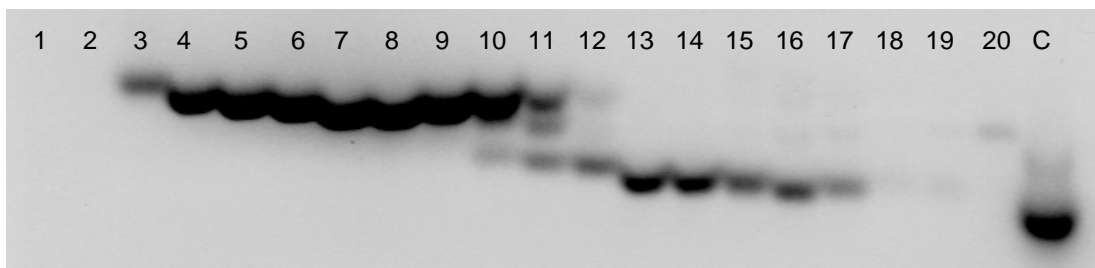


Fig. 3.14 Agarose gel analysis of the ion exchange chromatographic purification. Fractions, collected during ion exchange chromatographic purification of FoIA-PEG₂₄-siRNA were analyzed in a 2.5% agarose gel. 100 V were applied for 100 min. C: control (unmodified siRNA), 1-20: Fractions collected during purification.

As shown in Fig. 3.13 the targeted siRNA binds to the column, when a buffer containing 20 mM Hepes, pH 6.5 and 50 mM NaCl, 30% acetonitrile was used. During the sodium chloride gradient (10 mM/min, 1 mL/min) fractions showing absorption at 260 nm elute. The analytical gel electrophoresis reveals that these fractions contain siRNA. Two populations can be distinguished. One contained siRNA that migrates as far as free control siRNA in the gel, the other population containing retarded siRNA. Fractions containing retarded siRNA were pooled and used for further analysis.

3.2.2 *In vitro* gene silencing using FoIA-PEG₂₄-siRNA

It was hypothesized that the conjugate is not able to act as functional carrier itself, due to the absence of an endosomolytic function. The combination of the targeted siRNA with an endosomolytic active polymer should result in an efficient reporter gene knockdown. In an experimental setting, folic acid receptor positive KB cells stably expressing the eGFP-Luciferase gene were transfected with polyplexes containing different amounts of targeted siRNA and a defined polycation **229** (Fig. 3.15).

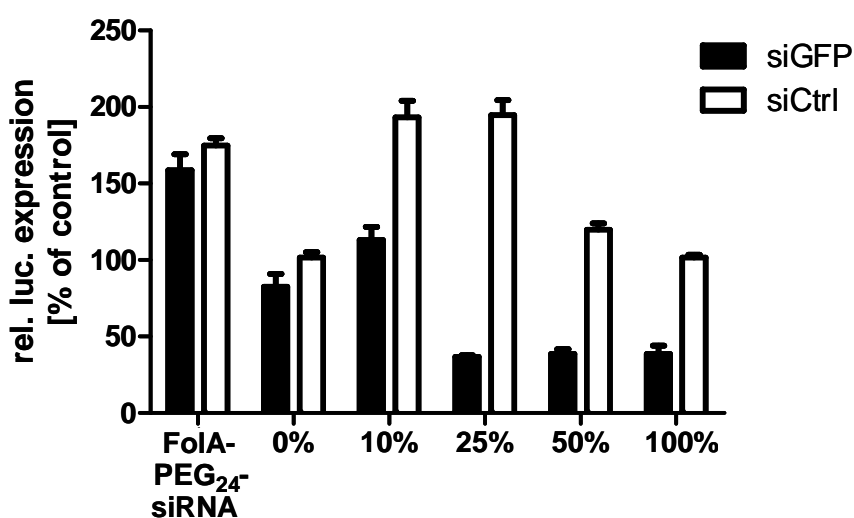


Fig. 3.15 *In vitro* target gene silencing using targeted siRNA. Folic acid receptor positive KB cells stably expressing eGFP-Luc were transfected with 400 nM siRNA polyplexes formed with polymer **229**. Indicated numbers represent the molar percentage of siRNA molecules replaced by FoIA-PEG₂₄-siRNA. Targeted siRNA without polymer was used for transfection as control. Used nitrogen to phosphate (N/P) ratio: 12.

As already expected, the FoIA-PEG₂₄-siRNA conjugate does not lead to a knockdown. Incubating the cells with polyplexes without targeted siRNA for 30 min does also not result in gene silencing. The addition of different amounts of targeted siRNA led at ratios above 25% to an efficient specific gene silencing to ~35% of expression. Using folic acid targeted siRNA leads to increased levels of luciferase expression without polymers and with 10% and 25% mixtures, while showing a slight toxicity at higher ratios.

3.2.3 Modified synthesis of targeted siRNA

As the proof of concept revealed, that the covalent attachment of a targeting ligand to siRNA resulted in a functional construct, the design was further improved. The used synthesis was laborious, time consuming and cost intensive due to three synthesis and purification steps (Fig. 3.12). To overcome these problems, a new reaction type, the Huisgen cycloaddition (1,3-dipolar cycloaddition) was chosen. Known to be very efficient and specific, this was a promising candidate for the synthesis of targeted siRNA. To enable the attachment of the ligand structure to the siRNAs alkyne the solid phase protocol to generate targeted structures (Fig. 3.9) was slightly modified. Instead of a resin bound Cys(Trt)-Fmoc, the synthesis was started with (S)-5-azido-2-(Fmoc-amino)pentanoic acid on solid support, resulting in the peptidic structure FoIA-PEG₂₄-azide as shown in Fig. 3.16. To maintain the advantage of a biodegradable disulfide linkage the siRNA was modified with a disulfide bond between backbone and alkyne group (see Fig. 3.17).

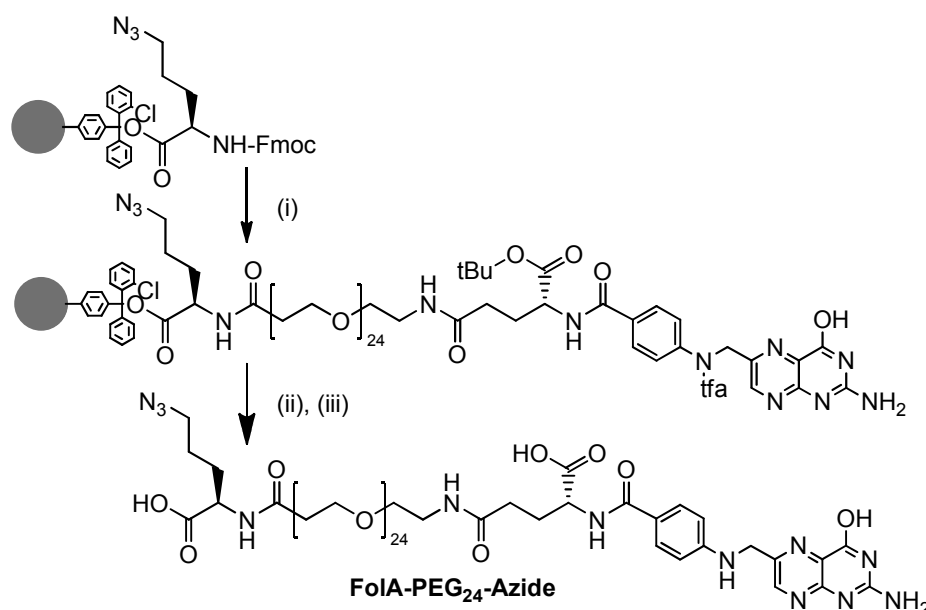


Fig. 3.16 Solid phase synthesis of FoIA-PEG₂₄-Azide. For synthesis, a 2-Chlorotrytyl chloride resin was chosen. After loading the resin with (S)-5-2-(Fmoc-amino)pentanoic acid, further components were attached, using standard Fmoc based synthesis strategy. (i) Deprotection: 20% (v/v) piperidine in DMF, four times 10 min; (ii) Coupling: AA/PyBop/HOBt/DIPEA (4/4/4/8) in DMF/DCM, 60 min; (iii) tfa-removal: 1 M ammonium hydroxide/DMF (1/1, v/v), four times 30 min; (iv) Cleavage: TFA/TIS/H₂O (95/2.5/2.5), 1 h.

Using Cu(I) as catalyst the synthesis could be reduced to one reaction and one purification step (Fig. 3.17). The resulting product is termed FoIA-PEG₂₄-click-siRNA in the following text. After purification *via* ion exchange chromatography and determination of fractions containing modified siRNA, the product was checked for identity by MALDI-TOF-MS analysis (Fig. 3.18).

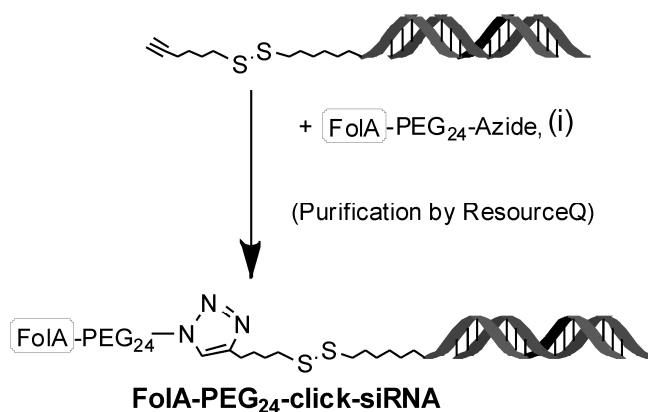


Fig. 3.17 One step synthesis of FoIA-PEG₂₄-click-siRNA. The targeting domain was coupled to the siRNA by Cu(I) catalyzed 1,3-dipolar cycloaddition. (i): TBTA/CuBr solution (0.1 M TBTA/0.1 M CuBr 2/1 (v/v) each in DMSO/tertiary Butanol 3/1 (v/v)), 2 h, 37°C, constant shaking.

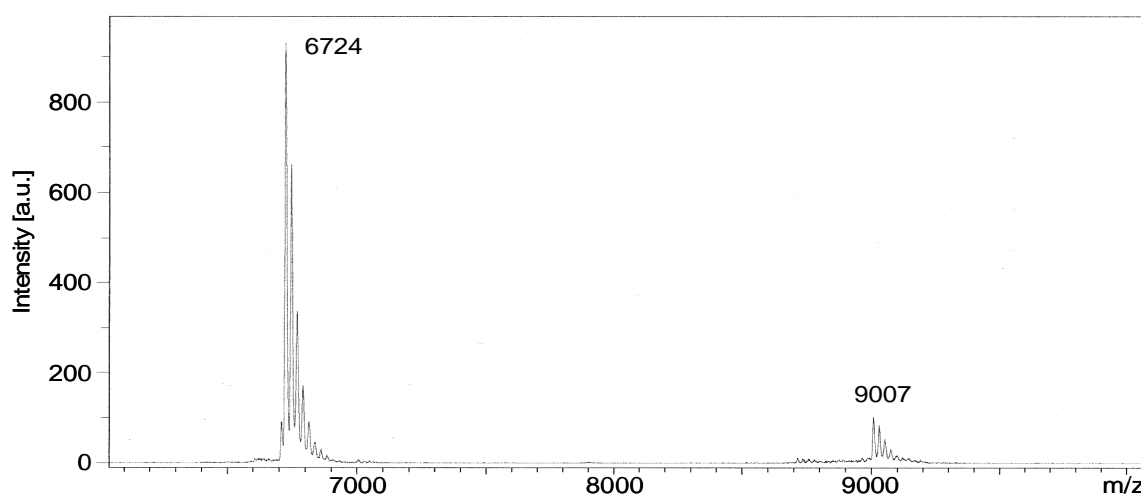


Fig. 3.18 MALDI-TOF-MS spectrum of FoIA-PEG₂₄-click-siCtrl. After purification *via* ion exchange chromatography and analysis with agarose gel electrophoresis, the FoIA-PEG₂₄-click-siRNA was identified by mass spectrometry. m/z 6724: antisense strand (Calculated mass: 6721 Da), m/z: 9007: modified sense strand (Calculated mass: 9004 Da). Used matrix: 3-hydroxypicolinic acid (HPA).

As demonstrated by mass analysis, the product is composed of pure modified siRNA. The two peak populations in Fig. 3.18 display the unmodified antisense strand (m/z 6724) and the modified sense strand (m/z 9007). Additional peaks result from salt adducts of the pure product.

3.2.4 Functional evaluation of FoIA-PEG₂₄-click-siRNA

As the modification of siRNA as well as folic acid can have a strong influence on its activity, the biological behaviour of the modified structure had to be shown, using the same assays.

3.2.4.1 Influence of the covalent siRNA attachment on the receptor binding ability of folic acid

The binding ability of siRNA bound folic acid was checked qualitatively by fluorescence microscopy (Fig. 3.19) and quantitatively by flow cytometry (Fig. 3.20). For that purpose the siRNA used in the synthesis was modified by a Cy5 label at the 5'-end of its antisense strand. As control sequence, nontargeted siRNA (PEG₂₄-click-siRNA-Cy5) was chosen.

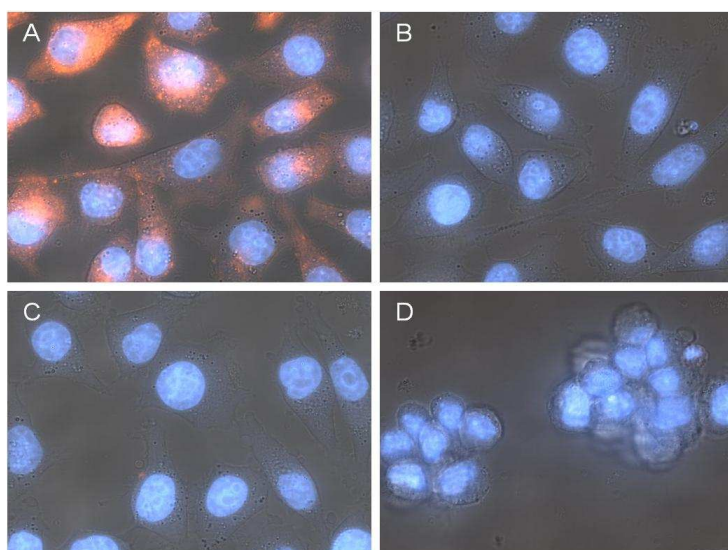


Fig. 3.19 Fluorescence microscopic pictures of the ligand mediated uptake of FoIA-PEG₂₄-click-siRNA. KB cells expressing the folic acid receptor were incubated for 30 min with A: Cy5 labeled FoIA-PEG₂₄-click-siRNA or C: labeled PEG₂₄-click-siRNA. To prove the specificity of uptake KB cells were B: preincubated with free folic acid for competitive inhibition or D: folic acid receptor negative Neuro2A cells were used. The experiment was performed by Thomas Fröhlich as part of his PhD thesis (in preparation).

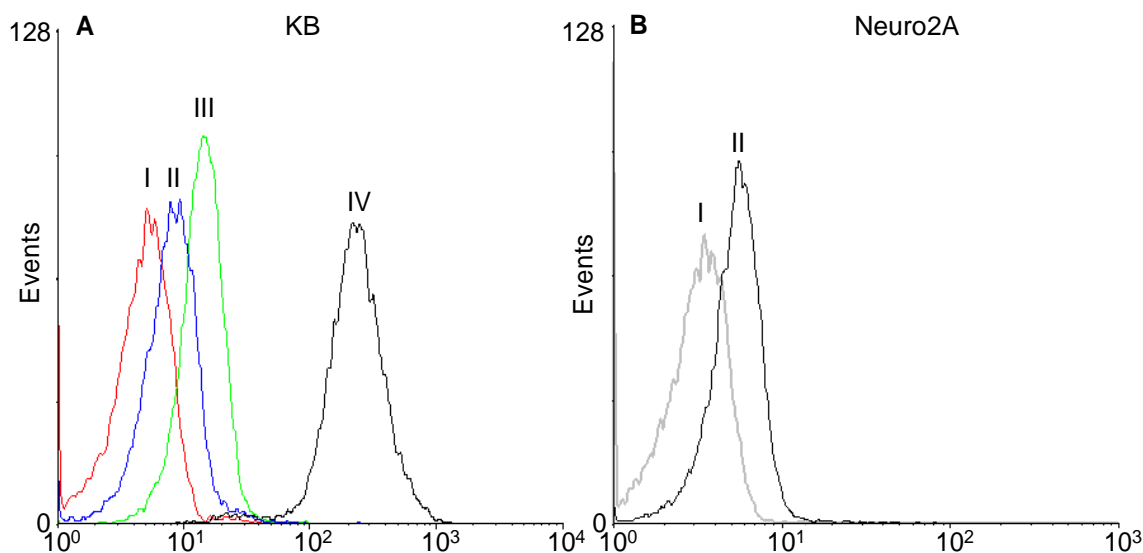


Fig. 3.20 Flow cytometric analysis for cell association of FoIA-PEG₂₄-click-siRNA. A: Folic acid receptor positive KB cells were treated with Cy5 labeled FoIA-PEG₂₄-click-siRNA or its analogues for 30 min. After washing, Cy5 positive cells were detected by flow cytometry. I: untransfected cells, II: FoIA-PEG₂₄-click-siRNA with folic acid competition, III: PEG₂₄-click-siRNA, IV: FoIA-PEG₂₄-click-siRNA; B: Folic acid receptor negative Neuro2A cells: I: untransfected cells, II: FoIA-PEG₂₄-click-siRNA. The experiment was performed by Thomas Fröhlich as part of his PhD thesis (in preparation).

Regarding the results of the fluorescence microscopy, the labeled FoIA-PEG₂₄-click-siRNA was efficiently taken up by KB cells (Fig. 3.19A), known for strong expression of the folic acid receptor. Nontargeted siRNA (Fig. 3.19C) showed no uptake, as does the targeted siRNA, when cells were preincubated with free folic acid before treatment (Fig. 3.19B). Folic acid receptor negative control cells did also not show a significant internalization of the conjugate (Fig. 3.19D). These qualitative results could be supported by flow cytometry. The treatment of KB cells with labelled FoIA-PEG₂₄-click-siRNA led to a significant shift of the fluorescent signal in the whole cell population (Fig. 3.20A IV), while all controls did not lead to a significant shift.

3.2.4.2 Influence of covalent attachment of FoIA-PEG₂₄ on the activity of siRNA

Although the modification of folic acid with a PEG-spacer and an attached siRNA did not alter its specificity and affinity to its receptor, the transfection of cells with FoIA-

PEG₂₄-siRNA did not lead to a significant reporter gene silencing. To exclude, that the conjugate as well as the type of reaction interferes with the silencing ability of the siRNA, the different constructs were transfected in a receptor independent setting to compare the influence of the modification on the silencing efficiency. As shown in Fig. 3.21 Neuro2A cells, with a low folic acid receptor level were transfected using a functional polycation (**230**).

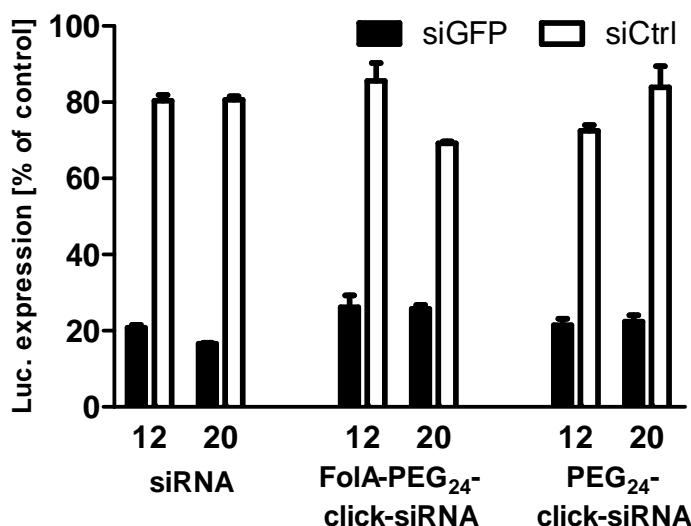


Fig. 3.21 Gene silencing activity of conjugated siRNA in comparison to unconjugated siRNA. Neuro2A cells stably expressing eGFP-Luciferase were transfected using the different siRNA conjugates in combination with polycation **230** at indicated N/P ratios of 12 or 20. The experiment was performed by Thomas Fröhlich as part of his PhD thesis (in preparation).

The knockdown efficiency of both siRNA conjugates is around 20% of the expression level of untreated cells and thus similar to that of unconjugated siRNA. As the controls of all three types of siRNA have a similar expression level the modifications show to have neither an influence on the silencing efficiency nor on specificity and toxicity.

3.2.5 Incorporation of FoIA-PEG₂₄-click-siRNA into an efficient and functional carrier system

Free FoIA-PEG₂₄-click-siRNA has shown to be not able to regulate the expression level of the target protein and thus is not able to silence a gene, although it is taken up very efficiently by specific interactions with the folic acid receptor and bears a

completely functional siRNA. Thus it was hypothesized that during intracellular delivery the endosomal escape is the crucial bottleneck of this conjugate. To develop a functional carrier system, the ligand PEG conjugated siRNA was combined with a simple, defined polycation known to force the proton sponge effect as an efficient endosomal escape mechanism. The used polycation, synthesized by solid phase supported peptide synthesis consists of three arms, each build of three Stp units terminated by a cysteine (**386**, for structure see Materials and Methods). In combination with the siRNA conjugate it should form stable polyplexes, present the pegylated ligand on its surface and lead to an efficient delivery system by combination of receptor mediated uptake and efficient endosomal escape.

3.2.5.1 Physicochemical characterization of FoIA-PEG₂₄-click-siRNA

To prove that this combination can result in an efficient delivery system, the ability to build polyplexes was tested in a gel migration assay and compared to free siRNA. The resulting gel picture is shown in Fig. 3.22. It shows siRNA, PEG₂₄-click-siRNA and FoIA-PEG₂₄-click-siRNA after complex formation with polymer **386** at two different N/P ratios.

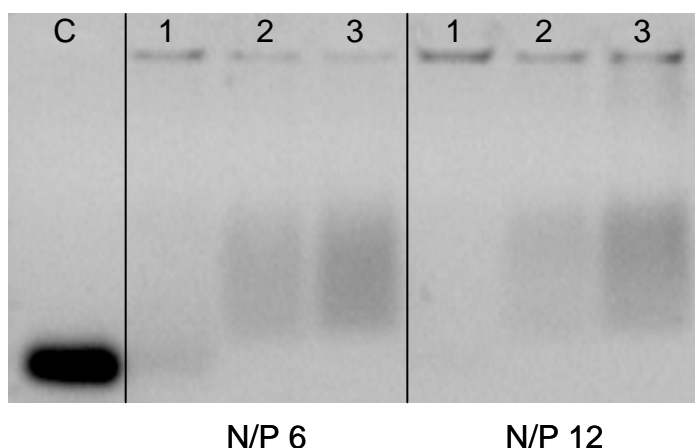


Fig. 3.22 Comparison of polyplex stability by agarose gel shift assay. Polyplex formation of unconjugated siRNA (1) FoIA-PEG₂₄-click-siRNA (2) or PEG₂₄-click-siRNA (3) in combination with polycation **386** was tested at indicated N/P ratios. C: control, free siRNA. The experiment was performed by Thomas Fröhlich as part of his PhD thesis (in preparation).

In contrast to free siRNA (C: control), the bands for all polyplexes are strongly reduced. In all pockets non migrating siRNA can be detected. Thus conjugated siRNA still retains its ability to interact with the polycationic carrier. Comparing conjugated (2, 3) to unconjugated siRNA, slight differences can be observed. In case of PEG₂₄-click-siRNA and FoliA-PEG₂₄-click-siRNA a small percentage of nucleic acids is able to migrate into the gel, while for unconjugated siRNA, no free nucleic acids can be detected, indicating a slight destabilization of polyplexes by PEG modification of siRNA. To further characterize the particle formation of conjugated and unconjugated siRNA, particle size and zeta potential of these structures was determined (table 3.3).

Table 3.3 Size and zeta potential of polyplexes of different siRNA conjugates in combination with polycation 386.

N/P	Polyplex	Diameter [nm]	Zeta potential [mV]
	siRNA	633 (±44)	20.1 (±1.0)
6/1	FoliA-PEG ₂₄ -click-siRNA	933 (±50)	11.0 (±0.6)
	PEG ₂₄ -click-siRNA	1075 (±64)	13.8 (±0.4)
	siRNA	597 (±32)	20.8 (±1.3)
12/1	FoliA-PEG ₂₄ -click-siRNA	953 (±145)	13.3 (±0.2)
	PEG ₂₄ -click-siRNA	1035 (±147)	15.6 (±0.5)

At both N/P ratios the polyplexes formed with unconjugated siRNA had a particle size around 600 nm and a zeta potential of 20 mV. In contrast particles formed with conjugated siRNA have a diameter between 933 nm – 1075 nm. The zeta potential of particles formed with siRNA conjugates is strongly reduced. At N/P 6 down to 11.0 – 13.8 mV (31-45% reduction) and at N/P 12 13.3 – 15.6 mV (25-36% reduction). These results show that interactions take place between polymer **386** and the different siRNA conjugates leading to stable particles. Although these particles are slightly bigger compared to particles formed with unconjugated siRNA, the pegylation significantly reduces the zeta potential.

The strong reduction of the zeta potential indicated, that PEG molecules and thus the targeting structures are presented on the polyplex surface. Thus a receptor specific uptake of particles should be enabled. To prove this, KB cells expressing the folic acid

receptor were transfected with the labeled FoIA-PEG₂₄-click-siRNA or its nontargeted analogue. Particle uptake was subsequently explored by flow cytometry. As the resulting data (Fig 3.23) demonstrate, cells transfected with particles consisting of nontargeted siRNA and polymer **386** show a slight positive Cy5 signal, indicating a weak polyplex association at N/P 6. Polyplexes carrying pegylated siRNA lead to an increased signal intensity. In contrast the introduction of folic acid into the structure leads to an 10- to 40-fold increase in cellular uptake at N/P 6 compared to pegylated siRNA or unconjugated siRNA. At N/P 12 the cell association is increased for all polyplex variants compared to N/P 6. As unconjugated and pegylated siRNA result in the same transfection efficiency folic acid targeted siRNA still leads to an 10-fold increased uptake of polyplexes.

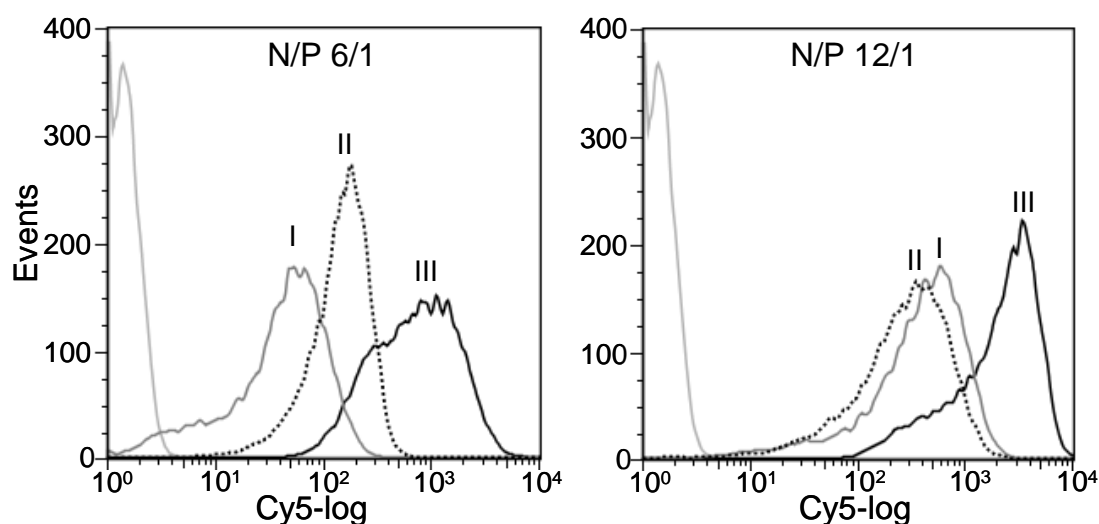


Fig. 3.23 Flow cytometric analysis for cell association of FoIA-PEG₂₄-click-siRNA in combination with polycation **386**. I: PEG₂₄-click-siRNA, II: FoIA-PEG₂₄-click-siRNA with folic acid competition, III: FoIA-PEG₂₄-click-siRNA. The experiment was performed by Thomas Fröhlich as part of his PhD thesis (in preparation).

3.2.5.2 FoIA-PEG₂₄-click-siRNA in combination with polymer **386** for efficient gene silencing

In the last sections the functionality of the FoIA-PEG₂₄-click-siRNA construct as well as its inefficiency in endosomal escape has been shown in detail. To overcome the limitation in intracellular delivery the conjugate was combined with the defined

polycation **386** that is able to escape out of the endosome due to the proton sponge ability of its Stp units.⁸⁰ These both molecules showed to be able to build stable particles with strongly reduced zeta potential due to the PEG shielding, compared to particles formed with unconjugated siRNA. Thus this combination of macromolecules shows to have the potential to act as efficient carrier system. To prove this, these polyplexes were used in an *in vitro* experimental setting to down regulate the eGFP-Luciferase fusion gene in KB cells expressing the folic acid receptor (Fig. 3.24).

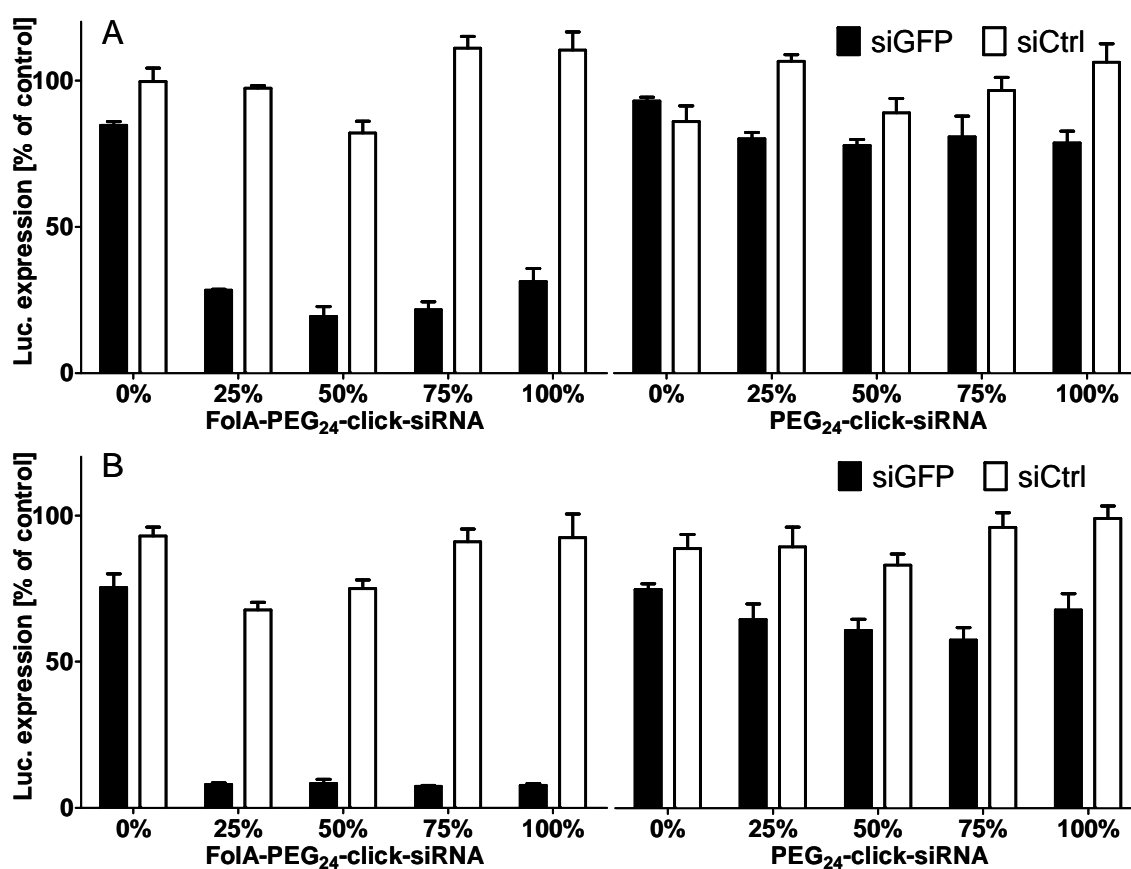


Fig. 3.24 Reporter gene silencing of targeted and nontargeted pegylated siRNA in combination with polycation 386. KB cells stably expressing eGFP-Luciferase were transfected either with 400 nM FoIA-PEG₂₄ modified siRNA (left bars) or 400 nM PEG₂₄-click-siRNA (right bars). For transfection polycation **386** was used at N/P 6 (A) or N/P 12 (B). The experiment was performed by Thomas Fröhlich as part of his PhD thesis (in preparation).

The transfection results reveal that the carrier system is able to silence the target gene in a receptor specific manner. Using 100% nontargeted siRNA for polyplex formation (0% FoIA-PEG₂₄-click-siRNA) resulted in the absence of gene silencing, while all polyplexes consisting either of a mixture of ligand conjugated and unconjugated

siRNA or pure ligand conjugated siRNA resulted in significant gene silencing down to 25% (for N/P 6) or 7% (for N/P 12) of the expression level of control cells. In contrast the use of pegylated siRNA did not lead to an effect on the target cells at N/P 6 and just to a slight regulation (~25% reduction) at N/P 12. The use of control siRNA resulted in full expression levels at any N/P ratio.

In conclusion, it could be demonstrated, that the synthesis of a defined FoliA-PEG-siRNA molecule is possible. Its identity and functionality could be proven in different assays, showing no significant differences between the two different synthesis strategies. As this molecule does not contain any functional group for endosomal escape, it does not lead to gene silencing when used as transfection agent. The combination with a defined carrier system, forcing endosomal escape, resulted in very efficient and specific reporter gene knockdown. Thus the presented structure reduces the role of the polymer to endosomal escape and particle formation and thus increases its design space.

3.3 Targeted polycation for cell specific siRNA delivery *in vitro* and *in vivo*

Targeting the cell of interest remains one of the major bottlenecks of today's RNAi technology. Reaching a specific cell population does in case of polyplex mediated delivery not only imply the enhancement of affinity to this special cell type, but also to avoid attachment processes to nontargeted cells. Thus, the common interpretation of Paul Ehrlich's "magic bullet" in case of polyplex mediated siRNA delivery is a polycation based particle incorporating the nucleic acid, which should be completely shielded by e.g. a surrounding layer of polyethylene glycol to avoid any unspecific cell attachment and an outer layer of ligands to enable interactions with the target cell. This idea was up to now limited by very unspecific synthesis strategies. Conjugation of polyethylene glycol (PEG) or pegylated targeting ligands was performed by random attachment to reactive groups of the polymeric backbone in most cases. The pegylation does not only shield the polymer of interaction with cells but also of its interaction with the nucleic acid. Thus the addition of high amounts of PEG to shield the particle could lead to a loss of particle formation ability. A solution for this problem was found by post-pegylation.¹⁴³ In this strategy the polyplex was formed prior to pegylation. Regarding reproducibility and analysis of the product, this method is inefficient for the production of defined structures. A more reasonable approach to separate the functionalities of shielding and nucleic acid binding ability is the synthesis of block copolymers.¹⁴⁴ These structures, consisting of two different subunits, one polycationic region for nucleic acid binding, attached to a second subunit consisting of one or several PEG molecules enable a maximum shielding capacity of the polyplex, maintaining a good nucleic acid binding ability. Until now these structures still lack definition due to substructures with a high polydispersity. This chapter deals with the synthesis, purification and biological evaluation of a peptide based, highly defined structure composed of a polycationic backbone and a defined PEG bearing folic acid as targeting ligand.

3.3.1 Design and synthesis of a structural defined targeted polycation

A highly defined structure for ligand based delivery of siRNA to target cells was the idea of this strategy. As solid phase peptide synthesis was already found out to be an excellent tool for the synthesis of defined polymers,¹⁴⁰ this method was chosen to generate this structure. The requirements of the planned structure were:

- ability to build stable complexes with nucleic acids, especially siRNA
- having a reasonable shielding *via* a PEG chain at a defined position
- containing an efficient targeting ligand

To enable the complexation of the carrier with siRNA, its synthesis was based on a linear backbone consisting of polyamino amides using Stp (16-Amino-4-oxo-5,8,11,14-tetraaza-hexadecanoic acid) as building block (previously described by Schaffert *et al.*¹⁴⁰). Improved polyplex stability should be reached by the incorporation of cysteines at both ends of the cationic backbone. To enable the defined attachment of PEG, a branching lysine was inserted in the middle of the polycation. For highest definition a commercially available, monodisperse, α -amino, ω -carboxy PEG₂₄ was chosen with folic acid as high affinity ligand. Synthesis and resulting structure is shown in Fig. 3.25.

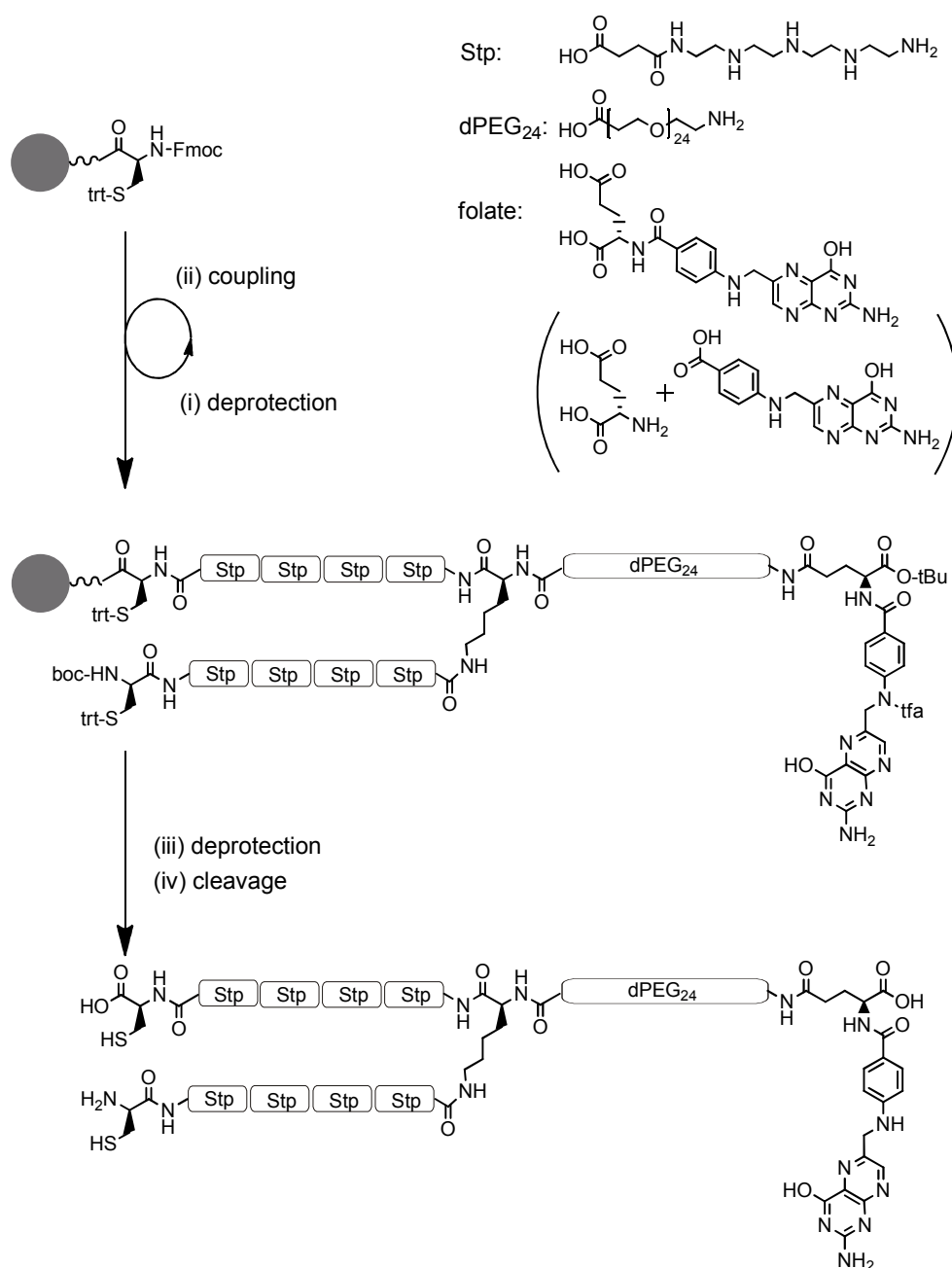


Fig. 3.25 Design and synthesis of Folate-PEG₂₄-K(Stp₄-C)₂. Stp: 16-Amino-4-oxo-5,8,11,14-tetraaza-hexadecanoic acid, dPEG₂₄: defined poly(ethylene glycol) consisting of 24 monomers, trt: trityl protection group, tBu: tert butyl protection group, boc: tert butyl protection group, tfa: trifluoroacetic acid protection group. (i) Deprotection: 20% (v/v) piperidine in DMF, four times 10 min; (ii) Coupling: AA/PyBop/HOBt/DIPEA (4/4/4/8) in DMF/DCM, 60 min; (iii) deprotection: 1 M ammonium hydroxide/DMF (1/1, v/v), four times 30 min; (iv) cleavage: TFA/TIS/H₂O (95/2.5/2.5), 2 h.

For further experiments, analogues lacking targeting or crosslinking ability were synthesized. For purification the peptidic structures were precipitated and lyophilized after cleavage from the resin and evaporation of solvents. Purity and identity were

shown by RP-HPLC (Fig. 3.26), MALDI-TOF-MS (Fig. 3.27) analysis and $^1\text{H-NMR}$ (see appendix).

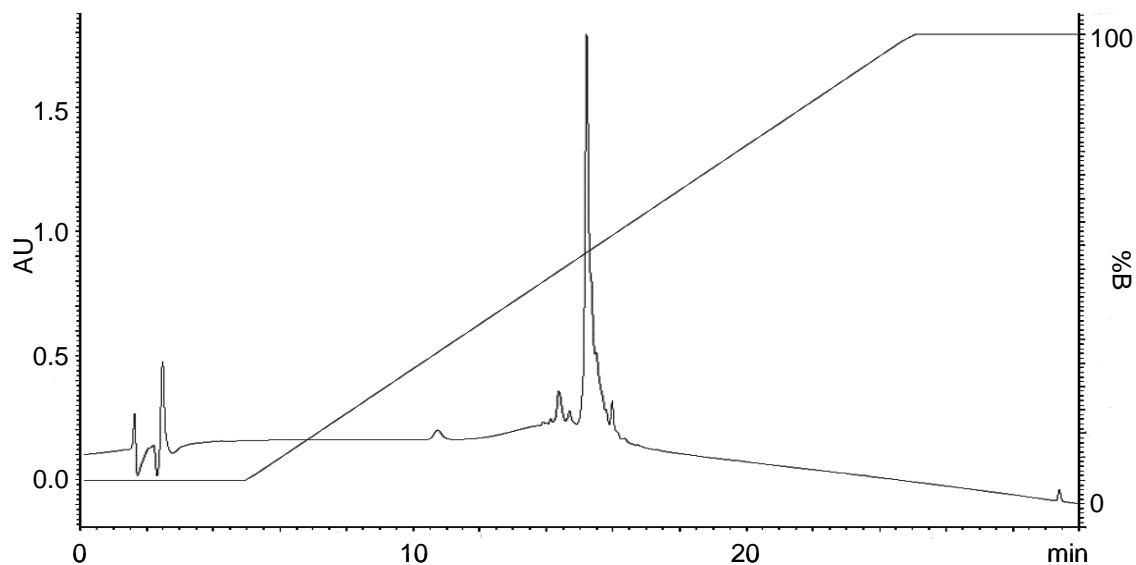


Fig. 3.26 Chromatogram of the analytical RP-HPLC of FoIA-PEG₂₄-K(Stp₄-C)₂. After cleavage of the product from the resin and precipitation the purity of the peptidic structure was analyzed by RP-HPLC using a sunfire C18 column (waters). A gradient from 5-100% (v/v) acetonitrile in water (0.1% (v/v) TFA) was applied in 20 min.

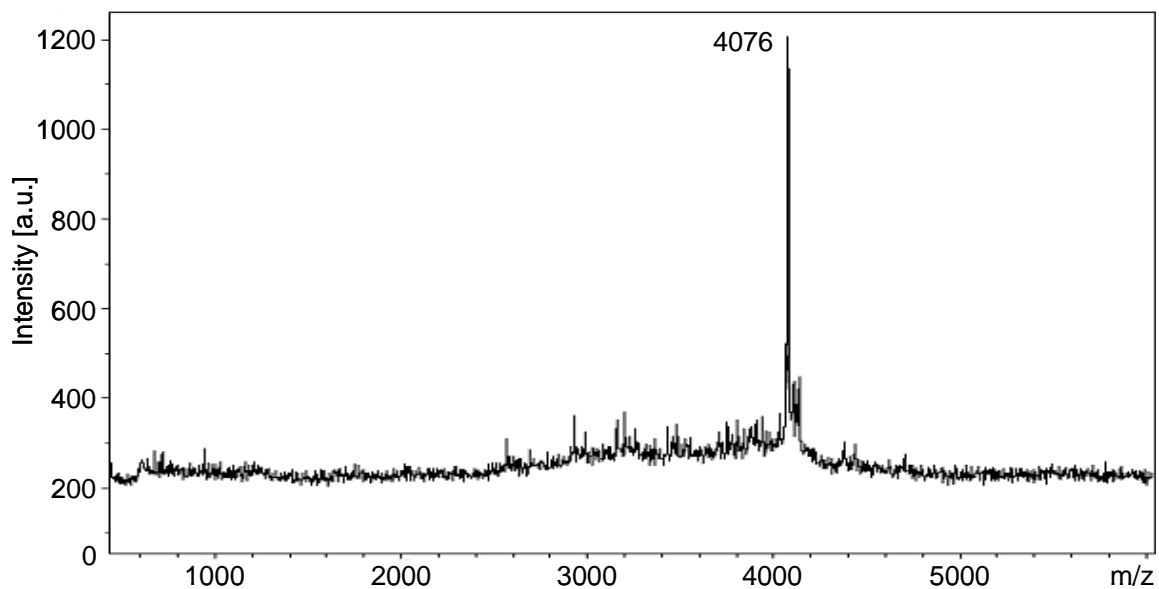


Fig. 3.27 MALDI-TOF-MS spectrum of FoIA-PEG₂₄-K(Stp₄-C)₂. After cleavage of the peptidic structure and purification by precipitation, the identity was checked by mass spectrometry (Calculated mass: 4076 Da). The analysis was performed by our collaborators at the Roche Kulmbach GmbH. Used matrix: 2,5-dihydroxybenzoic acid (DHB).

The analysis reveals purity above 90% and a single mass peak at the estimated position. Same results could be found for both synthesized analogues as shown in table 3.3 (see appendix for detailed information).

Table 3.4 Solid phase peptide synthesis based polycationic structures. Sequences are written from C- to N-terminus as synthesized on solid support.

Sequence	Formula	Calculated mass [M+H] ⁺	Detected mass [M+H] ⁺
A-PEG ₂₄ -K(Stp ₄ -C) ₂	C162H330N46O46S2	3723	3720
C-Stp ₄ -K(Stp ₄ -C)-PEG ₂₄ -FolA	C178H342N52O50S2	4076	4077
S-Stp ₄ -K(Stp ₄ -S)-PEG ₂₄ -FolA	C178H342N52O52	4043	4043

3.3.2 Showing targeting by DNA delivery - A proof of concept

First knockdown experiments using the targeted polycationic structure in combination with siRNA resulted in absence of silencing efficiency (data not shown). As this delivery system is very complex, having several substructures with different functionality, it was decided to show the proof of concept by DNA delivery. DNA delivery has certain parallels in comparison to siRNA delivery. Although complexation, stability, cell attachment, endocytosis and endosomal escape are not the same, they are in certain issues comparable. For this reason DNA delivery is a feasible model to show the efficiency and functionality of a delivery vehicle. Detection of 1% cells showing expression of a transgene is more sensitive than detecting the silencing of a gene by 1%. Thus this model gives a hint whether the system is able to work under certain conditions or whether it is completely inefficient.

As model KB cells, known for high expression of the folate receptor were chosen. First transfection experiments revealed no transgene expression for the targeted as well as for the nontargeted structure (Fig. 3.28A), indicating that the carrier did not work. Addition of chloroquine 1 h after transfection resulted in transgene expressions shown in Fig. 3.28B. Toxicity studies did not show differences between targeted and nontargeted structures (Fig 3.28C,D).

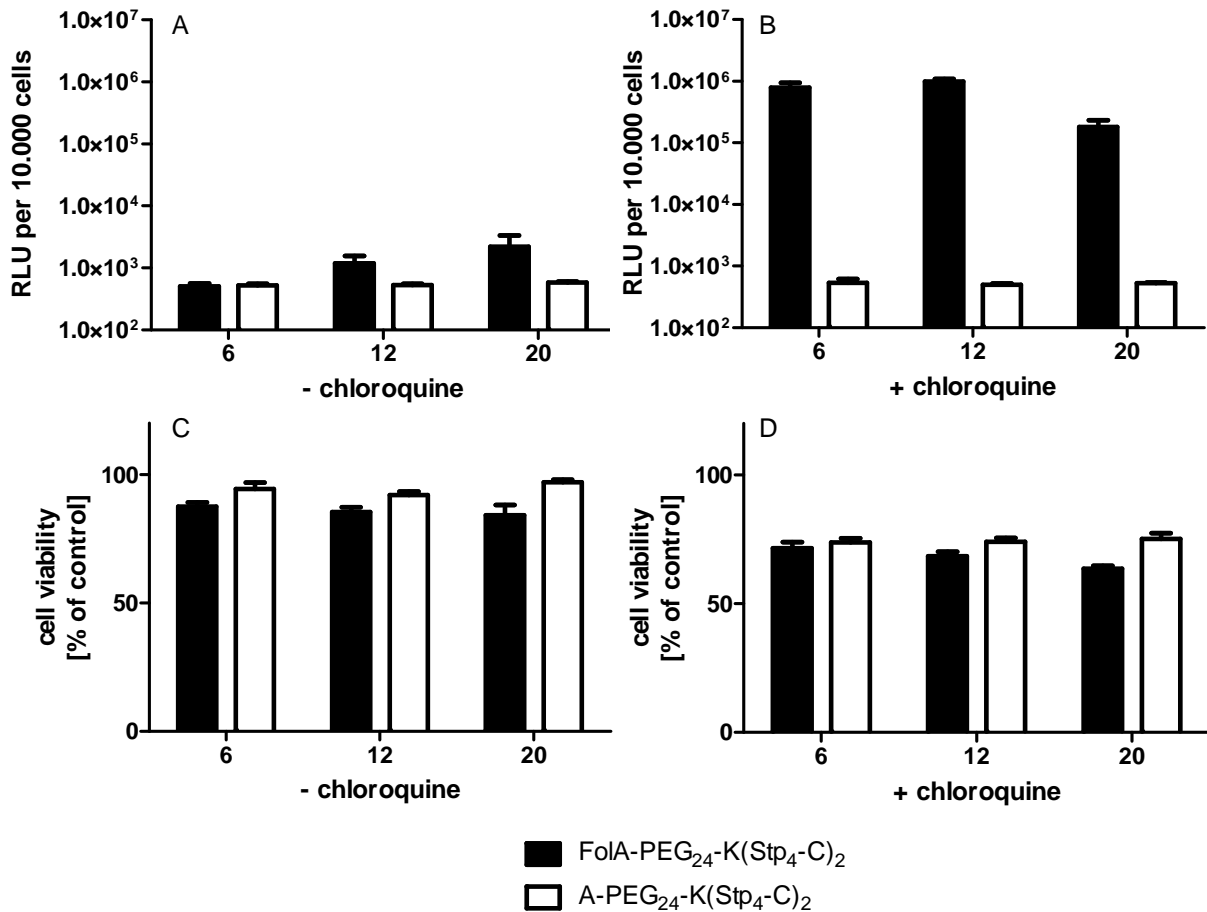


Fig. 3.28 DNA delivery using defined folic acid targeted poly amines. Folic acid receptor positive KB cells were transfected with pDNA encoding for the eGFP-Luciferase fusion protein. A/B: luciferase gene expression 24h after transfection. C/D: Relative cell viability, compared to HBG treated cells.

Using chloroquine after transfection, results in expression levels up to 10^6 relative light units per 10.000 cells. Chloroquine is known to enhance the endosomal escape. Thus this experiment shows that the system is lacking endosomal escape ability. Beside this, results show, that targeting and shielding are very efficient, because the uptake of polyplexes resulting in transgene expression can just be shown with the ligand containing polymer.

As the endosomal escape is the crucial bottleneck using this delivery vehicle, it was decided to combine this carrier-system with the in chapter 3.1 described endosomolytic peptide-siRNA hybrid.

3.3.3 Functional evaluation of FoIA-PEG₂₄-K(Stp₄-C)₂ in combination with Inf7-siRNA

The designed carrier system shows a high complexity, consisting of different substructures with specific functionality. Although the combination was expected to have synergistic effects, nonfunctionality of one part could lead to an overall inefficient system, as already shown for endosomal escape. Hence the functionality and necessity of every single compound had to be tested in detail.

3.3.3.1 Stabilization by disulfide bond formation

As already described in the work of Schaffert *et al.*,⁸⁰ short Stp units are not able to bind nucleic acids efficient enough to be stable during the delivery process. Thus stabilizing moieties have to be incorporated to enhance polyplex stability. In the described system, cysteines were introduced to enable disulfide bond formation among the oligo-Stp chains after polyplex formation and thus raise its stability. To prove the effect of the used mechanism, the functional carrier was compared with a carrier bearing serines instead of cysteines. Polyplexes were formed and loaded on an agarose gel to test their stability (Fig. 3.29).

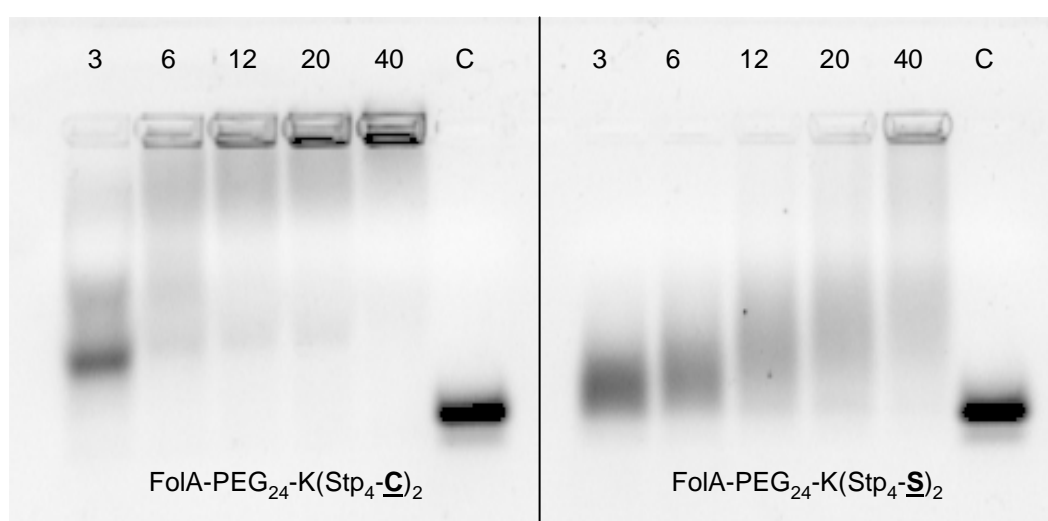


Fig. 3.29 Comparison of polyplex stability by agarose gel shift assay. FoIA-PEG₂₄-K(Stp₄-C)₂ was compared with a structural analogue containing serine instead of cysteine. 3-40: nitrogen to phosphate (N/P) ratio for polyplex formation, C: control (free siRNA).

The analysis of the gel reveals that polyplexes formed with the functional polymer, are able to interact with the nucleic acid, hampering its migration in the gel at a nitrogen to phosphate (N/P) ratio of 6 or higher. The mutant lacking cysteines shows a significantly reduced interaction with siRNA. Just a slight ability to hamper the siRNA migration can be observed. This demonstrates that the construct is able to interact with the nucleic acid. To further identify the kind of interaction and to distinguish between particle formation and aggregation, particle size measurements *via* fluorescence correlation spectroscopy (FCS) were performed. Results are shown in table 3.5 and 3.6.

Table 3.5 Particle size of polyplexes of FolA-PEG₂₄-K(Stp₄-C)₂ and Inf7-siRNA. Particles have been formed in HBS buffer. r_h : hydrodynamic radius.

N/P	r_h [nm]
0 (siRNA)	2.1 (± 0.1)
3	2.7 (± 0.1)
6	2.9 (± 0.1)
12	3.0 (± 0.1)
16	3.0 (± 0.1)
20	2.8 (± 0.1)
40	2.8 (± 0.1)

Table 3.6 Influence of buffer compounds and polymer targeting on particle size. Particles have been formed at an N/P ratio of 16. r_h : hydrodynamic radius.

Conjugate	buffer	r_h [nm]
FolA-PEG ₂₄ -K(Stp ₄ -C) ₂	HEPES	3.0 (± 0.1)
FolA-PEG ₂₄ -K(Stp ₄ -C) ₂	HBS	3.0 (± 0.1)
A-PEG ₂₄ -K(Stp ₄ -C) ₂	HBS	2.9 (± 0.1)

Particle measurements reveal that the gel retardation of siRNA is not due to aggregation but due to the formation of particles between polycation and siRNA. The polyplexes have a hydrodynamic radius between 2.7 and 3.0 nm. Compared with free siRNA (2.1 nm) these particles are very small, composed of one siRNA surrounded by

a thin polymer layer (see table 3.5). Polyplex size is neither significantly influenced by the used mixing buffer nor by type of targeting (table 3.6).

3.3.3.2 Pegylation for polyplex shielding

Pegylation is a very important tool in case of targeted delivery. Besides targeting of a certain cell, shielding the polyplex from interactions with other cells is very important to get the vehicle to its target cell. Polyethylene glycol (PEG) has shown its shielding ability in many different studies. As it is non-toxic and highly soluble in water, it is ideal for use in a carrier system. In the described molecule a defined PEG, consisting of exactly 24 ethylene glycol subunits was used. To prove the shielding ability of this PEG chain, the zeta potential of particles formed under common conditions, was measured. As control the same structure lacking the PEG chain was used (table 3.7).

Table 3.7 Zeta potential of pegylated and nonpegylated polyplexes. N/P: nitrogen to phosphate ratio for polyplex formation, n.d.: no zeta potential measurable

N/P	Zetapotential [mV]	
	A-PEG ₂₄ -K(Stp ₄ -C) ₂	A-K(Stp ₄ -C) ₂
3	0.0 (±1.6)	9.3 (±1.8)
6	0.0 (±1.7)	12.7 (±1.9)
12	0.0 (±2.4)	14.2 (±1.7)
20	0.0 (±2.4)	12.9 (±1.9)
40	0.1 (±2.7)	n.d.

The measurement data show that the zeta potential of nonpegylated particles is around 9-15 mV. In comparison the zeta potential of pegylated particles is completely neutral at all N/P ratios. As the difference of the carrier systems is just the PEG chain, this indicates that the degree of pegylation is enough to shield the particle completely.

3.3.3.3 Ligand incorporation for cell specific delivery of siRNA

As it has been shown, that FoIA-PEG₂₄-K(Stp₄-C)₂ is able to bind siRNA efficiently, shielding its positive charge completely, a targeting ligand for specific cell attachment and uptake becomes very important. In this case folic acid was chosen, because it is described to have an extremely high affinity for its receptor. To test the functionality of the ligand, cell uptake was analyzed qualitatively by fluorescence microscopy (Fig. 3.30) and quantitatively by flow cytometry on KB cells expressing the folate receptor (Fig. 3.31).

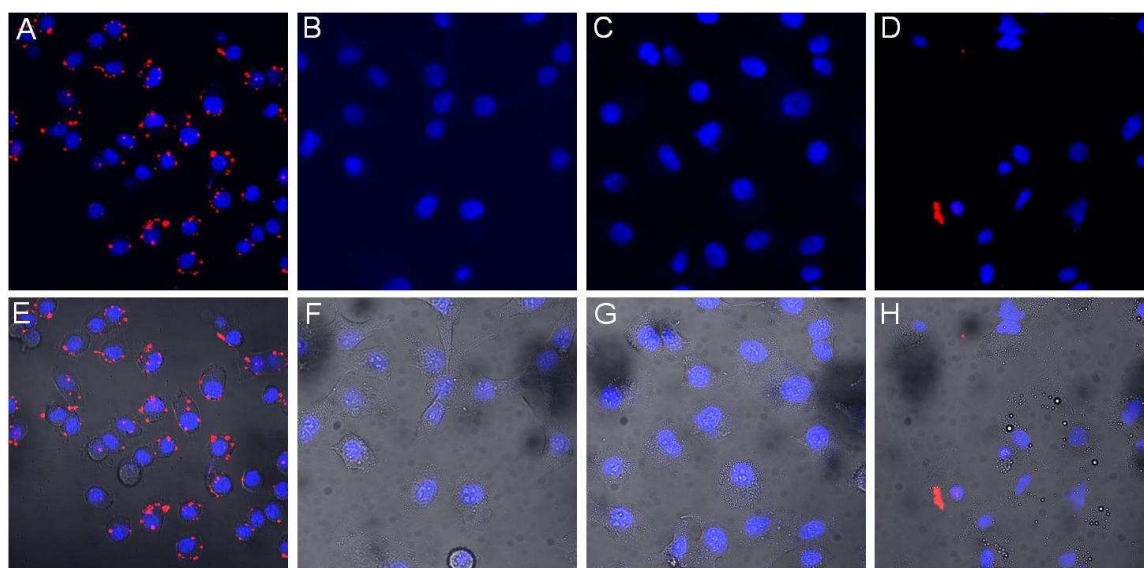


Fig. 3.30 Fluorescence microscopic pictures of the internalization of FoIA-PEG₂₄-K(Stp₄-C)₂ polyplexes. A-D: overlay of DAPI and Cy5 channel; E-H: overlay of DAPI, Cy5 and transmission channel. A,E: KB cell transfected with FoIA-PEG₂₄-K(Stp₄-C)₂; B,F: KB cell transfected with FoIA-PEG₂₄-K(Stp₄-S)₂, C,G: KB cells transfected with A-PEG₂₄-K(Stp₄-C)₂; D,H: Neuro2A cells transfected with FoIA-PEG₂₄-K(Stp₄-C)₂. For all transfection Inf7-siAHA1-Cy5 was used. The experiment was performed by Thomas Fröhlich as part of his PhD thesis (in preparation).

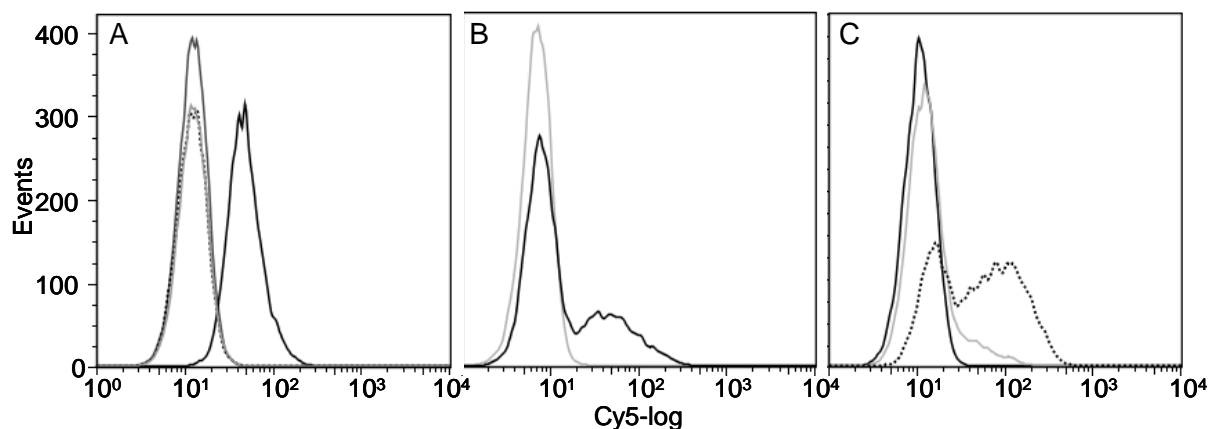


Fig. 3.31 Flow cytometric analysis of receptor mediated cell uptake of FoliA-PEG₂₄-K(Stp₄-C)₂ polyplexes. A: KB cell were transfected using functional FoliA-PEG₂₄-K(Stp₄-C)₂ (black line), non-functional A-PEG₂₄-K(Stp₄-C)₂ (dashed line) or non-functional FoliA-PEG₂₄-K(Stp₄-S)₂ (light grey line). Untransfected cells: dark grey line. B: Folic acid receptor negative Neuro2A cells were transfected using functional FoliA-PEG₂₄-K(Stp₄-C)₂ (dark line). Control cells: light grey line. C: cell association assay on ice. KB cells were incubated on ice with FoliA-PEG₂₄-K(Stp₄-C)₂ without (dashed line) and with (grey line) preincubation with free folic acid. Untransfected control cells: black line. The experiment was performed by Thomas Fröhlich as part of his PhD thesis (in preparation).

The resulting histogram (Fig. 3.31) shows that polyplexes formed with folic acid targeted polymers were taken up very efficiently, indicated by the strong shift of the graph (Fig. 3.31A). In comparison polyplexes carrying just a PEG chain without ligand do not enter the cell. The uptake of folate receptor targeted polyplexes is strongly reduced on a folate receptor negative Neuro2A cell line (Fig. 3.31B) and can be inhibited by preincubation with free folic acid (Fig. 3.31C). Results were supported by microscopic pictures (Fig. 3.30). Summarizing, these results prove that the uptake of these particles is only receptor mediated lacking unwanted unspecific cell attachment.

3.3.4 Specific *in vitro* gene silencing activity of FoliA-PEG₂₄-K(Stp₄-C)₂ in combination with endosomolytic active siRNA

In the last chapter the functionality of every single substructure of the carrier system has been shown. Although the carrier works as expected, the system does not lead to an efficient knockdown when complexed with siRNA (data not shown). Initial experiments on DNA delivery revealed, that the carrier system shows no endosomal

escape ability. Thus it was decided to combine this defined and efficient carrier system with the endosomolytic active peptide-siRNA hybrid described in chapter 3.1. If the endosomal escape is the only remaining bottleneck of the system, this combination should lead to an efficient knockdown in KB cells, stably expression eGFP-Luciferase. To show the necessity and functionality of all substructures not only in special designed experimental settings but also during *in vitro* transfection, controls lacking targeting, crosslinking ability, the endosomolytic peptide or the reducible linkage between Inf7 and siRNA were used for transfection as well (Fig. 3.32).

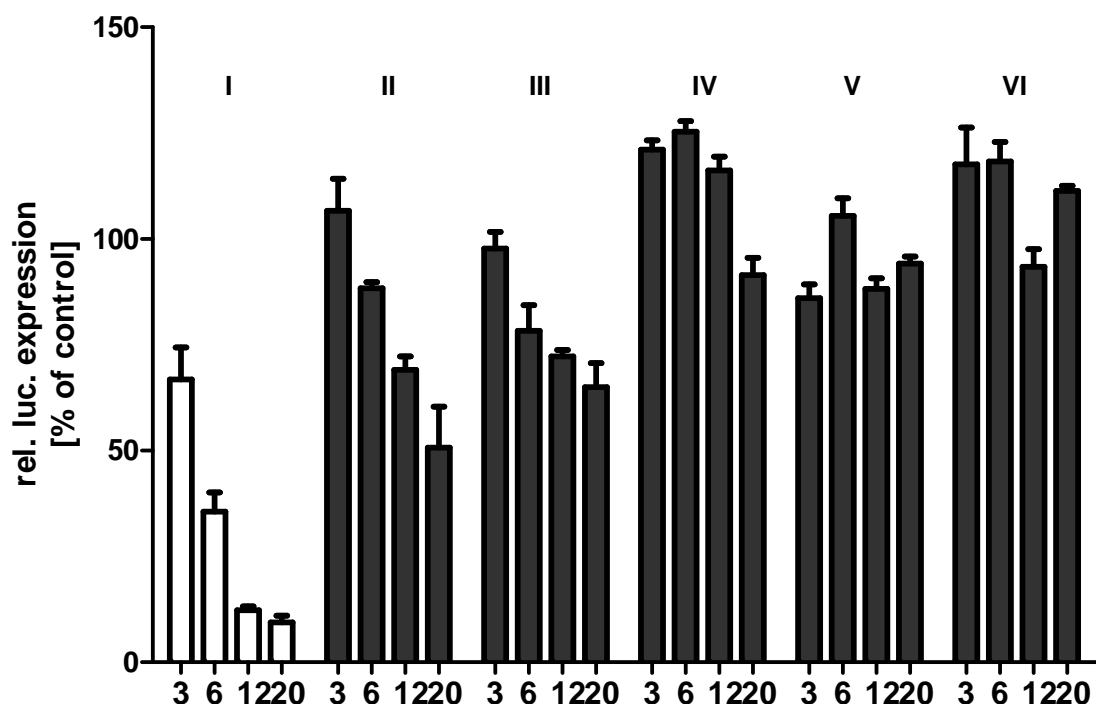


Fig. 3.32 *In vitro* gene silencing combining FoliA-PEG₂₄-K(Stp₄-C)₂ with Inf7-siRNA. Folic acid receptor positive KB cells stably expressing the eGFP-Luciferase gene were transfected with FoliA-PEG₂₄-K(Stp₄-C)₂ combined with Inf7-siGFP (I), FoliA-PEG₂₄-K(Stp₄-C)₂ combined with Inf7-Mal-siGFP (II), FoliA-PEG₂₄-K(Stp₄-C)₂ combined with siGFP (III), A-PEG₂₄-K(Stp₄-C)₂ combined with Inf7-siGFP (IV), FoliA-PEG₂₄-K(Stp₄-S)₂ combined with Inf7-siGFP (V) or FoliA-PEG₂₄-K(Stp₄-C)₂ combined with Inf7-siCtrl (VI). 3-20: used nitrogen to phosphate (N/P) ratio for polyplex formation.

As expected, the only combination of structures that leads to a specific knockdown, is the functional carrier in combination with the endosomolytic active siRNA. All other structures do not show any effect on gene expression. The only controls showing a slight concentration dependent knockdown, is the combination of the functional carrier with unmodified siRNA or same construct with non-reducible linkage between Inf7 and siGFP, indicating that the endosomal escape has been a crucial bottleneck.

After the specific knockdown of an “artificial” gene could be demonstrated, this system was used to silence the endogenous target EG5 (KSP). This protein is active in spindle formation during mitosis. Literature describes that the down regulation of this protein leads to a mitotic arrest, showing a characteristic mitotic figure in the nucleus (aster formation).¹⁴¹ As this allows readout by microscopy, this system was chosen as endogenic target. The comparison of the targeted carrier with the untargeted analogue led to the results shown in Fig. 3.33.

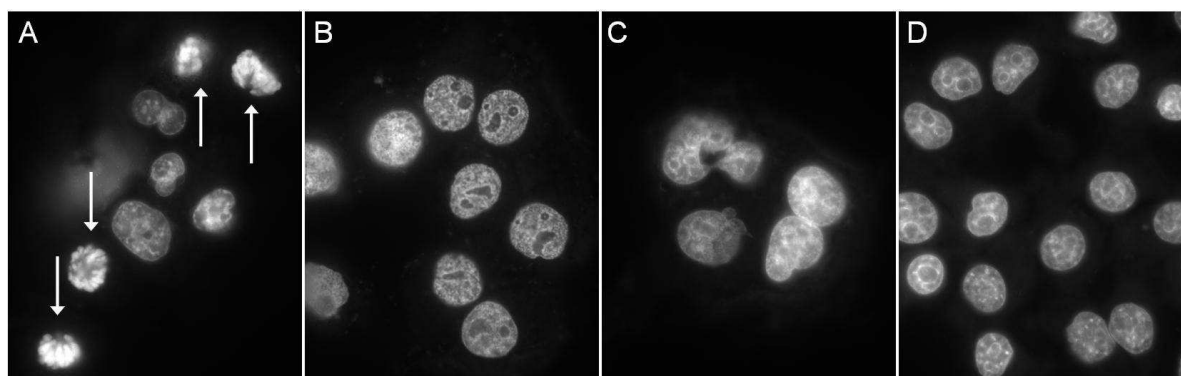


Fig. 3.33 Microscopic pictures of *in vitro* knockdown experiments using EG5 as endogenic target. KB cells were transfected using Inf7-siEG5 in combination with Fola-PEG₂₄-K(Stp₄-C)₂ (A) or A-PEG₂₄-K(Stp₄-C)₂ (C), or Inf7-siCtrl in combination with Fola-PEG₂₄-K(Stp₄-C)₂ (B) or A-PEG₂₄-K(Stp₄-C)₂ (D). Arrows: detected spindle arrest. The experiment was performed by Daniel Edinger as part of his PhD thesis (in preparation).

As the microscopic pictures demonstrate, the only experimental setting showing the specific mitotic figure is the combination of Fola-PEG₂₄-K(Stp₄-C)₂ with Inf7-siEG5 for transfection (Fig. 3.33 A). In all other settings no aster formation could be observed (Fig 3.33 B-D).

Summarizing this chapter, the synthesis of a pure and defined polycationic carrier including shielding and targeting could be demonstrated. The functionality of the substructures could be shown, resulting in an efficient and specific gene silencing *in vitro*.

3.3.5 Biodistribution of siRNA using FoIA-PEG₂₄-K(Stp₄-C)₂ in combination with Inf7-siRNA

After the positive results of characterization and evaluation of the new carrier system *in vitro*, it was decided to test the efficiency of the delivery system *in vivo*. For this purpose KB cells were used in a subcutaneous tumor model in NMRI nude mice.

As the particle size of the designed carrier system was measured to be around 6 nm in diameter and therefore below the molecular cut off of the kidney, it was hypothesized that these particles are not able to circulate stable after systemic application. This could be demonstrated in initial experiments (data not shown). Therefore different analogues have been designed and synthesized in a further screen to increase the particle size and explore the particle behaviour during systemic circulation. Two concepts were chosen:

- elongation of the PEG chain for an increased shielding layer
- incorporation of lipid structures to force agglomeration to bigger particles and/or interactions with blood compounds

These criteria led to the structures shown in Fig. 3.34 and 3.35 for the *in vivo* screen.

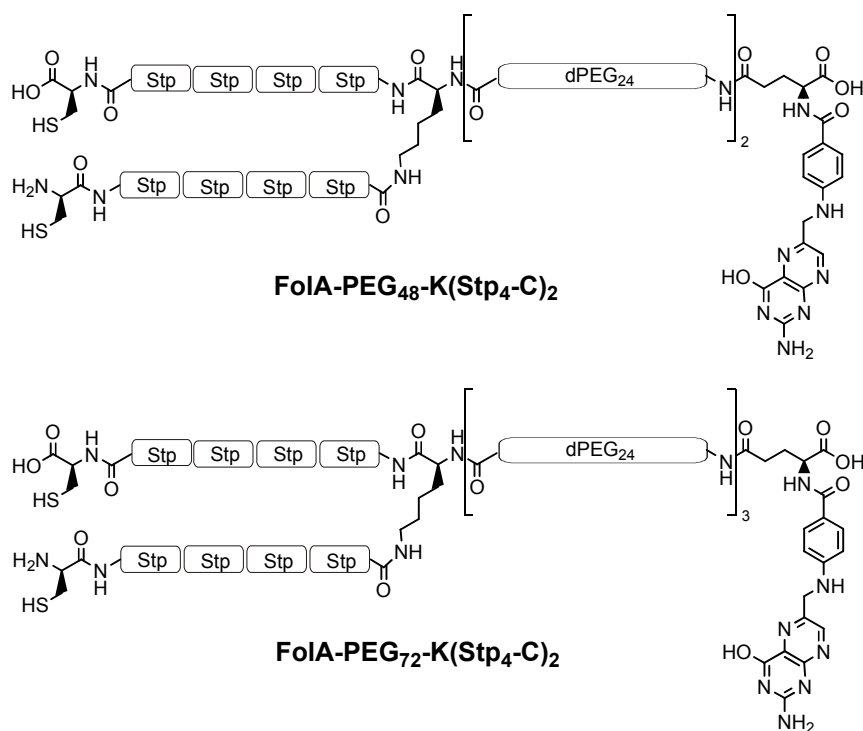


Fig. 3.34 FoIA-PEG₂₄-K(Stp₄-C)₂ analogues with increased PEG length.

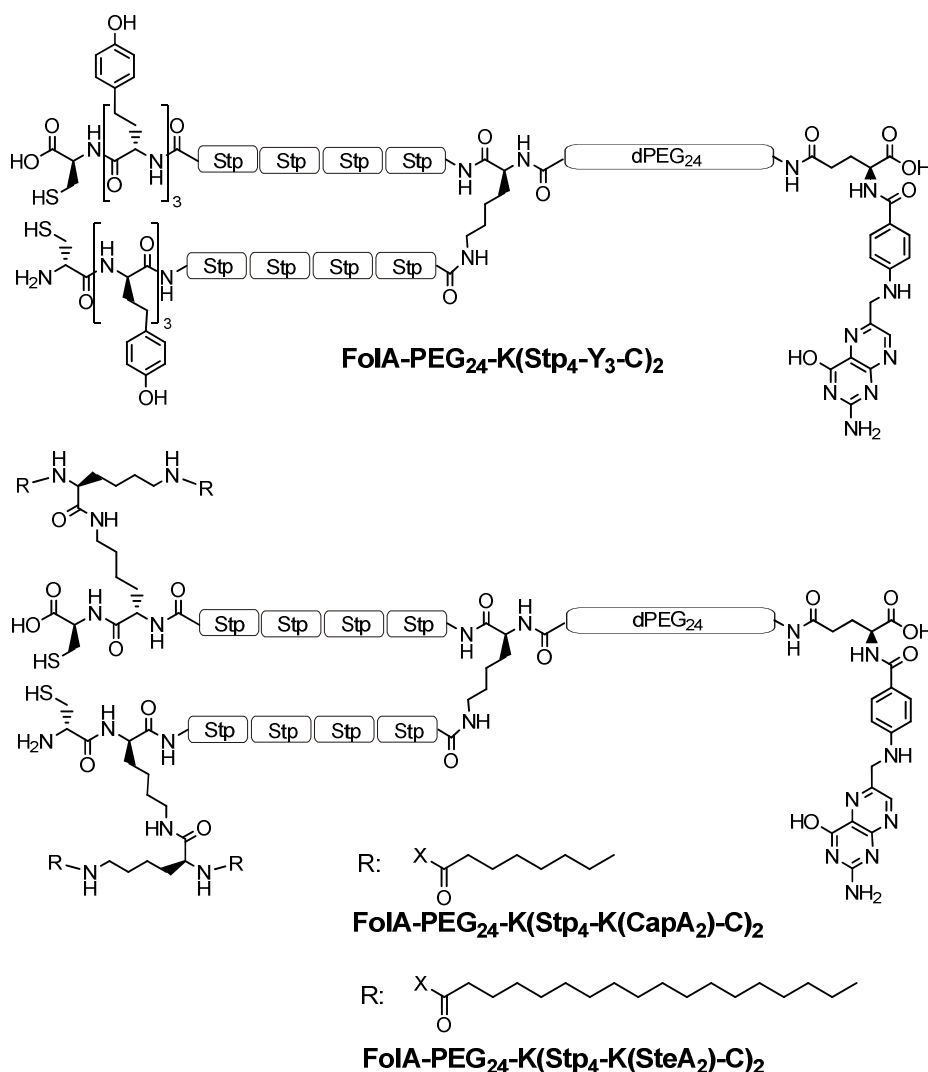


Fig. 3.35 FoIA-PEG₂₄-K(Stp₄-C)₂ variations with hydrophobic modifications.

The elongation of the PEG chain was performed, repeating the conjugation step of Fmoc-amido-dPEG₂₄-acid two- or three times. As hydrophobic domains for increased aggregation and interaction with blood compounds three different variants were tested: tyrosines as short hydrophobic domain, caprylic acid with a medium length, and stearic acid as long hydrophobic modification.

After synthesis these carriers were used in combination with Inf7-siRNA to determine the influence of the modification on the particle size of the polyplex. Therefore the diameter was determined by fluorescence correlation spectroscopy (FCS) measurements. Results (table 3.8) demonstrate that these small variations in carrier design lead to significant differences in particle size.

Table 3.8 Particle size of polyplexes of different carrier variants and Inf7-siRNA. Particles have been formed in HBS buffer. r_h : hydrodynamic radius.

Carrier	r_h [nm]
FoIA-PEG ₄₈ -K(Stp ₄ -C) ₂	3.2 (± 0.1)
FoIA-PEG ₇₂ -K(Stp ₄ -C) ₂	4.4 (± 0.1)
FoIA-PEG ₂₄ -K(Stp ₄ -Y ₃ -C) ₂	2.8 (± 0.2)
FoIA-PEG ₂₄ -K(Stp ₄ -K(K(CapA) ₂ -C) ₂	16.9 (± 0.2)
FoIA-PEG ₂₄ -K(Stp ₄ -K(K(SteA) ₂ -C) ₂	160.3 (± 0.6)

The elongation of the PEG chain has a moderate effect, increasing the hydrodynamic radius from 3.0 nm (1 PEG) to 3.2 nm (2 PEG) and 4.4 nm (3 PEG). In contrast the hydrophobic modifications led to particles with great differences in particle size. While the tyrosine motif did not change the particle size, modification with caprylic- and steric acid resulted in particles with a size of 16.9 and 160 nm.

To exclude that the modification of the structure leads to a negative impact on toxicity or silencing efficiency all structures were tested in the standard *in vitro* screen as explained under 3.3.4 (Fig. 3.36).

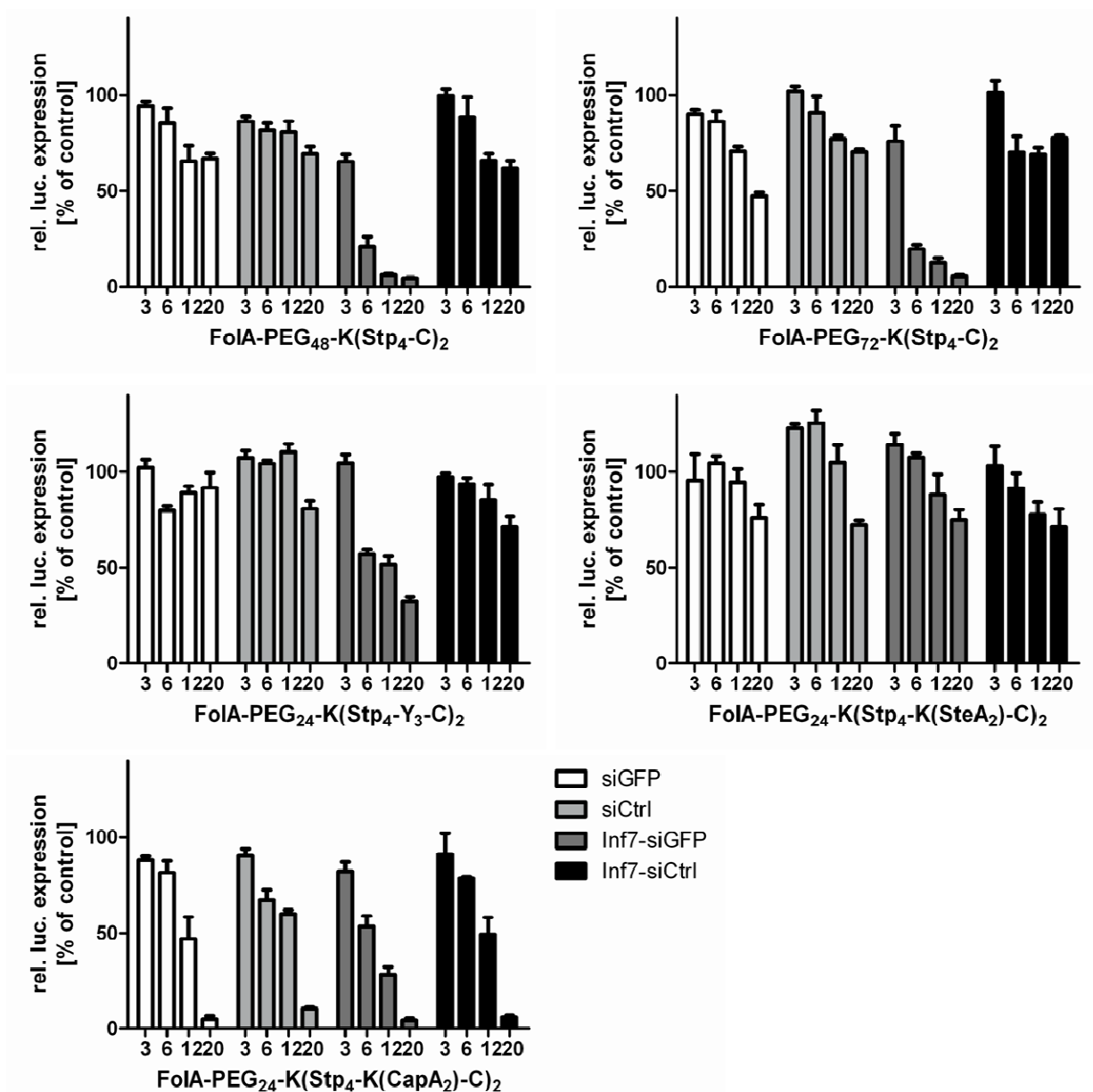


Fig. 3.36 *In vitro* gene silencing, using different variations of FoIA-PEG₂₄-K(Stp₄-C)₂. Folic acid receptor positive KB cells stably expressing the eGFP-Luciferase gene were transfected with the different modified versions of FoIA-PEG₂₄-K(Stp₄-C)₂ in combination with siGFP (white bars) siCtrl (light grey bars), Inf7-siGFP (dark grey bars) or Inf7-siCtrl (black bars). 3-20 used nitrogen to phosphate (N/P ratio for polyplex formation. Data is presented as relative value compared to HBG treated cells.

The transfection results show that the modification of the carrier backbone has a strong influence on the silencing efficiency *in vitro*. For the two constructs with the elongated PEG chain (FoIA-PEG₄₈-K(Stp₄-C)₂ and FoIA-PEG₇₂-K(Stp₄-C)₂) the combination with Inf7-siRNA resulted in a specific reporter gene silencing comparable with the efficiency of the initial construct (FoIA-PEG₂₄-K(Stp₄-C)₂), while transfection with unmodified siRNA resulted in absence of gene regulation. In contrast to this

finding the combination of the three hydrophobic modified versions of the model compound with Inf7-siRNA did not result in an efficient knockdown. The use of Fola-PEG₂₄-K(Stp₄-Y₃-C)₂ showed a medium silencing effect of approximately 50% expression under used conditions, while the use of fatty acid modified carriers did not result in a significant difference in reporter gene silencing between Inf7-siGFP and Inf7-siCtrl or unconjugated siRNA. In contrast to the PEG variants carriers containing fatty acids led to a medium (in case of stearic acid) or high (in case of caprylic acid) concentration dependent toxicity.

Although not all constructs were efficient in *in vitro* gene silencing, the constructs were used to perform studies on the influence of particle size on the biodistribution *in vivo*. For this purpose polyplexes of the single constructs in combination with 50 µg Cy7 labeled siRNA in an N/P ratio of 16 were injected intravenously into NMRI nude mice, carrying a subcutaneous KB tumor. Animals were imaged 0.25, 1 and 4 h after injection by near infrared fluorescence imaging using an IVIS Lumina system. Exemplary images of one animal per group are shown in Fig. 3.37 and 3.38.

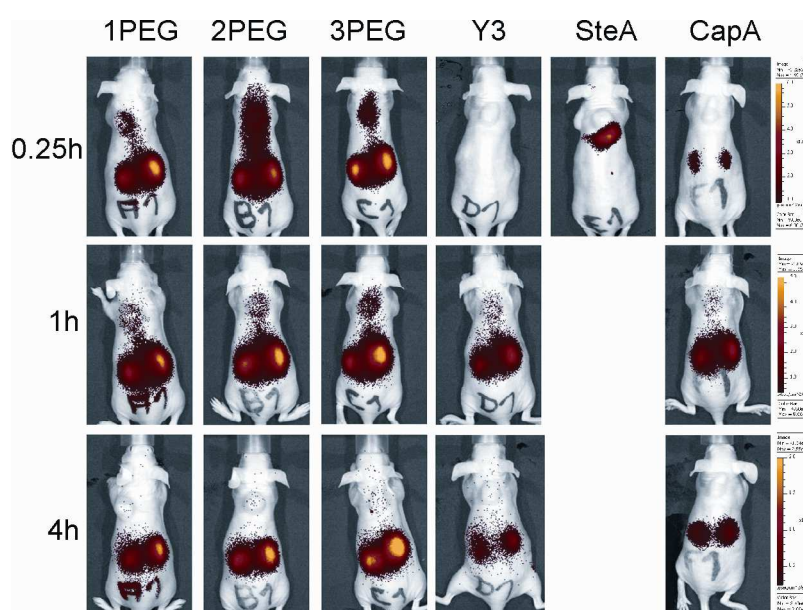


Fig. 3.37 Biodistribution of siRNA in combination with different polycationic backbones, ventral position. Polyplexes containing Cy7-labeled siRNA and one of the six targeted, polycationic backbones were injected systemically into NRMI nude mice. Mice were imaged 0.25, 1, 4 h after injection. The experiment was performed by Laura Schreiner and Daniel Edinger as part of their PhD thesis (in preparation).

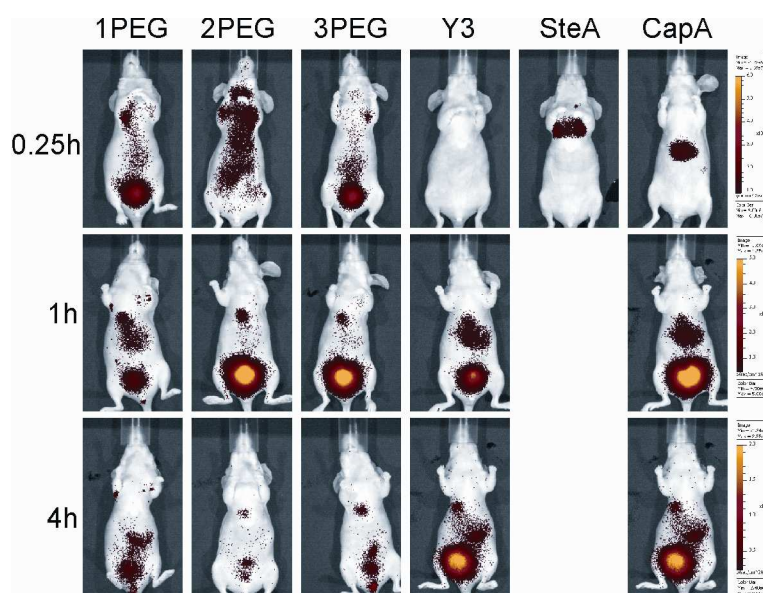


Fig. 3.38 Biodistribution of siRNA in combination with different polycationic backbones, dorsal position. Polyplexes containing Cy7-labeled siRNA and one of the six targeted, polycationic backbones were injected systemically into NRM1 nude mice. Mice were imaged 0.25, 1 and 4 h after injection. The experiment was performed by Laura Schreiner and Daniel Edinger as part of their PhD thesis (in preparation).

As demonstrated by the NIR fluorescence images the different structures of the polycationic carriers led to alterations in biodistribution. Comparing the carriers with altered PEG length no significant changes can be observed. All particles do not interact with any tissue and are cleared efficiently *via* renal filtration. In contrast particles with hydrophobic modifications showed a different behaviour. With increasing hydrophobicity ($Y_3 < CapA$) the particles have an increased delay within the liver before the Cy7 signal appears in kidney and bladder. Particles containing stearic acid showed a strong accumulation in the lung and a high toxicity. The animal died after injection.

As the detected Cy7 label was covalently attached to the backbone of the siRNA the imaging experiments show just the distribution of siRNA molecules and not of siRNA bound in a polyplex. Thus the fast renal filtration could be a result of a low particle stability and thus filtration of released siRNA and not of particles. In case of hydrophobic modified particles, this could be excluded due to the observed retention in liver or lung that cannot be observed in case of the injection of free siRNA. To prove the theory of stable particles that are cleared due to small size, the urine of mice was

checked for appearance of particles and free siRNA after systemic administration of FoIA-PEG₂₄-K(Stp₄-C)₂ and FoIA-PEG₇₂-K(Stp₄-C)₂. For this purpose the urine was analyzed in an agarose gel with (+) or without (-) preincubation with particle disruptive agents (Fig. 3.39).

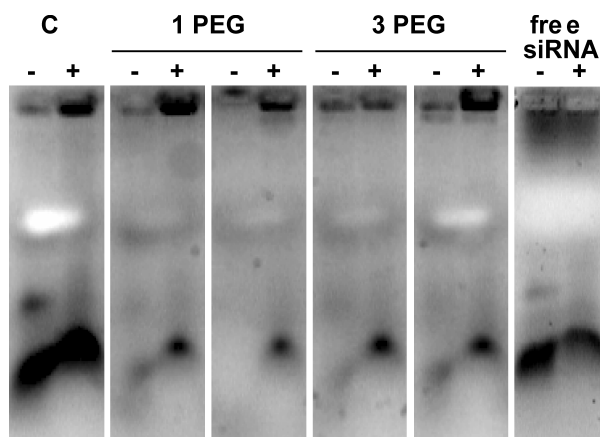


Fig. 3.39 Gel migration assay of urine samples. Urine of NMRI nude mice was collected by punctation 4 h after systemic injection of polyplexes containing Inf7-siRNA in combination with FoIA-PEG₂₄-K(Stp₄-C)₂, (1PEG) or FoIA-PEG₇₂-K(Stp₄-C)₂, (3PEG). C: Control (free siRNA as internal standard; free siRNA: siRNA that has been injected without complexation with polymer. -: Sample was analyzed without further treatment, +: Sample was treated with TCEP and heparin and incubated for 10 min before analysis. The experiment was performed by Laura Schreiner as part of her PhD thesis (in preparation).

In this gel migration assay urine samples of animals treated with polyplexes of siRNA with the two polycations were compared with the urine of animals treated with free siRNA and a siRNA sample that has not been injected into an animal. Both control siRNA samples show a similar migration pattern. Thus free siRNA is rapidly cleared *via* the kidney and not processed inside the body. Although the migration distance is slightly different when the samples were preincubated with TCEP and heparin, the strength of the band is not altered. In comparison, the urine samples of mice treated with polyplexes show a different pattern. While there is just a minimal signal of free siRNA if the urine is not preincubated with TCEP and heparin, the band signal increases significantly when the polyplex destabilizing agents are used. This indicates that the signal detected in the urine by imaging experiments is labeled siRNA bound in polyplexes. Thus the polyplexes are stable during blood circulation and are cleared if not detected by the target tissue.

The absence of a Cy7 signal in the tumor tissue does not necessarily result in the absence of gene knockdown. Just few siRNA molecules might have to enter the tumor cells to result in efficient target gene silencing. Therefore Inf7-siEG5 was injected in combination with FoliA-PEG₂₄-K(Stp₄-C)₂ using the same *in vivo* model as already described. At 24 h after treatment animals were sacrificed, tumors harvested and analyzed for mitotic figure by cryosection and microscopy (Fig. 3.40).

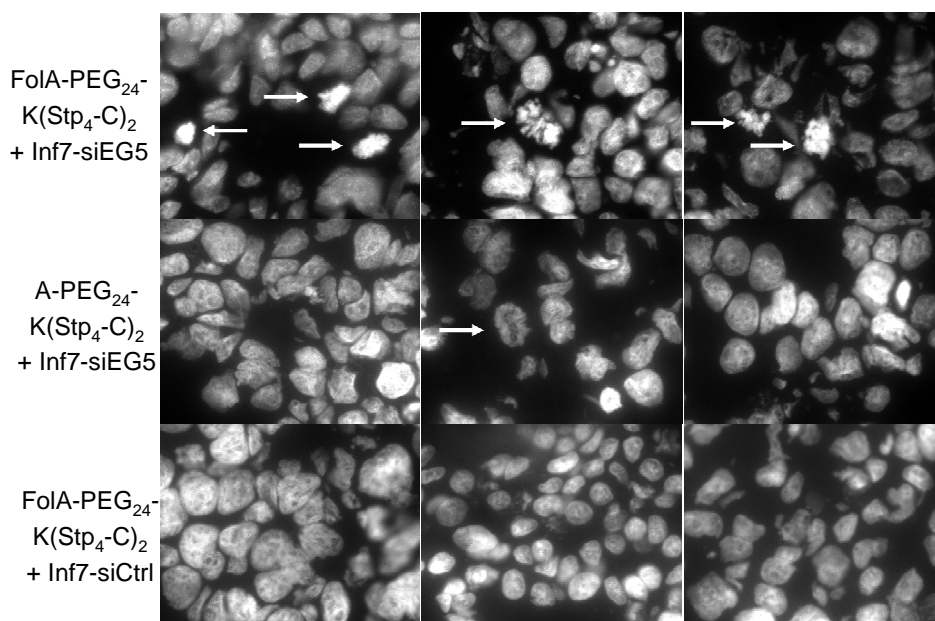


Fig. 3.40 Aster formation after systemic application of Inf7-EG5. 24 h after systemic treatment of NMRI mice, bearing a subcutaneous KB tumor, with Inf7-EG5 in combination with FoliA-PEG₂₄-K(Stp₄-C)₂ or controls, tumors were harvested. Slices were stained with DAPI to visualize the nucleic. Arrows: detected mitotic figures. The experiment was performed by Laura Schreiner and Daniel Edinger as part of their PhD thesis (in preparation).

The tumor sections show aster formation when EG5-siRNA was injected either in combination with the targeted or the nontargeted polycation. Treatment with control siRNA did not result in the formation of mitotic figures. Thus gene silencing could be demonstrated, although just small amounts of siRNA enter the tumor tissue. As the detection of mitotic figures is just a semiquantitative method, a clear benefit of folic acid targeted particles could neither be proved nor be disproved. Therefore further experiments had to be carried out.

3.3.6 Proving *in vivo* tumor targeting *via* intratumoral treatment.

In the last section the behaviour and functionality of the designed carrier system was evaluated *in vivo*. It could be demonstrated, that the particles are stable during blood circulation, inert to nontargeted tissue and cleared when not recognised by the target tissue. Although just small amounts of siRNA reached the tumor side, the carrier system was efficient enough to lead to target gene silencing as shown by the appearance of mitotic figures after treatment with Inf7-siEG5. Although more asters were observed for targeted structures, in the analyzed tumor slices, this method is not applicable for quantification. An *in vivo* bioimaging method should give a more quantitative result for the targeting ability of a carrier system. As the detection of the Cy7 signal after systemic administration was not sensitive enough to quantify the accumulation of siRNA in the tumor tissue, the amount of siRNA that reaches the tumor should be maximized in a second imaging experiment. Therefore labeled siRNA was injected intratumoral into the subcutaneous KB NMRI nude model.

The tumor signal of free siRNA was compared to polyplexes in combination with either FoIA-PEG₂₄-K(Stp₄-C)₂ or A-PEG₂₄-K(Stp₄-C)₂. Resulting kinetic is shown in Fig. 3.41.

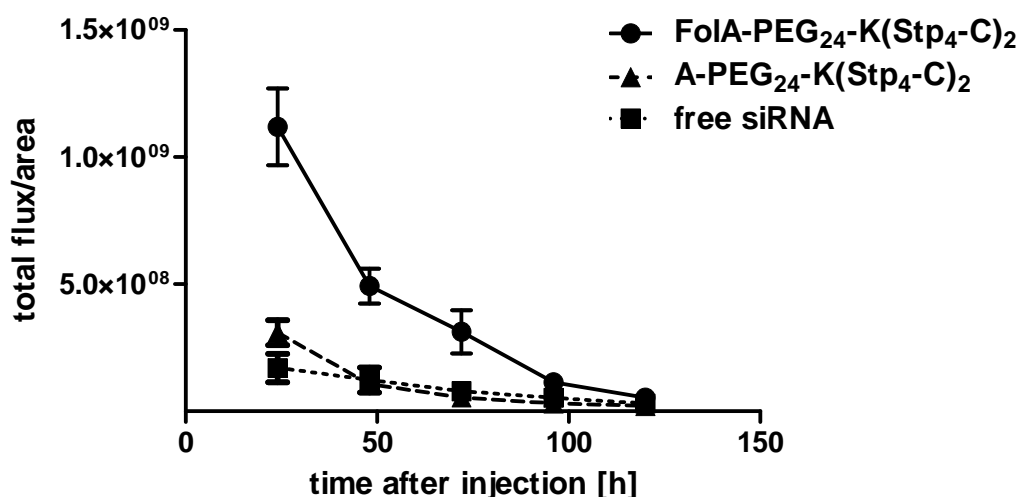


Fig. 3.41 Tumor retention of folic acid targeted polyplexes. After local injection of 50 µg Cy7-labeled siRNA in combination with FoIA-PEG₂₄-K(Stp₄-C)₂ or its controls in a N/P ratio of 16, animals were imaged for NIR fluorescence every 24 h. The experiment was performed by Laura Schreiner and Daniel Edinger as part of their PhD thesis (in preparation).

The intratumoral application of labeled siRNA shows a significant increased retention of targeted polyplexes over nontargeted polyplexes and free siRNA. These data prove that tumor targeting by folic acid results in polyplexes with an increased affinity to its target tissue.

In conclusion this chapter demonstrates the synthesis of a molecular defined, monodisperse, polycationic carrier by solid phase supported peptide synthesis. This carrier bears special functionalities, addressing single steps during the delivery process. Due to the synthesis strategy, the design of the molecule can be controlled in every single detail. In combination with Inf7-siRNA this carrier is able to silence a specific gene *in vitro*, demonstrating the synergistic effect of the single functional domains. Although resulting particles were shown to be very small and thus get cleared *via* the kidney, these particles were able to generate gene silencing in their target tissue and show high tolerability to the animal, due to a perfect shielding. Significant influence of the targeting moiety was demonstrated by intratumoral application of this complex carrier.

4 Discussion

4.1 An endosomolytic active peptide-siRNA hybrid as structural defined molecule for enhanced endosomal escape in siRNA carrier systems

The delivery of siRNA to target cells is a very complex process, wherein many different steps play a role. A perfect delivery system addresses every single step of this process, overcoming its limitation as efficient as possible. One of the most crucial hurdles is the escape out of the endosomal compartment. After cell attachment of the delivery system *via* unspecific ionic interactions or *via* specific target cell interactions, common polyplexes are taken up into the cell by endocytosis. The resulting endosomes are further processed to lysosomes in order to inactivate their payload and protect the cell. Thus an efficient escape out of the endosome is crucial for a functional carrier system. Overcoming this hurdle, different approaches have been investigated that can be divided into two groups. One possibility is the enhancement of the buffering capacity of the carrier system, based on e.g. ethylenimine units¹⁴⁵ or the incorporation of histidines.¹⁴⁶ The second possibility is the incorporation of membrane active structures like fatty acids or lytic peptides.^{128, 147} Both approaches imply the chemical modification of the carrier system. Working with polymers and common linker chemistry, this leads to very heterogenic products. In general the chemical characterization is limited or disabled.

For the current study structural definition of compounds was a key criterion. Thus the idea was to design an endosomolytic active peptide-siRNA hybrid. This structure should be combined with a polymeric delivery system (with or without endosomal escape ability) to improve its efficiency. A peptidic endosomolytic modification in contrast to a polymeric buffering domain was chosen, because published work already showed that the incorporation of such peptides into a carrier system leads to a strongly enhanced delivery.^{123, 128} The attachment of the peptide to siRNA was chosen for different reasons. (i) The hybrid leads to a covalent attachment of endosomolytic domain and siRNA and therefore to a stable interaction of structures that have to end up in one endosome to be functional. (ii) This design leads to a structural defined molecule. To show a general proof of concept, Inf7, a designed peptide based on the amino-terminus of the influenza virus hemagglutinin was chosen as model peptide. Its

negatively charged sequence minimises undesired interactions with the siRNA, while its pH dependant lytic activity has shown to enhance the endosomal escape of delivery systems.¹²³

For the synthesis of the construct a thiol modified siRNA has been chosen. The conjugation was performed by activation of the thiol group followed by attachment of the cysteine modified peptide (Fig. 3.1). This synthesis route allows a controlled reaction. The siRNA is highly soluble under aqueous conditions. Its high charge density allows a fast and scalable purification. Thus educts such as DTNB and Inf7 can be used in high excess, shifting the reaction to the product side. Furthermore this reaction type enables an easy adoption to other siRNA sequences and different peptides. As shown in chapter 3.2 the same protocol has shown to be effective for the synthesis of targeted and pegylated siRNA constructs. Qualitative (Fig. 3.4) as well as quantitative analyses (Fig. 3.3) revealed the identity of the reaction product and a purity above 95%.

The covalent conjugation of peptides to siRNA has already been published by different groups. Leading approaches show the covalent attachment of cell penetrating peptides (CPPs) or protein transduction domains (PTDs) to the siRNA backbone.¹⁴⁸⁻¹⁵¹ These peptides are derived from sequences of proteins that are able to cross the cell membrane. The conjugation was performed to mediate cellular uptake of siRNA by cells. In all these approaches the conjugation was performed in different ways. Acid cleavable linkers have been used as well as linkers cleaved under reductive conditions or non-cleavable linkers. But literature reveals that the possibility of siRNA modification is discussed controversial.¹⁴² Modifications have been described at all four ends of the siRNA double strand.¹⁵⁰⁻¹⁵³ A modification of siRNA always can have an influence on its silencing efficiency. To be active, the siRNA has to be recognized by, and incorporated into the RISC. A modification of one end could alter its structural accessibility and thus hamper the interaction with the RISC, resulting in a reduced activity. The position of the attachment as well as the type of linkage has therefore to be chosen carefully. In most cases a reduced activity has been explained by delivery processes, but a side by side comparison of the activity of modified and unmodified siRNA has just been performed in a few cases.^{151, 154} In this approach the endosomolytic active peptide Inf7 was covalently attached to the 5'-end of the siRNAs sense strand. As it is reported that the 5'-end of the antisense strand is very important for RNA interference, this position should be the least influencing position and thus

ideal for conjugation. The functionality assay revealed that our hypothesis was right. The modification of the antisense strand with Inf7 at this position did not influence its activity (Fig. 3.6).

A second important question in the design of a peptide-siRNA hybrid is the influence of the siRNA attachment on the activity of the peptide. In case of CPPs or PTDs no separate examination has been described yet. In this thesis the lytic activity of the attached peptide could be demonstrated in an isolated assay (Fig. 3.5). Incubation of erythrocytes with free Inf7 peptide and the Inf7-siRNA hybrid revealed that the covalent modification with a negatively charged macromolecular siRNA does not influence the peptides activity nor its pH specificity in this conjugate. Within these experiments it could be shown in a side by side comparison in isolated assays that the activity of both, siRNA and Inf7 peptide are not significantly influenced by the synthesis of a hybrid structure.

Further experiments combining endosomolytic siRNA and polymers with a low endosomal escape efficiency (Fig. 3.8 and Fig. 3.32) show that this construct is able to increase the silencing efficiency of the carrier system. Control experiments reveal that the raised activity is due to an enhancement of endosomal escape. Both tested polymers, the nontargeted structure **76**, as well as the targeted polymer FoIA-PEG₂₄-K(Stp₄-C)₂ do just show an increased knockdown if peptide modified target siRNA is used. All controls lacking either the peptide or the siRNA target sequence do not lead to an efficient down regulation of expression. As an increased particle size (e.g. due to aggregation) is known to have an influence on the silencing efficiency *in vitro*, it was checked, if the modification leads to an altered polyplex formation. Results showed that particles formed with modified siRNA do not differ from particles formed with unmodified siRNA (Fig. 3.7, table 3.2).

In combination with FoIA-PEG₂₄-K(Stp₄-C)₂ it could also be shown that the disulfide bridge connecting siRNA and peptide is very important. A control, where the reducible disulfide bond is replaced by a non-cleavable maleimid, resulted in a strong reduction of gene knockdown. Thus it seems to be very important for the silencing efficiency of the siRNA that the peptide is cleaved in the reductive cytosolic environment to result in an active siRNA (Fig. 3.32).

Concluding these results, the synthesis of a structural defined hybrid of functional siRNA and endosomolytic active Inf7 peptide could be realized. Structure and purity could be verified. The functionality of the substructures has been shown in detail

leading to an efficient delivery system when combined with a polycationic carrier. Raised activity in comparison to unmodified siRNA could be shown to be exclusively due to an enhanced endosomal escape. Thus endosomolytic siRNA displays a beneficial method to overcome the bottleneck of endosomal escape. This increases the design space of used carriers, because they are no longer limited to an own endosomal escape ability.

4.2 Targeted siRNA as defined structure for enhanced cell specificity and uptake

RNA interference takes place in the cytosol. Thus siRNA has to cross the cellular membrane to become an active drug. As negatively charged macromolecule, the nucleic acid needs a delivery system to overcome this hurdle. Besides endosomal escape (discussed in section 4.1) the specific attachment and uptake by the cell is one of the main limitations during the delivery process. Basic approaches on siRNA delivery with polymers used the positive charge of the resulting polyplex to attach to the negative charged cell surface. This rather unspecific attachment leads to cell entry *via* endocytosis.¹⁴⁵ This method has been shown to result in gene silencing under *in vitro* as well as under *in vivo* conditions for several polymers. Although the method is very efficient, it bears disadvantages. Positive charged polyplexes have the same affinity to all cells, not distinguishing between target and nontarget cells. This causes undesired transfection of cells and thus side effects especially *in vivo*. For an efficient delivery the polyplex has to be highly charged which also leads to interactions with several compounds in the extracellular environment, resulting in aggregation or loss of function. To reduce side effects and increase siRNA delivery to target cells, specific ligands have been incorporated into the delivery vehicle. These ligands address specific receptors, ideally highly expressed on target cells. Attachment of the ligand to the receptor results in specific internalization of the carrier.

Incorporation of specific ligands into a carrier system has been described using several methods. The type of conjugation can be separated into two main groups. Either the ligand is attached covalently to the polymer^{105, 155} or to the siRNA backbone.¹⁵⁶⁻¹⁵⁷

As described in chapter 3.2 a targeted siRNA was synthesized enabling the specific delivery of the nucleic acid to its target cell in this work. As structural definition was the

main topic of this thesis a synthesis route had to be designed that allowed the construction of a molecular defined ligand structure and a conjugation method that allows the purification and identification of the product.

As synthesis platform for the ligand structure, Fmoc based solid phase supported peptide synthesis (SPPS) was chosen. This method first published by Merrifield *et al.*¹³⁷ allows the controlled generation of defined macromolecules on a solid support using a high excess of educts, eliminating unreacted material by simple filtration steps. Although this strategy allows the generation of pure products it limited the choice of ligands to structures that can be integrated *via* a solid phase coupling step. Besides peptide ligands like GE11 or B6, folic acid displays a feasible structure for SPPS. Being composed of glutamic acid and pteric acid connected *via* an amide bond, this structure could be synthesized in two steps on solid support, as already been shown by Kazanova *et al.*¹¹⁸ Protected educts were commercially available and therefore an ideal candidate for targeting. Folic acid was preferred as model, because it is a small molecular ligand with a high binding affinity to its receptor. It has been used in several approaches for targeted delivery to tumor cells. Its ligand is reported to be upregulated in many different cancer types,¹¹¹⁻¹¹² while it is almost absent on other cells, despite of the apical membrane of epithelial cells in the kidney proximal tubules¹¹⁵ and activated monocytes and macrophages.¹¹⁶ Therefore it bears all criteria for an efficient model structure. In general targeting ligands, especially small molecules are attached to its cargo *via* a polyethylene glycol (PEG) spacer. This structure allows the local separation of targeting moiety from the nucleic acid and thus an increased recognition by the receptor. Considering structural definition, the PEG spacer in general represents the most crucial part in these kinds of constructs. In similar constructs described in literature, bifunctional PEG linkers have been used.¹⁵⁸⁻¹⁶⁰ The ligand has selectively been attached to one side, the siRNA to the other side. The application of two different reaction types for attachment limits the use of ligand structures and decreases precision. As these PEG-linkers are synthesized by random polymerization, they show a high degree of polydispersity. In the approach described in this thesis, a monodisperse PEG chain was used bearing exactly 24 ethylene glycol subunits (dPEG₂₄). As this structure is commercially available with a ω -carboxyl and an Fmoc-protected α -amino group, it can easily be introduced into the targeting structure *via* SPPS. As coupling domain for the attachment of the siRNA two different structures have been evaluated. First the synthesis was performed similar to the

construction of the endosomolytic siRNA using a terminal cysteine for disulfide formation (Fig. 3.12). Improving the synthesis, the ability to use the 1,3-dipolar cycloaddition was explored. Thus cysteine was replaced by an azide containing building block in later syntheses (Fig. 3.17). For the first studies, the attachment was performed as already described for the peptide-siRNA hybrid *via* a disulfide bond. This bond was used for two reasons. (i) It allowed performing the synthesis analogous to the synthesis of Inf7-siRNA. (ii) Disulfide bonds are thought to be cleaved under the reductive cytosolic environment. Incorporation of a disulfide bond allows the removal of the ligand-PEG structure after cell entry and thus avoids undesired effects. As shown in Fig. 3.14 this strategy leads to a pure and functional conjugate after purification. The disadvantage of this synthesis is its laborious, material- and time-consuming strategy. Three reaction steps (deprotection, activation and coupling) have to be performed, each intermitted by a purification step. As the purification always leads to a loss of 10-20% of the material, shorting the synthesis route would be beneficial. The 1,3-dipolar cycloaddition displays a reaction type that is reported to be very efficient and does not lead to undesired side reactions. Thus it was a useful tool to generate ligand attached siRNA. As mentioned before, the synthesis of the SPPS generated part of the construct was adapted for this purpose by exchanging the thiol bearing cysteine against (S)-5-Azido-2-(Fmoc-amino)pentanoic acid. The siRNA was modified by an alkyne linker, allowing the coupling of the altered construct. The disulfide remained in the structure and was included in the alkyne linker (see Fig. 3.17). This strategy allowed the conjugation *via* a one-step synthesis and one purification step. The resulting product showed same purity and functionality as the former construct. Thus the 1,3-dipolar cycloaddition displays an efficient reaction method for the construction of precise structures.

Functionality assays for the determination of the effect of the conjugation on the biological activity of ligand as well as of siRNA were performed. Using a polymer that already had been reported to work efficiently for siRNA delivery *in vitro* showed that neither the conjugation of PEG nor the additional modification with folic acid influences the silencing efficacy of the siRNA (Fig. 3.21). This result is consistent with the results obtained with Inf7-siRNA. The modification of the double stranded nucleic acid at the 5'-end of its sense strand does not influence the siRNA activity, when the attachment is performed *via* a reducible disulfide bond. In a second assay the binding ability of folic acid to its receptor was determined after coupling. The conjugation of folic acid to

a polymer or biomolecule for cell specific targeting has already been reported in different publications. The most discussed point is the influence of conjugation on the activity of the ligand. The attachment can be performed *via* one of the two carboxyl-groups. As it has been shown, that the attachment *via* the α -carboxyl group results in a strong reduction in receptor affinity, the optimal position would be the γ -carboxyl group of the glutamic acid. In common solution chemistry the conjugation is in general performed by activation of the carboxyl group and conjugation to an amino function. As this method does not allow a determination between the α - and γ -carboxyl function, this leads by theory to ~50% product carrying a ligand with reduced activity. Within the synthesis and conjugation method presented in this thesis, the attachment of PEG-spacer and siRNA was always performed to 100% at the γ -carboxyl function. Therefore all of the modified molecules should retain its high affinity to the receptor. This could also be underlined by uptake studies of the free Folate-PEG₂₄-click-siRNA conjugate. The flow cytometric analysis (Fig. 3.20) as well as the fluorescence microscopy (Fig. 3.19), using labeled siRNA, shows an efficient and very specific uptake of the conjugate *via* the folic acid receptor.

Although it has been proven in single assays that both biomolecules retain its functionality after conjugation, it does not lead to gene silencing after transfection of folic acid receptor expressing KB cells. The same findings were already observed in the work of Thomas *et al.*,¹⁵⁷ where they also did not find any functionality of a similar but more imprecise targeted structure. The reason for the negative result could be shown during this thesis. As no functionality for endosomal escape was incorporated into the structure, the transfection route could not be completed and therefore did not result in gene silencing. This hypothesis could further be underlined, combining the defined structure with a defined polycation, having an endosome disruptive proton sponge property in one polyplex. Addressing this last step of *in vitro* delivery, the construct mediated a very efficient knockdown of the target gene (Fig. 3.24).

In summary, chapter 3.2 proves that the synthesis of a defined monodisperse conjugate of folic acid, PEG and siRNA can be realized. The presented design and strategy allows the control of the molecular structure of the conjugate and enables a clear and distinct analysis with state-of-the-art methods. Due to the knowledge of published findings on the influence of attachment site on activity, the synthesis resulted in a macromolecule with maximal activity. Although this structure is not able to address every single step during the delivery process, it results in specific and

efficient gene silencing when combined with an endosomolytic active polycation. Thus the molecule reduces the role of the polycation to polyplex formation and endosomal escape and therefore increases its design space.

4.3 The combination of a structurally defined, targeted polymer and an endosomolytic active peptide-siRNA hybrid results in a delivery system for specific gene silencing *in vitro* as well as *in vivo*

As already described in the last section, targeting is a crucial step in the delivery of nanoparticles. Besides covalent attachment of a targeting ligand to the backbone of siRNA described in chapter 3.2, coupling the ligand to the polycationic backbone is the most popular strategy in the design of targeted polyplexes. Methods described in literature, in general use polymers with a high polydispersity and chemistry based on rather random attachment of linker molecules to the polymeric side chains.⁵⁷ This strategy leads to the desired result of a targeted polyplex but bears several problems. (i) The high polydispersity of the polymer in combination with the imprecise chemistry results in a very heterogenic mixture of molecules. Further incorporation of e.g. endosomolytic or shielding domains would further increase the heterogeneity. (ii) The resulting polymers fail any possibility of precise structural analysis. The only information that can be gained is an averaged ratio of molecules in the mixture. (iii) Data obtained from physical or biological evaluation of resulting polyplexes are just an average of influences of all single slightly differing molecules, making the analysis of a real structure activity relationship impossible.

In this thesis part the design and synthesis of a polycationic backbone is described. Within this structure, a defined pegylation was incorporated for shielding purpose, combined with folic acid as targeting ligand. Goal of this construct was the design of a structural defined targeted polycationic macromolecule that allows clear functional evaluation of substructures. As model structure a polycationic backbone consisting of 8 Stp units was chosen. Schaffert *et al.* already showed that this kind of short structures are not able to bind nucleic acids efficiently.¹⁴⁰ Thus cysteines were incorporated at both ends of the chains to mediate crosslinking between the backbones after complexation. Functional assays on the nucleic acid binding ability (Fig. 3.29) indicate that this crosslinking is essential for the formation of stable

polyplexes. Hence transfection efficiency was absent, when the cysteines were replaced by serines (Fig. 3.32). These findings are consistent with literature, where short polycations have to be complexed before or after polyplex formation to generate stable carriers.⁷⁵ The advantage of disulfide bridges is their biodegradability. After cellular transport of its payload the stabilized particles degrade into their small substructures due to cleavage of disulfide bonds in the reductive cytosolic environment.

The carrier design included a pegylation to shield the polyplexes positive charge and generate a particle with low interactions with blood components and nontargeted cells. Thus a branching point was introduced into the backbone during synthesis by attachment of lysine. This branching point was used to attach a defined PEG chain consisting of exactly 24 ethylene glycol subunits. As this commercially available PEG was modified with a ω -carboxyl group and an Fmoc protected α -amino group, it was fully compatible to solid phase synthesis. This shielded polymer was tested for its functionality using different methods. Fluorescence correlation spectroscopy (FCS) measurements revealed that the shielded particles had a hydrodynamic radius of ~ 3 nm (naked siRNA ~ 2 nm; table 3.5), while its zeta potential was around 0 mV (10-14 mV lower than the control structure; table 3.7). This indicates that this structure is able to efficiently build small, fully shielded particles. Further experiments on cell association and transfection efficiency demonstrated that these fully protected particles do not interact with the cell surface and thus do not deliver siRNA in an unspecific manner (Fig. 3.30, 3.31, 3.32). The reduced interaction with the cell surface avoids undesired cell and protein interactions *in vivo* but necessitates the incorporation of a homing structure for the target cells. Folic acid presents a high affinity ligand which is also well compatible with solid phase supported synthesis. The incorporation of folate clearly showed that the lost transfection efficiency of a pegylated particle could be recovered (Fig. 3.28, Fig. 3.32). In flow cytometric analyses the targeted carrier showed a strongly enhanced uptake efficiency on receptor expressing cells and an almost absent cell association in nontargeted cells (Fig. 3.31). Several transfection systems have been designed in the last few years using folic acid as targeting domain. Although the attachment never was defined, leading to a loss of targeting efficiency, all these systems gave similar results on the strong targeting effect of this molecule.¹⁶¹ Despite the shown targeting, published data

up to now did not show a fully protected particle with absence of transfection efficiency without the ligand.

Although the biophysical behaviour of the particles was as expected, they did not show any transfection efficiency due to a lack of endosomal escape (Fig. 3.28, Fig. 3.32). It was hypothesized that the Stp units lead to disruption of the endosomal compartment, forcing the proton sponge effect. Transfection results with DNA and with siRNA show that this effect is not strong enough. This finding could be explained by the phenomenon, known as “PEG dilemma”.¹⁶² It is reported that the endosomal escape ability of functional polymers gets strongly reduced by the incorporation of PEG into its structure. As the PEG per polycation ratio is very high in the designed carrier, this could explain its behaviour after internalization. To enhance the delivery process the structural defined polycationic carrier was combined with the endosomolytic peptide-siRNA hybrid in one carrier system. This combination resulted in a very defined efficient delivery vehicle addressing every limitation during the delivery process. Moreover efficient silencing of an “artificial” as well as an endogenous target could be achieved *in vitro*.

In vivo delivery studies could further demonstrate the specific characteristics of the carrier system. As already performed during *in vitro* characterisation, the particle properties were checked step by step using different assays and readout systems. Flow cytometry and fluorescence microscopy could also prove in cell culture that unspecific interactions with nontargeted cells could be strongly reduced due to charge neutralization by pegylation. *In vivo* results on biodistribution confirm these results. In contrast to published work, showing almost always accumulation in liver and spleen (due to clearance by the reticuloendothelial system) or lung (due to aggregation and ionic interactions) these particles circulate stably without interactions with any tissue or short time after systemic injection, but are rapidly cleared by the kidney (Fig. 3.37, Fig. 3.38). The only arising signal showing accumulation of siRNA can be detected in kidney and bladder. Consistent with the small particle size of 6 nm in diameter, these particles are efficiently cleared by kidney filtration. Analysis of urine fractions proved that the detected signal is not free uncomplexed siRNA after dissociation from unstable polyplexes, but the signal of siRNA bound in stable polyplexes (Fig. 3.39). As no tumor accumulation was found during these imaging experiments, it was hypothesized that the circulation time is not long enough for the particle to “recognize” its target tissue. Hence the particle size was modified by redesigning the carrier and

modification of the backbone (Fig. 3.34, Fig. 3.35). The elongation of the PEG-chain by a factor of two or three resulted in an increase of particle size by a factor of only 1.1 or 1.5. The incorporation of hydrophobic domains showed different results. Short hydrophobic modifications (Y_3) did not alter the particle size, while longer hydrophobic chains (caprylic acid, stearic acid) resulted in bigger particles, having a diameter of 33.8 nm or 320.4 nm. These results indicate that two factors influence the particle size. A high degree of pegylation leads to decreased particle size due to the generation of polyplexes with a low amount of siRNAs and reduced aggregation, while hydrophobic domains force aggregation, resulting in increased particle size. Studies on biodistribution prove this hypothesis (Fig. 3.37, Fig. 3.38). Small, pegylated polyplexes still circulate without unspecific interactions but show no significant enhanced circulation time triggered by the only slightly increased particle size. In contrast hydrophobic modifications show accumulation in liver or in case of stearic acid aggregation and accumulation in the lung. Thus these modifications did not result in the desired elongated circulation time due to strong side effects.

Although no fluorescence signal could be detected during biodistribution studies, the system is efficient enough to result in gene regulation. Studies performed with Inf7-siEG5 and FoIA-PEG₂₄-K(Stp₄-C)₂ showed specific mitotic figure formation after intravenous injection (fig. 3.40). As just small amounts of siRNA are necessary for these findings, this indicates that the delivery route can be completed very efficiently.

The low tumor signal after systemic injection as well as the semiquantitative readout of mitotic figure formation disabled a clear determination of the influence of the targeting ligand. The function of the targeting ligand is the attachment to its receptor and thus elongation of the retention, after the carrier reached the target tissue, and an increased uptake by the target cell. To prove the elongated retention time, the amount polyplexes reaching the tumor side was maximized by intratumoral injection. Measuring the fluorescence signal of injected polyplexes (Cy7 labeled siRNA complexed with FoIA-PEG₂₄-K(Stp₄-C)₂) showed a significant elongated retention in the tissue compared to nontargeted polyplexes and free siRNA (Fig. 3.42).

5 Summary

siRNA induced RNA interference is one of the most promising mechanisms for the treatment of various diseases including cancer. The introduction of siRNA into cells has been shown to allow the regulation of former undruggable targets. The most crucial limitation, hampering the development of a therapeutic drug, remains the delivery process. As many efforts had been invested in the improvement of polycationic delivery vehicles, as much the complexity of structures had increased. Carrier systems were modified with functional substructures that improve the different delivery steps by random attachment. This design results in very heterogeneous structures, preventing clear structure activity correlation studies. In this thesis multifunctional siRNA carrier systems were developed, composed of precise and well defined structures, allowing reproducibility, state-of-the-art analytics and the determination of a clear structure activity relationship. In one concept, siRNA was covalently attached to the pegylated targeting ligand folic acid. The structure was synthesized by solid phase peptide synthesis, using a PEG with a defined length. *Via* 1,3-dipolar cycloaddition or disulfide formation this structure was covalently attached to the siRNA backbone. This design allowed full control of the synthesis by purification and analysis. In *in vitro* assays it could be proven that this structure is able to get the siRNA efficiently across the cellular membrane *via* receptor mediated endocytosis but lacks the ability to escape the endosome. In combination with a defined polycationic carrier, enabling an efficient endosomal escape *via* the proton sponge effect, this carrier system enabled efficient receptor specific gene silencing.

In a second approach, a polycationic carrier, composed of a cationic backbone, cysteines for nanoparticle stability by internal crosslinking, a defined PEG chain for shielding, and folic acid as targeting ligand was synthesized using solid phase supported peptide synthesis. Again a very defined monodisperse structure could be generated. Functionality of the structure regarding nucleic acid binding, crosslinking, shielding and receptor specific cell targeting could be demonstrated in separate assays *in vitro*. In combination with the third developed structure, an endosomolytic peptide- siRNA conjugate, this structure was able to overcome all single limitations during the delivery process resulting in very efficient and specific gene silencing *in vitro*. The nanosized appearance (only 6 nm hydrodynamic diameter) and complete

surface shielding of the particles was found very favourable for *in vivo* application tested in mice, resulting in a low accumulation in nontargeted tissue, clearance *via* the kidney and thus high tolerability by the organism after systemic application. Intratumoral injection proved increased tumor retention due to folic acid receptor targeting. Both intratumoral and intravenous injection resulted in specific target gene silencing in the folate-receptor expressing tumor.

In conclusion, this thesis demonstrates that the synthesis of defined highly functionalized carrier systems is possible, allows the control of the appearance of the structures as well as its analysis *via* state-of-the-art methods. This design enables a full control over the carrier enabling the determination of a clear structure activity relationship. This thesis gives the proof of concept for the design of such carrier systems. Based on this strategy a tremendous variety of structures might be synthesized, providing numerous opportunities for the design of siRNA drugs.

6 References

1. Fire, A. et al. Potent and specific genetic interference by double-stranded RNA in *Caenorhabditis elegans*. *Nature* **391**, 806-811 (1998).
2. Sczakiel, G. Antisense strategies for the control of aberrant gene expression. *J Hematother* **3**, 305-313 (1994).
3. Zamore, P.D., Tuschl, T., Sharp, P.A. & Bartel, D.P. RNAi: double-stranded RNA directs the ATP-dependent cleavage of mRNA at 21 to 23 nucleotide intervals. *Cell* **101**, 25-33 (2000).
4. Elbashir, S.M. et al. Duplexes of 21-nucleotide RNAs mediate RNA interference in cultured mammalian cells. *Nature* **411**, 494-498 (2001).
5. Bernstein, E., Caudy, A.A., Hammond, S.M. & Hannon, G.J. Role for a bidentate ribonuclease in the initiation step of RNA interference. *Nature* **409**, 363-366 (2001).
6. Matranga, C., Tomari, Y., Shin, C., Bartel, D.P. & Zamore, P.D. Passenger-strand cleavage facilitates assembly of siRNA into Ago2-containing RNAi enzyme complexes. *Cell* **123**, 607-620 (2005).
7. Ameres, S.L., Martinez, J. & Schroeder, R. Molecular basis for target RNA recognition and cleavage by human RISC. *Cell* **130**, 101-112 (2007).
8. Song, J.J., Smith, S.K., Hannon, G.J. & Joshua-Tor, L. Crystal structure of Argonaute and its implications for RISC slicer activity. *Science* **305**, 1434-1437 (2004).
9. McCaffrey, A.P. et al. RNA interference in adult mice. *Nature* **418**, 38-39 (2002).
10. Behlke, M.A. Progress towards in vivo use of siRNAs. *Mol Ther* **13**, 644-670 (2006).
11. Hannon, G.J. & Rossi, J.J. Unlocking the potential of the human genome with RNA interference. *Nature* **431**, 371-378 (2004).
12. Stenvang, J. & Kauppinen, S. MicroRNAs as targets for antisense-based therapeutics. *Expert Opin Biol Ther* **8**, 59-81 (2008).
13. Zhang, J. et al. Therapeutic potential of RNA interference against cellular targets of HIV infection. *Mol Biotechnol* **37**, 225-236 (2007).
14. Hede, K. Blocking cancer with RNA interference moves toward the clinic. *J Natl Cancer Inst* **97**, 626-628 (2005).
15. Devi, G.R. siRNA-based approaches in cancer therapy. *Cancer Gene Ther* **13**, 819-829 (2006).
16. Shen, Y. Advances in the development of siRNA-based therapeutics for cancer. *IDrugs* **11**, 572-578 (2008).
17. Bitko, V., Musiyenko, A., Shulyayeva, O. & Barik, S. Inhibition of respiratory viruses by nasally administered siRNA. *Nat Med* **11**, 50-55 (2005).
18. Palliser, D. et al. An siRNA-based microbicide protects mice from lethal herpes simplex virus 2 infection. *Nature* **439**, 89-94 (2006).
19. Wang, B. et al. NAMPT overexpression in prostate cancer and its contribution to tumor cell survival and stress response. *Oncogene* **30**, 907-921 (2011).
20. Mangala, L.S., Han, H.D., Lopez-Berestein, G. & Sood, A.K. Liposomal siRNA for ovarian cancer. *Methods Mol Biol* **555**, 29-42 (2009).
21. Wu, L., Wang, Y. & Tian, D. Knockdown of survivin expression by siRNA induces apoptosis of hepatocellular carcinoma cells. *J Huazhong Univ Sci Technolog Med Sci* **27**, 403-406 (2007).

22. Sliwkowski, M.X. et al. Nonclinical studies addressing the mechanism of action of trastuzumab (Herceptin). *Semin Oncol* **26**, 60-70 (1999).
23. Navaratna, D. et al. A peptide inhibitor of the urokinase/urokinase receptor system inhibits alteration of the blood-retinal barrier in diabetes. *FASEB J* **22**, 3310-3317 (2008).
24. Tolentino, M.J. et al. Intravitreal injection of vascular endothelial growth factor small interfering RNA inhibits growth and leakage in a nonhuman primate, laser-induced model of choroidal neovascularization. *Retina* **24**, 132-138 (2004).
25. Dash, P.R., Read, M.L., Barrett, L.B., Wolfert, M.A. & Seymour, L.W. Factors affecting blood clearance and in vivo distribution of polyelectrolyte complexes for gene delivery. *Gene Ther* **6**, 643-650 (1999).
26. Braasch, D.A. et al. Biodistribution of phosphodiester and phosphorothioate siRNA. *Bioorg Med Chem Lett* **14**, 1139-1143 (2004).
27. Deshayes, S., Morris, M.C., Divita, G. & Heitz, F. Cell-penetrating peptides: tools for intracellular delivery of therapeutics. *Cell Mol Life Sci* **62**, 1839-1849 (2005).
28. Ho, A., Schwarze, S.R., Mermelstein, S.J., Waksman, G. & Dowdy, S.F. Synthetic protein transduction domains: enhanced transduction potential in vitro and in vivo. *Cancer Res* **61**, 474-477 (2001).
29. Meade, B.R. & Dowdy, S.F. Exogenous siRNA delivery using peptide transduction domains/cell penetrating peptides. *Adv Drug Deliv Rev* **59**, 134-140 (2007).
30. Ezzat, K. et al. Scavenger receptor-mediated uptake of cell-penetrating peptide nanocomplexes with oligonucleotides. *FASEB J* **26**, 1172-1180 (2012).
31. Limmon, G.V. et al. Scavenger receptor class-A is a novel cell surface receptor for double-stranded RNA. *FASEB J* **22**, 159-167 (2008).
32. Soifer, H.S. et al. Silencing of gene expression by gymnotic delivery of antisense oligonucleotides. *Methods Mol Biol* **815**, 333-346 (2012).
33. Zhang, Y. et al. Down-modulation of cancer targets using locked nucleic acid (LNA)-based antisense oligonucleotides without transfection. *Gene Ther* **18**, 326-333 (2011).
34. Li, H. & Qian, Z.M. Transferrin/transferrin receptor-mediated drug delivery. *Med Res Rev* **22**, 225-250 (2002).
35. Bausinger, R. et al. The transport of nanosized gene carriers unraveled by live-cell imaging. *Angew Chem Int Ed Engl* **45**, 1568-1572 (2006).
36. Turner, J.J., Jones, S.W., Moschos, S.A., Lindsay, M.A. & Gait, M.J. MALDI-TOF mass spectral analysis of siRNA degradation in serum confirms an RNase A-like activity. *Mol Biosyst* **3**, 43-50 (2007).
37. Marques, J.T. & Williams, B.R. Activation of the mammalian immune system by siRNAs. *Nat Biotechnol* **23**, 1399-1405 (2005).
38. Aigner, A. Gene silencing through RNA interference (RNAi) in vivo: strategies based on the direct application of siRNAs. *J Biotechnol* **124**, 12-25 (2006).
39. Sliva, K. & Schnierle, B.S. Selective gene silencing by viral delivery of short hairpin RNA. *Virology* **7**, 248 (2010).
40. Christie, R.J., Nishiyama, N. & Kataoka, K. Delivering the code: polyplex carriers for deoxyribonucleic acid and ribonucleic acid interference therapies. *Endocrinology* **151**, 466-473 (2010).
41. Hughes, J., Yadava, P. & Mesaros, R. Liposomal siRNA delivery. *Methods Mol Biol* **605**, 445-459 (2010).

42. Green, N.K. et al. Retargeting polymer-coated adenovirus to the FGF receptor allows productive infection and mediates efficacy in a peritoneal model of human ovarian cancer. *J Gene Med* **10**, 280-289 (2008).
43. Prill, J.M. et al. Modifications of adenovirus hexon allow for either hepatocyte detargeting or targeting with potential evasion from Kupffer cells. *Mol Ther* **19**, 83-92 (2011).
44. Tatsis, N. & Ertl, H.C. Adenoviruses as vaccine vectors. *Mol Ther* **10**, 616-629 (2004).
45. Kreppel, F. & Kochanek, S. Modification of adenovirus gene transfer vectors with synthetic polymers: a scientific review and technical guide. *Mol Ther* **16**, 16-29 (2008).
46. Merten, O.W. State-of-the-art of the production of retroviral vectors. *J Gene Med* **6 Suppl 1**, S105-124 (2004).
47. McIntyre, G.J. & Fanning, G.C. Design and cloning strategies for constructing shRNA expression vectors. *BMC Biotechnol* **6**, 1 (2006).
48. Paddison, P.J., Caudy, A.A., Bernstein, E., Hannon, G.J. & Conklin, D.S. Short hairpin RNAs (shRNAs) induce sequence-specific silencing in mammalian cells. *Genes Dev* **16**, 948-958 (2002).
49. Kaiser, J. Gene therapy. Seeking the cause of induced leukemias in X-SCID trial. *Science* **299**, 495 (2003).
50. Hacein-Bey-Abina, S. et al. A serious adverse event after successful gene therapy for X-linked severe combined immunodeficiency. *N Engl J Med* **348**, 255-256 (2003).
51. Li, S.D. & Huang, L. Non-viral is superior to viral gene delivery. *J Control Release* **123**, 181-183 (2007).
52. Santel, A. et al. A novel siRNA-lipoplex technology for RNA interference in the mouse vascular endothelium. *Gene Ther* **13**, 1222-1234 (2006).
53. Semple, S.C. et al. Rational design of cationic lipids for siRNA delivery. *Nat Biotechnol* **28**, 172-176 (2010).
54. Akinc, A. et al. Development of lipidoid-siRNA formulations for systemic delivery to the liver. *Mol Ther* **17**, 872-879 (2009).
55. Podesta, J.E. & Kostarelos, K. Chapter 17 - Engineering cationic liposome siRNA complexes for in vitro and in vivo delivery. *Methods Enzymol* **464**, 343-354 (2009).
56. Wagner, E., Cotten, M., Foisner, R. & Birnstiel, M.L. Transferrin-polycation-DNA complexes: the effect of polycations on the structure of the complex and DNA delivery to cells. *Proc Natl Acad Sci U S A* **88**, 4255-4259 (1991).
57. Meyer, M. et al. Synthesis and biological evaluation of a bioresponsive and endosomolytic siRNA-polymer conjugate. *Mol Pharm* **6**, 752-762 (2009).
58. Oskuee, R.K., Philipp, A., Dehshahri, A., Wagner, E. & Ramezani, M. The impact of carboxyalkylation of branched polyethylenimine on effectiveness in small interfering RNA delivery. *J Gene Med* **12**, 729-738 (2010).
59. Howard, K.A. et al. Chitosan/siRNA nanoparticle-mediated TNF-alpha knockdown in peritoneal macrophages for anti-inflammatory treatment in a murine arthritis model. *Mol Ther* **17**, 162-168 (2009).
60. Navarro, G. et al. Low generation PAMAM dendrimer and CpG free plasmids allow targeted and extended transgene expression in tumors after systemic delivery. *J Control Release* **146**, 99-105 (2010).
61. Zintchenko, A., Philipp, A., Dehshahri, A. & Wagner, E. Simple modifications of branched PEI lead to highly efficient siRNA carriers with low toxicity. *Bioconjug Chem* **19**, 1448-1455 (2008).

62. Russ, V., Gunther, M., Halama, A., Ogris, M. & Wagner, E. Oligoethylenimine-grafted polypropylenimine dendrimers as degradable and biocompatible synthetic vectors for gene delivery. *J Control Release* **132**, 131-140 (2008).
63. Huth, S. et al. Insights into the mechanism of magnetofection using PEI-based magnetofectins for gene transfer. *J Gene Med* **6**, 923-936 (2004).
64. Ogris, M., Steinlein, P., Carotta, S., Brunner, S. & Wagner, E. DNA/polyethylenimine transfection particles: influence of ligands, polymer size, and PEGylation on internalization and gene expression. *AAPS PharmSci* **3**, E21 (2001).
65. Hobel, S. & Aigner, A. Polyethylenimine (PEI)/siRNA-mediated gene knockdown in vitro and in vivo. *Methods Mol Biol* **623**, 283-297 (2010).
66. Behr, J.P. The Proton Sponge: a Trick to Enter Cells the Viruses Did Not Exploit. *CHIMIA International Journal for Chemistry* **51**, 34-36 (1997).
67. Sonawane, N.D., Szoka, F.C., Jr. & Verkman, A.S. Chloride accumulation and swelling in endosomes enhances DNA transfer by polyamine-DNA polyplexes. *J Biol Chem* **278**, 44826-44831 (2003).
68. Funhoff, A.M. et al. Endosomal escape of polymeric gene delivery complexes is not always enhanced by polymers buffering at low pH. *Biomacromolecules* **5**, 32-39 (2004).
69. Wagner, E. Polymers for siRNA Delivery: Inspired by Viruses to be Targeted, Dynamic, and Precise. *Acc Chem Res* **in press** (2011).
70. Grayson, A.C., Doody, A.M. & Putnam, D. Biophysical and structural characterization of polyethylenimine-mediated siRNA delivery in vitro. *Pharm Res* **23**, 1868-1876 (2006).
71. Urban-Klein, B., Werth, S., Abuharbeid, S., Czubayko, F. & Aigner, A. RNAi-mediated gene-targeting through systemic application of polyethylenimine (PEI)-complexed siRNA in vivo. *Gene Ther* **12**, 461-466 (2005).
72. Fischer, D., Li, Y., Ahlemeyer, B., Krieglstein, J. & Kissel, T. In vitro cytotoxicity testing of polycations: influence of polymer structure on cell viability and hemolysis. *Biomaterials* **24**, 1121-1131 (2003).
73. Wagner, E. Functional Polymer Conjugates for Medicinal Nucleic Acid Delivery. *Adv Polym Sci* **247**, 1-30 (2012).
74. Knorr, V., Russ, V., Allmendinger, L., Ogris, M. & Wagner, E. Acetal linked oligoethylenimines for use as pH-sensitive gene carriers. *Bioconjug Chem* **19**, 1625-1634 (2008).
75. Russ, V. et al. Improved in vivo gene transfer into tumor tissue by stabilization of pseudodendritic oligoethylenimine-based polyplexes. *J Gene Med* **12**, 180-193 (2010).
76. Yu, H., Russ, V. & Wagner, E. Influence of the molecular weight of bioreducible oligoethylenimine conjugates on the polyplex transfection properties. *AAPS J* **11**, 445-455 (2009).
77. Jiang, T. et al. Tumor imaging by means of proteolytic activation of cell-penetrating peptides. *Proc Natl Acad Sci U S A* **101**, 17867-17872 (2004).
78. Creusat, G. & Zuber, G. Tyrosine-modified PEI: a novel and highly efficient vector for siRNA delivery in mammalian cells. *Nucleic Acids Symp Ser (Oxf)*, 91-92 (2008).
79. Alshamsan, A. et al. Formulation and delivery of siRNA by oleic acid and stearic acid modified polyethylenimine. *Mol Pharm* **6**, 121-133 (2009).
80. Schaffert, D. et al. Solid-Phase Synthesis of Sequence-Defined T-, i-, and U-Shape Polymers for pDNA and siRNA Delivery. *Angew Chem Int Ed Engl* **50**, 8986-8989 (2011).

81. Rozema, D.B. et al. Dynamic PolyConjugates for targeted in vivo delivery of siRNA to hepatocytes. *Proc Natl Acad Sci U S A* **104**, 12982-12987 (2007).
82. Harris, J.M. & Chess, R.B. Effect of pegylation on pharmaceuticals. *Nat Rev Drug Discov* **2**, 214-221 (2003).
83. Immordino, M.L., Dosio, F. & Cattel, L. Stealth liposomes: review of the basic science, rationale, and clinical applications, existing and potential. *Int J Nanomedicine* **1**, 297-315 (2006).
84. Ulasov, A.V. et al. Properties of PEI-based polyplex nanoparticles that correlate with their transfection efficacy. *Mol Ther* **19**, 103-112 (2011).
85. Wu, Y. et al. The investigation of polymer-siRNA nanoparticle for gene therapy of gastric cancer in vitro. *Int J Nanomedicine* **5**, 129-136 (2010).
86. Verbaan, F.J. et al. Steric stabilization of poly(2-(dimethylamino)ethyl methacrylate)-based polyplexes mediates prolonged circulation and tumor targeting in mice. *J Gene Med* **6**, 64-75 (2004).
87. Dash, P.R. et al. Decreased binding to proteins and cells of polymeric gene delivery vectors surface modified with a multivalent hydrophilic polymer and retargeting through attachment of transferrin. *J Biol Chem* **275**, 3793-3802 (2000).
88. Oupicky, D., Ogris, M. & Seymour, L.W. Development of long-circulating polyelectrolyte complexes for systemic delivery of genes. *J Drug Target* **10**, 93-98 (2002).
89. Philipp, A., Zhao, X., Tarcha, P., Wagner, E. & Zintchenko, A. Hydrophobically modified oligoethylenimines as highly efficient transfection agents for siRNA delivery. *Bioconjug Chem* **20**, 2055-2061 (2009).
90. Maeda, H. The enhanced permeability and retention (EPR) effect in tumor vasculature: the key role of tumor-selective macromolecular drug targeting. *Adv Enzyme Regul* **41**, 189-207 (2001).
91. Folkman, J. Angiogenesis in cancer, vascular, rheumatoid and other disease. *Nat Med* **1**, 27-31 (1995).
92. Maeda, H. Tumor-selective delivery of macromolecular drugs via the EPR effect: background and future prospects. *Bioconjug Chem* **21**, 797-802 (2010).
93. Ming, X. Cellular delivery of siRNA and antisense oligonucleotides via receptor-mediated endocytosis. *Expert Opin Drug Deliv* **8**, 435-449 (2011).
94. Davis, M.E. The first targeted delivery of siRNA in humans via a self-assembling, cyclodextrin polymer-based nanoparticle: from concept to clinic. *Mol Pharm* **6**, 659-668 (2009).
95. Tietze, N. et al. Induction of apoptosis in murine neuroblastoma by systemic delivery of transferrin-shielded siRNA polyplexes for downregulation of Ran. *Oligonucleotides* **18**, 161-174 (2008).
96. Shir, A., Ogris, M., Wagner, E. & Levitzki, A. EGF receptor-targeted synthetic double-stranded RNA eliminates glioblastoma, breast cancer, and adenocarcinoma tumors in mice. *PLoS Med* **3**, e6 (2006).
97. Oba, M. et al. Cyclic RGD peptide-conjugated polyplex micelles as a targetable gene delivery system directed to cells possessing $\alpha v \beta 3$ and $\alpha v \beta 5$ integrins. *Bioconjug Chem* **18**, 1415-1423 (2007).
98. Biswal, B.K., Debata, N.B. & Verma, R.S. Development of a targeted siRNA delivery system using FOL-PEG-PEI conjugate. *Mol Biol Rep* **37**, 2919-2926 (2010).
99. Schneider, Y.J. et al. The role of receptor-mediated endocytosis in iron metabolism. *Prog Clin Biol Res* **91**, 495-521 (1982).

100. Sorkin, A. & Goh, L.K. Endocytosis and intracellular trafficking of ErbBs. *Exp Cell Res* **315**, 683-696 (2009).
101. Lee, R.J., Wang, S. & Low, P.S. Measurement of endosome pH following folate receptor-mediated endocytosis. *Biochim Biophys Acta* **1312**, 237-242 (1996).
102. Cressman, S. et al. Binding and Uptake of RGD-Containing Ligands to Cellular avb3 Integrins. *Int J Pept Res Ther* **15**, 10 (2009).
103. Xia, H., Anderson, B., Mao, Q. & Davidson, B.L. Recombinant human adenovirus: targeting to the human transferrin receptor improves gene transfer to brain microcapillary endothelium. *J Virol* **74**, 11359-11366 (2000).
104. Li, Z. et al. Identification and characterization of a novel peptide ligand of epidermal growth factor receptor for targeted delivery of therapeutics. *FASEB J* **19**, 1978-1985 (2005).
105. Schafer, A. et al. Disconnecting the yin and yang relation of epidermal growth factor receptor (EGFR) mediated delivery: a fully synthetic, EGFR-targeted gene transfer system avoiding receptor activation. *Hum Gene Ther* (2011).
106. Goodman, S.L., Holzemann, G., Sulyok, G.A. & Kessler, H. Nanomolar small molecule inhibitors for alphav(beta)6, alphav(beta)5, and alphav(beta)3 integrins. *J Med Chem* **45**, 1045-1051 (2002).
107. Aumailley, M. et al. Arg-Gly-Asp constrained within cyclic pentapeptides. Strong and selective inhibitors of cell adhesion to vitronectin and laminin fragment P1. *FEBS Lett* **291**, 50-54 (1991).
108. Mendelsohn, J. & Baselga, J. The EGF receptor family as targets for cancer therapy. *Oncogene* **19**, 6550-6565 (2000).
109. Molina, M.A. et al. Trastuzumab (herceptin), a humanized anti-Her2 receptor monoclonal antibody, inhibits basal and activated Her2 ectodomain cleavage in breast cancer cells. *Cancer Res* **61**, 4744-4749 (2001).
110. Low, P.S., Henne, W.A. & Doorneweerd, D.D. Discovery and development of folic-acid-based receptor targeting for imaging and therapy of cancer and inflammatory diseases. *Acc Chem Res* **41**, 120-129 (2008).
111. Weitman, S.D. et al. Distribution of the folate receptor GP38 in normal and malignant cell lines and tissues. *Cancer Res* **52**, 3396-3401 (1992).
112. Toffoli, G. et al. Overexpression of folate binding protein in ovarian cancers. *Int J Cancer* **74**, 193-198 (1997).
113. Elnakat, H. & Ratnam, M. Distribution, functionality and gene regulation of folate receptor isoforms: implications in targeted therapy. *Adv Drug Deliv Rev* **56**, 1067-1084 (2004).
114. Kamen, B.A. & Caston, J.D. Properties of a folate binding protein (FBP) isolated from porcine kidney. *Biochem Pharmacol* **35**, 2323-2329 (1986).
115. Birn, H., Nielsen, S. & Christensen, E.I. Internalization and apical-to-basolateral transport of folate in rat kidney proximal tubule. *Am J Physiol* **272**, F70-78 (1997).
116. Nakashima-Matsushita, N. et al. Selective expression of folate receptor beta and its possible role in methotrexate transport in synovial macrophages from patients with rheumatoid arthritis. *Arthritis Rheum* **42**, 1609-1616 (1999).
117. Stella, B. et al. Design of folic acid-conjugated nanoparticles for drug targeting. *J Pharm Sci* **89**, 1452-1464 (2000).
118. Kazanova, E.V. et al. A convenient solid-phase method for the synthesis of novel oligonucleotide-folate conjugates. *Nucleosides Nucleotides Nucleic Acids* **26**, 1273-1276 (2007).

119. Wang, S., Lee, R.J., Mathias, C.J., Green, M.A. & Low, P.S. Synthesis, purification, and tumor cell uptake of ⁶⁷Ga-deferoxamine--folate, a potential radiopharmaceutical for tumor imaging. *Bioconjug Chem* **7**, 56-62 (1996).
120. Meyer, M., Zintchenko, A., Ogris, M. & Wagner, E. A dimethylmaleic acid-melittin-polylysine conjugate with reduced toxicity, pH-triggered endosomolytic activity and enhanced gene transfer potential. *J Gene Med* **9**, 797-805 (2007).
121. Wagner, E. Application of membrane-active peptides for nonviral gene delivery. *Adv Drug Deliv Rev* **38**, 279-289 (1999).
122. Wagner, E., Plank, C., Zatloukal, K., Cotten, M. & Birnstiel, M.L. Influenza virus hemagglutinin HA-2 N-terminal fusogenic peptides augment gene transfer by transferrin-polylysine-DNA complexes: toward a synthetic virus-like gene-transfer vehicle. *Proc Natl Acad Sci U S A* **89**, 7934-7938 (1992).
123. Plank, C., Oberhauser, B., Mechtler, K., Koch, C. & Wagner, E. The influence of endosome-disruptive peptides on gene transfer using synthetic virus-like gene transfer systems. *J Biol Chem* **269**, 12918-12924 (1994).
124. Chen, C.P., Kim, J.S., Steenblock, E., Liu, D. & Rice, K.G. Gene transfer with poly-melittin peptides. *Bioconjug Chem* **17**, 1057-1062 (2006).
125. Ogris, M., Carlisle, R.C., Bettinger, T. & Seymour, L.W. Melittin enables efficient vesicular escape and enhanced nuclear access of nonviral gene delivery vectors. *J Biol Chem* **276**, 47550-47555 (2001).
126. Tosteson, M.T. & Tosteson, D.C. The sting. Melittin forms channels in lipid bilayers. *Biophys J* **36**, 109-116 (1981).
127. Boeckle, S., Wagner, E. & Ogris, M. C- versus N-terminally linked melittin-polyethylenimine conjugates: the site of linkage strongly influences activity of DNA polyplexes. *J Gene Med* **7**, 1335-1347 (2005).
128. Meyer, M., Philipp, A., Oskuee, R., Schmidt, C. & Wagner, E. Breathing life into polycations: functionalization with pH-responsive endosomolytic peptides and polyethylene glycol enables siRNA delivery. *J Am Chem Soc* **130**, 3272-3273 (2008).
129. Li, W., Nicol, F. & Szoka, F.C., Jr. GALA: a designed synthetic pH-responsive amphipathic peptide with applications in drug and gene delivery. *Adv Drug Deliv Rev* **56**, 967-985 (2004).
130. Wyman, T.B. et al. Design, synthesis, and characterization of a cationic peptide that binds to nucleic acids and permeabilizes bilayers. *Biochemistry* **36**, 3008-3017 (1997).
131. Simoes, S. et al. Transfection of human macrophages by lipoplexes via the combined use of transferrin and pH-sensitive peptides. *J Leukoc Biol* **65**, 270-279 (1999).
132. Sasaki, K. et al. An artificial virus-like nano carrier system: enhanced endosomal escape of nanoparticles via synergistic action of pH-sensitive fusogenic peptide derivatives. *Anal Bioanal Chem* **391**, 2717-2727 (2008).
133. Akita, H. et al. Nanoparticles for ex vivo siRNA delivery to dendritic cells for cancer vaccines: programmed endosomal escape and dissociation. *J Control Release* **143**, 311-317 (2010).
134. Lee, S.H., Kim, S.H. & Park, T.G. Intracellular siRNA delivery system using polyelectrolyte complex micelles prepared from VEGF siRNA-PEG conjugate and cationic fusogenic peptide. *Biochem Biophys Res Commun* **357**, 511-516 (2007).
135. Kircheis, R. et al. Coupling of cell-binding ligands to polyethylenimine for targeted gene delivery. *Gene Ther* **4**, 409-418 (1997).

136. Blessing, T., Kursa, M., Holzhauser, R., Kircheis, R. & Wagner, E. Different strategies for formation of pegylated EGF-conjugated PEI/DNA complexes for targeted gene delivery. *Bioconjug Chem* **12**, 529-537 (2001).
137. Merrifield, R.B. Solid Phase Peptide Synthesis. I. The Synthesis of a Tetrapeptide. *Journal of the American Chemical Society* **85**, 2149-2155 (1963).
138. Hartmann, L., Krause, E., Antonietti, M. & Borner, H.G. Solid-phase supported polymer synthesis of sequence-defined, multifunctional poly(amidoamines). *Biomacromolecules* **7**, 1239-1244 (2006).
139. Hartmann, L., Hafele, S., Peschka-Suss, R., Antonietti, M. & Borner, H.G. Tailor-made poly(amidoamine)s for controlled complexation and condensation of DNA. *Chemistry* **14**, 2025-2033 (2008).
140. Schaffert, D., Badgular, N. & Wagner, E. Novel Fmoc-polyamino acids for solid-phase synthesis of defined polyamidoamines. *Org Lett* **13**, 1586-1589 (2011).
141. Judge, A.D. et al. Confirming the RNAi-mediated mechanism of action of siRNA-based cancer therapeutics in mice. *J Clin Invest* **119**, 661-673 (2009).
142. Jeong, J.H., Mok, H., Oh, Y.K. & Park, T.G. siRNA conjugate delivery systems. *Bioconjug Chem* **20**, 5-14 (2009).
143. Kong, W.H. et al. Efficient intracellular siRNA delivery strategy through rapid and simple two steps mixing involving noncovalent post-PEGylation. *J Control Release* **138**, 141-147 (2009).
144. Mao, S. et al. Influence of polyethylene glycol chain length on the physicochemical and biological properties of poly(ethylene imine)-graft-poly(ethylene glycol) block copolymer/SiRNA polyplexes. *Bioconjug Chem* **17**, 1209-1218 (2006).
145. Boussif, O. et al. A versatile vector for gene and oligonucleotide transfer into cells in culture and in vivo: polyethylenimine. *Proc Natl Acad Sci U S A* **92**, 7297-7301 (1995).
146. Yu, G.S. et al. Synthesis of PAMAM Dendrimer Derivatives with Enhanced Buffering Capacity and Remarkable Gene Transfection Efficiency. *Bioconjug Chem* **22**, 1046-1055 (2011).
147. Wang, X.L., Nguyen, T., Gillespie, D., Jensen, R. & Lu, Z.R. A multifunctional and reversibly polymerizable carrier for efficient siRNA delivery. *Biomaterials* **29**, 15-22 (2008).
148. Moschos, S.A. et al. Lung delivery studies using siRNA conjugated to TAT(48-60) and penetratin reveal peptide induced reduction in gene expression and induction of innate immunity. *Bioconjug Chem* **18**, 1450-1459 (2007).
149. Detzer, A. et al. Increased RNAi is related to intracellular release of siRNA via a covalently attached signal peptide. *RNA* **15**, 627-636 (2009).
150. Chiu, Y.L., Ali, A., Chu, C.Y., Cao, H. & Rana, T.M. Visualizing a correlation between siRNA localization, cellular uptake, and RNAi in living cells. *Chem Biol* **11**, 1165-1175 (2004).
151. Muratovska, A. & Eccles, M.R. Conjugate for efficient delivery of short interfering RNA (siRNA) into mammalian cells. *FEBS Lett* **558**, 63-68 (2004).
152. Soutschek, J. et al. Therapeutic silencing of an endogenous gene by systemic administration of modified siRNAs. *Nature* **432**, 173-178 (2004).
153. Nishina, K. et al. Efficient in vivo delivery of siRNA to the liver by conjugation of alpha-tocopherol. *Mol Ther* **16**, 734-740 (2008).
154. Bartlett, D.W., Su, H., Hildebrandt, I.J., Weber, W.A. & Davis, M.E. Impact of tumor-specific targeting on the biodistribution and efficacy of siRNA nanoparticles measured by multimodality in vivo imaging. *Proc Natl Acad Sci U S A* **104**, 15549-15554 (2007).

155. Schiffelers, R.M. et al. Cancer siRNA therapy by tumor selective delivery with ligand-targeted sterically stabilized nanoparticle. *Nucleic Acids Res* **32**, e149 (2004).
156. Kim, S.H., Jeong, J.H., Lee, S.H., Kim, S.W. & Park, T.G. LHRH receptor-mediated delivery of siRNA using polyelectrolyte complex micelles self-assembled from siRNA-PEG-LHRH conjugate and PEI. *Bioconjug Chem* **19**, 2156-2162 (2008).
157. Thomas, M. et al. Ligand-targeted delivery of small interfering RNAs to malignant cells and tissues. *Ann N Y Acad Sci* **1175**, 32-39 (2009).
158. Zhu, L. & Mahato, R.I. Targeted delivery of siRNA to hepatocytes and hepatic stellate cells by bioconjugation. *Bioconjug Chem* **21**, 2119-2127 (2010).
159. Oishi, M., Nagasaki, Y., Itaka, K., Nishiyama, N. & Kataoka, K. Lactosylated poly(ethylene glycol)-siRNA conjugate through acid-labile beta-thiopropionate linkage to construct pH-sensitive polyion complex micelles achieving enhanced gene silencing in hepatoma cells. *J Am Chem Soc* **127**, 1624-1625 (2005).
160. Oishi, M., Sasaki, S., Nagasaki, Y. & Kataoka, K. pH-responsive oligodeoxynucleotide (ODN)-poly(ethylene glycol) conjugate through acid-labile beta-thiopropionate linkage: preparation and polyion complex micelle formation. *Biomacromolecules* **4**, 1426-1432 (2003).
161. Zhao, X., Li, H. & Lee, R.J. Targeted drug delivery via folate receptors. *Expert Opin Drug Deliv* **5**, 309-319 (2008).
162. Wang, T., Upponi, J.R. & Torchilin, V.P. Design of multifunctional non-viral gene vectors to overcome physiological barriers: Dilemmas and strategies. *Int J Pharm* (2011).

7 Appendix

7.1 Abbreviations

AA	Amino acid
a.u.	Absorption units
B6	Peptide sequence with affinity for the transferrin receptor
brPEI	Branched polyethylenimine
CapA	Caprylic acid
CPP	Cell penetrating peptide
CTC-resin	2-chlorotriyl chloride resin
CuBr	Copper bromide
DAPI	4',6-diamidino-2-phenylindole
DCM	Dichloromethane
DHB	2,5-dihydroxybenzoic acid
DIPEA	Diisopropylethylamine
DMF	N,N-Dimethylformamide
DMMA _n	2,3-Dimethylmaleic anhydride
DNA	Deoxyribonucleic acid
dsRNA	Double stranded ribonucleic acid
DTNB	5,5'-dithiobis-(2-nitrobenzoic acid)
EDTA	Ethylenediaminetetraacetic acid
e.g.	exempli gratia (for example)
EG5	Eglin 5, or KSP, Kinesin spindle protein
eGFP	Enhanced green fluorescent protein
EGF-R	Epidermal growth factor receptor
EPR	Enhanced permeability and retention effect
EtOH	Ethanol
FCS	Fluorescence correlation spectroscopy or Fetal calf serum
Fe ³⁺	Trivalent iron
Fig.	Figure
Fmoc	Fluorenylmethyloxycarbonyl chloride
FoIA	Folic acid
FoIA-R	Folic acid receptor
GALA	Peptide with the sequence Glutamic acid-Alanine-Leucine-Alanine

GE11	Peptide binding to the EGF-receptor
GMP	Good manufacturing practice
HEPES	N-(2-hydroxyethyl) piperazine-N'-(2-ethansulfonic acid)
HES	Hydroxy ethyl starch
HBG	Hepes buffered glucose
HBS	Hepes buffered saline
HOBt	Hydroxybenzotriazole
HPA	3-Hydroxypicolinic acid
KALA	Peptide with the sequence Lysine-Alanine-Leucine-Alanine
KCN	Potassium cyanide
K _d	Dissociation constant
KSP	Kinesin spindle protein
LinA	Linoleic acid
LPEI	Linear polyethylenimine
MALDI-TOF-MS	Matrix-Assisted-Laser-Desorption/Ionization-Time-Of-Flight-Mass-Spectrometry
MeOH	Methanol
MTBE	Methyl tertiary butyl ether
mRNA	Messenger ribonucleic acid
n.d.	Not defined
N/P	Polymer nitrogen to nucleic acid phosphate ratio
nt	Nucleotide
OEI	Oligoethylenimine
OleA	Oleic acid
PAMAM	Polyamidoamine
pDNA	Plasmid deoxyribonucleic acid
PEG	Polyethylene glycol
PEG ₂₄	Polyethylene glycol with exactly 24 monomers
pHPMA	poly(N-(2-hydroxypropyl)methacrylamide
PLL	poly-L-lysine
PPI	polypropylenimine
PTD	protein transduction domain
PyBop®	benzotriazole-1-yl-oxy-tris-(dimethylamino)- phosphonium hexafluorophosphate

r_h	hydrodynamic radius
RGD	peptide sequence (arginine, glycine, aspartic acid)
RISC	ribonucleic acid induced silencing complex
RNA	Ribonucleic acid
rpm	Rounds per minute
RNAi	Ribonucleic acid interference
RP-HPLC	Reverse phase high pressure liquid chromatography
RT	Room temperature
shRNA	Small hairpin ribonucleic acid
siRNA	Small interfering ribonucleic acid
SPPS	Solid phase peptide synthesis
Stp	Succinoyl-tetraethylenpentamine
TBE-buffer	Tris-Boric acid-EDTA-buffer
TBTA	Tris[(1-benzyl-1 <i>H</i> -1,2,3-triazol-4-yl)methyl]amine
TCEP	tris(2-carboxyethyl)phosphine
Tfa	Trifluoroacetic acid
Tf-R	Transferrin receptor
TIS	triisopropyl-silane
Trt	trityl
v/v	volume per volume
v/v/v	volume per volume per volume
w/v	weight per volume

7.2 Supporting Info Chapter 3.3

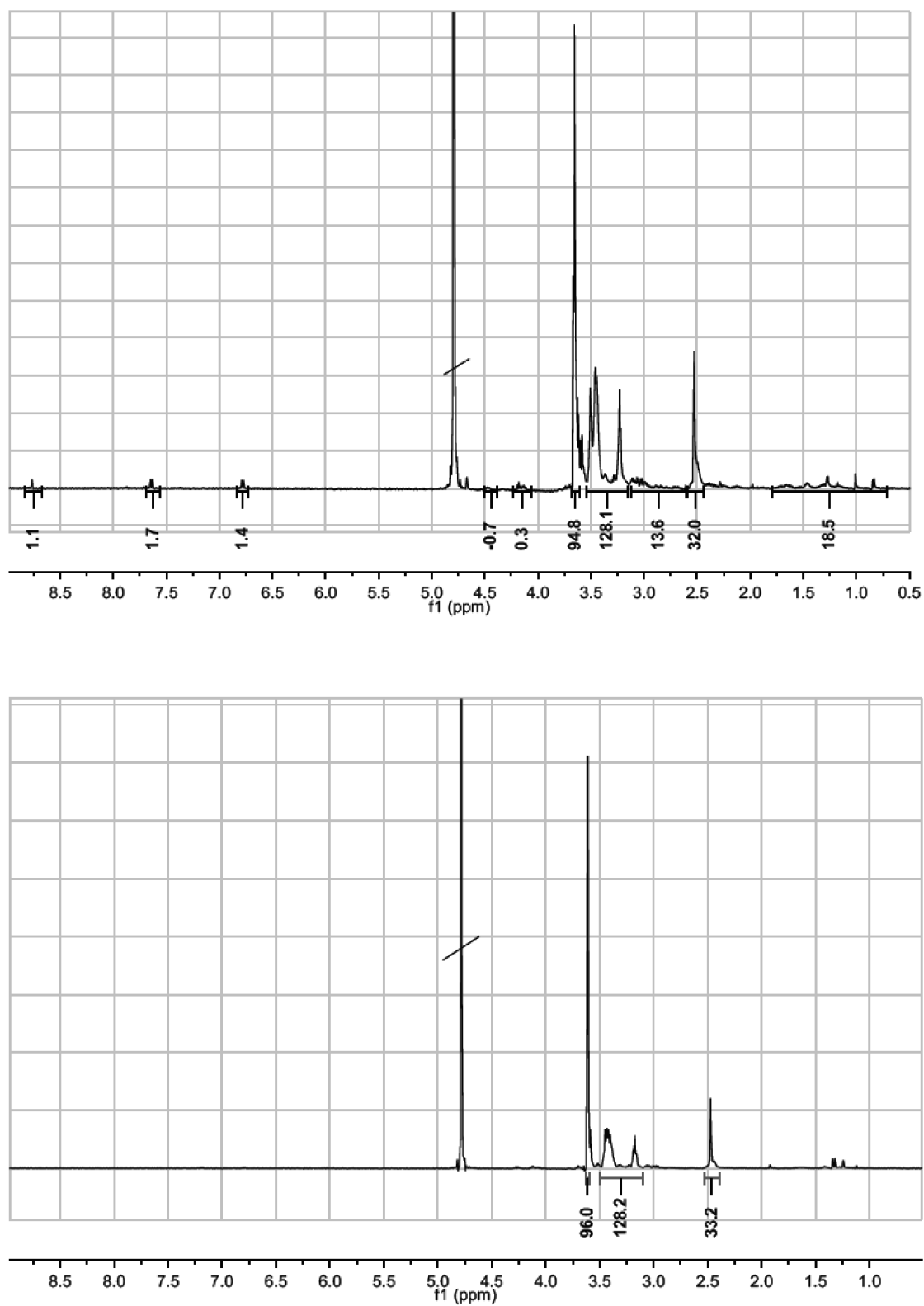


Fig. 7.1 $^1\text{H-NMR}$ spectra of FoIA-PEG₂₄-K(Stp₄-C)₂ and A-PEG₂₄-K(Stp₄-C)₂ in D₂O.

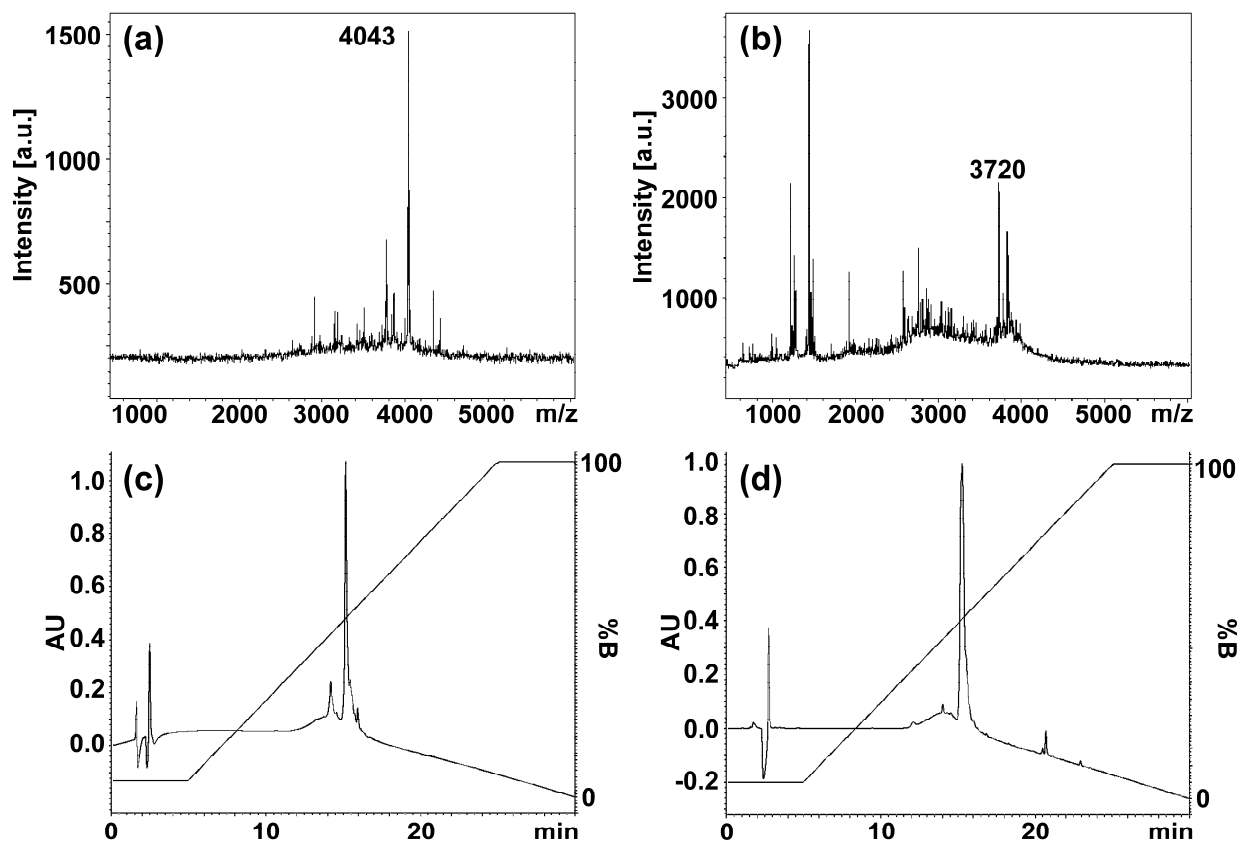


Fig. 7.2 Analysis of structural analogues of Fola-PEG₂₄-K(Stp₄-C)₂. MALDI-TOF-MS spectra and chromatogram of the analytical RP-HPLC of Fola-PEG₂₄-K(Stp₄-S)₂ (a,c) and A-PEG₂₄-K(Stp₄-C)₂ (b,d). Calculated mass [M+H]⁺: Fola-PEG₂₄-K(Stp₄-S)₂: 4043, A-PEG₂₄-K(Stp₄-C)₂: 3720.

7.3 Publications

7.3.1 Original papers

Dohmen C, Edinger D, Fröhlich T, Schreiner L, Lächelt U, Troiber C, Rädler J, Hadwiger P, Vornlocher H-P, Wagner E, *Nano sized multifunctional polyplexes for receptor mediated siRNA delivery*, submitted

Martin I, Dohmen C, Mas- Moruno C, Troiber C, Kos P, Schaffert D, Lächelt U, Teixidó M, Günther M, Kessler H, Giralt E, Wagner E, *Solid-phase-assisted synthesis of targeting peptide-PEG-oligo(ethane amino)amides for receptor-mediated gene delivery*, Org Biomol Chem. 2012;10(16):3258-68

Dohmen C, Fröhlich T, Lächelt U, Roehl I, Vornlocher H-P, Hadwiger P, Wagner E; *Defined Folate-PEG-siRNA Conjugates for Receptor Specific Gene Silencing*, Mol. Ther. Nucleic Acid 2012, 1, e7

Schaffert D, Troiber C, Salcher E, Fröhlich T, Martin I, Badgujar N, Dohmen C, Edinger D, Kläger R, Maiwald G, Farkasova K, Hadwiger P, Wagner E, *Solid-Phase Synthesis of Sequence-Defined T-, i-, and U-Shape Polymers for pDNA and siRNA Delivery*, Angew Chem Int Ed Engl 2011;50(38):8986-9

Schlossbauer A, Dohmen C, Schaffert D, Wagner E, Bein T, *pH-responsive release of acetal-linked melittin from SBA-15 mesoporous silica*, Angew Chem Int Ed Engl 2011, 50(30):6828-30

Klutz K, Willhauck M, Dohmen C, Wunderlich N, Knoop K, Zach C, Senekowitsch-Schmidtke R, Gildehaus F, Ziegler S, Fürst S, Göke B, Wagner E, Ogris M, Spitzweg C, *Image-Guided Tumor-Selective Radioiodine Therapy of Liver Cancer After Systemic Nonviral Delivery of the Sodium Iodide Symporter Gene*, Hum. Gene Ther. 2011, 22(12):1563-74

Haijun Y, Nie Y, Dohmen C, Yunquin L, Wagner E, *Epidermal growth factor-PEG functionalized PAMAM-pentaethylenehexamine dendron for targeted gene delivery produced by click chemistry*, *Biomacromolecules*, 2011, 12(6):2039-47

Meyer M, Dohmen C, Philipp A, Kiener D, Mailwald G, Scheu C, Ogris M, Wagner E; *Synthesis and biological evaluation of a bioresponsiv and endosomolytic siRNA-polymer conjugate*, *Mol Pharm.* 2009, 6(3):752-62

7.3.2 Patents

Schaffert D, Dohmen C, Lächelt U, Günther M, Wagner E, *Polymers for Nucleic Acid Delivery*, European Patent Application (WO2011154331A1, EP2395041A1) in cooperation with Roche Kulmbach

7.3.3 Book chapters

Dohmen C, Wagner E; *Multifunctional CPP polymer system for tumor-targeted pDNA and siRNA delivery*, *Methods Mol Biol.* 2011, 683:453-463

Dohmen C, Ogris M, *Receptor-Mediated Delivery of Proteins and Peptides to Tumors*, *Pharmaceutical Perspectives of Cancer Therapeutics*, 2009, 269-96

8 Acknowledgements

This thesis would not have been possible to be completed without the cooperation and assistance of various people who deserve my acknowledgement.

First of all I want to thank all my colleagues for their help and support as well as for the great atmosphere in the lab. It always was a pleasure to work in this big team.

I want to thank my supervisor Professor Dr. Ernst Wagner for giving me the opportunity to become a member of his working group, time and trust to develop own ideas, but also for the scientific guidance enabling this thesis.

Special thanks to the Axiolabs GmbH (former Roche Kulmbach GmbH) especially to Philipp Hadwiger and Hans-Peter Vornlocher for scientific cooperation and siRNA support.

Thank you to Martin Meyer and David Schaffert for getting me started in the scientific world and never getting tired of answering a lot of questions.

Many thanks to my lab mate Kevin Maier. I know you were the best person I could ever find to work next to me.

Furthermore I want to thank Thomas Fröhlich for performing the *in vitro* studies, Daniel Edinger and Laura Schreiner for the *in vivo* studies and a lot of hours in the animal house, David Schaffert, Ulrich Lächelt, Irene Martin, Claudia Scholz, Edith Salcher and Christina Troiber for a lot of fruitful discussions about chemistry and peptide synthesis.

Thank you to Martin Ruffer for help and support. A special thank goes to Wolfgang Rödl who always had a helping hand on problems concerning broken machines, computers, chromatographic topics or any other difficulty in the lab. Almost everything could be fixed within minutes.

I also want to thank all the other technicians Markus, Miriam, Melinda, Ursula for their help with all problems and keeping the lab routine running.

My special thanks go to the “PhD-room group” and all included members. You always found a tool to make work easy when I wanted to give up. It was a pleasure working with you.

But life is more than just science. Therefore a very heartfelt thank goes to Rebekka for her support and a lot of patience during the whole time.

Finally, I want to thank most of all my parents for their trust, appreciation and indefatigable support during my whole life for so many reasons!